8-AL

PRESSURE LOSSES IN SUBSEA CHOKE LINES DURING WELL CONTROL OPERATIONS

A Thesis

Submitted to the Graduate Faculty of the
Louisiana State University and
Agricultural and Mechanical College
in partial fulfillment of the
requirements for the degree of
Master of Science

in

The Department of Petroleum Engineering

by
Fawzi A. Elfaghi
B.S., University of Tripoli, 1975
May, 1982

ACKNOWLEDGMENTS

The author wishes to express his sincere appreciation to the faculty and staff of the Petroleum Engineering Department at Louisiana State University for their guidance during his graduate study.

He is especially grateful to Dr. Julius P. Langlinais, under whose supervision this work was accomplished. Professor Adam "Ted" Bourgoyne, Chairman of the department, gave much help and guidance in the development of this work, and Professor William R. Holden provided valuable advice. For this assistance, the author is grateful to them both. The considerable help of Professor Oscar K. Kimbler, Professor Walter R. Whitehead, Professor Zaki Bassiouni and Mr. Jim Sykora is also greatly appreciated.

The author, also, would like to thank his mother Fatema, his wife, Najah, and his brothers and sisters for their endless support and encouragement in making this work possible.

Finally, he would like to dedicate this work to his daughter, Haneen, who was born during the course of its preparation and who aided in her own way to its achievement.

TABLE OF CONTENTS

LIST OF TABLES

LIST OF FIGURES

ABSTRACT

As the offshore drilling industry expands to deeper water depths, the pressure losses in choke lines during well control operations become more significant. The main objective of this experimental work is to study the pressure losses in subsea choke lines. The study includes the measurement of pressure losses of clay-water muds and nitrogen-mud mixtures using a full-scale model consisting of 3000 feet of 2-3/8 inch subsurface choke line. These measurements were used to evaluate some available non-Newtonian and vertical two-phase flow correlations. The non-Newtonian correlations include the Bingham plastic and the power law models, while the two-phase correlations include those of Poettmann and Carpenter, Hagedorn and Brown, and Beggs and Brill. The Bingham plastic and the power law models were combined with the two-phase flow correlations when the gas-mud mixtures were studied.

It was found that choke line pressure losses due to the flow of kick fluids and/or drilling muds can be accurately predicted. For single phase mud flow, both the Bingham plastic and the power law non-Newtonian models provided acceptable comparisons with observed data. For simultaneous vertical flow of gas and mud through the choke line, all the two-phase flow correlations except

the Poettmann and Carpenter correlation provided acceptable results. However, Hagedorn and Brown predictions had the least deviation from observed data.

CHAPTER I

INTRODUCTION

A kick is defined as the uncontrolled entry of formation fluid into the well bore, which tends to cause the well to blowout if proper well control procedures are not taken. A blowout is considered the most expensive and potentially dangerous problem encountered during drilling operations.

The basic idea of any well control procedure is to close the blowout preventors and circulate the kick fluid out of the hole while holding a constant bottom hole pressure just slightly above the formation pressure. Constant bottom hole pressure is maintained by circulating the well through a surface adjustable choke. The choke is linked to the well annulus at a point below the blowout preventor equipment through a choke line. Adjusting the choke at the proper position requires consideration of the pressure drop in the choke line as mud and kick fluid continue to flow to the surface. A better understanding of the behavior of the mud and kick fluid, as well as the characteristics of the equipment is essential in the development of practical and efficient contingency plans for pressure control operations.

Kick fluids are generally salt water or gas. A salt water kick is easier to handle since salt water

does not significantly expand as it is brought to the surface. A gas kick, however, is completely different. Since gas is highly compressible, it must be allowed to expand as it is circulated to the surface, if a constant bottom hole pressure is to be maintained. The expansion of the gas will force the drilling mud out of the hole, reducing the hydrostatic pressure of the fluid column, thus requiring a higher back pressure in order to maintain a constant bottom hole pressure. A complicating factor of applying too much back pressure is the danger of fracturing a weaker unprotected stratum which could result in an underground blowout. Another source of pressure loss is the frictional flow pressure associated with the movement of mud and kick fluid up the well annulus and through the choke line. The frictional pressure losses in the annulus are generally small at the circulating rates commonly used in well control operations. Unfortunately, frictional pressure losses in the choke line cannot always be ignored. In land rigs and bottom supported marine rigs, where a short choke line is used, the associated pressure losses are small. However, in deep offshore drilling operations, the problem is more complicated because the pressure losses in the choke line are too significant to be ignored.

As offshore drilling operations were extended to deeper water depths, more significant modifications in

blowout equipment were needed. The first major modification was the location of the blowout preventer equipment on the seafloor, rather than the surface. Having the blowout preventer equipment located on the seafloor requires long subsea choke lines to link the well annulus to the surface choke manifold. Subsea choke lines added several more complications to the problem of well control operations. These complications are due to the fact that hydrostatic as well as frictional pressure drops in subsea choke lines are very significant in pressure control operations. The high frictional pressure loss is developed as a result of the return flow of mud and gas-mud mixtures through the choke line. Moreover, if a gas kick is being circulated from the well, a greater loss of hydrostatic head, associated with a mud-gas two-phase frictional loss, will be developed as the gas flows through the choke line. The loss of hydrostatic head tends to lower the bottom hole pressure, while the frictional pressure loss tends to increase the pressure on the exposed formations. Figure 1.2 shows a typical well pressure profile that must be held by the adjustable choke when formation gas being circulated from the well reaches the well-control equipment at the seafloor.

Another major problem, as illustrated in Figure 1.3, is the maximum drilling fluid density which can be used without fracturing the exposed formation. Note,

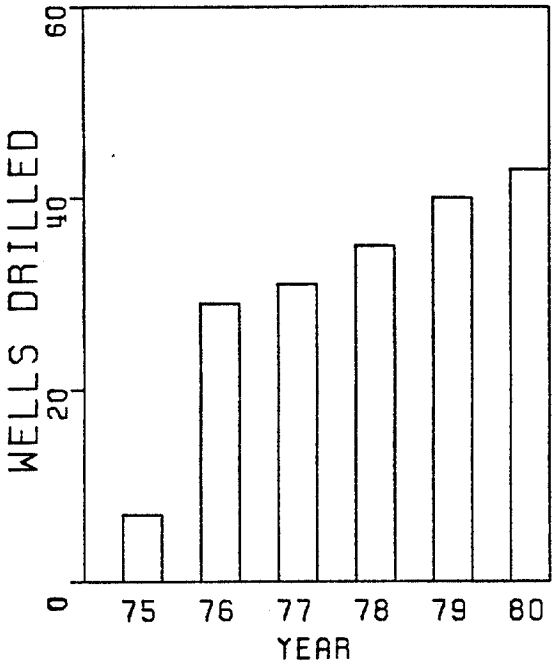

FIG.1.1-ANNUAL NUMBER OF WELLS DRILLED OVER 1000 FT OF WATER[13]

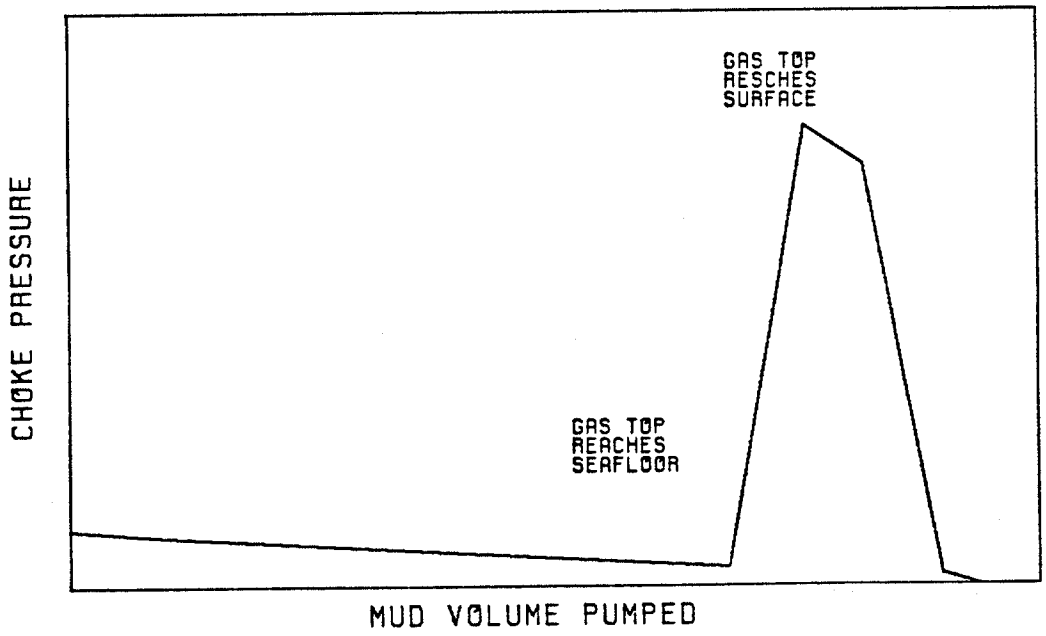

FIG.1.2-A TYPICAL CHOKE PRESSURE PROFILE

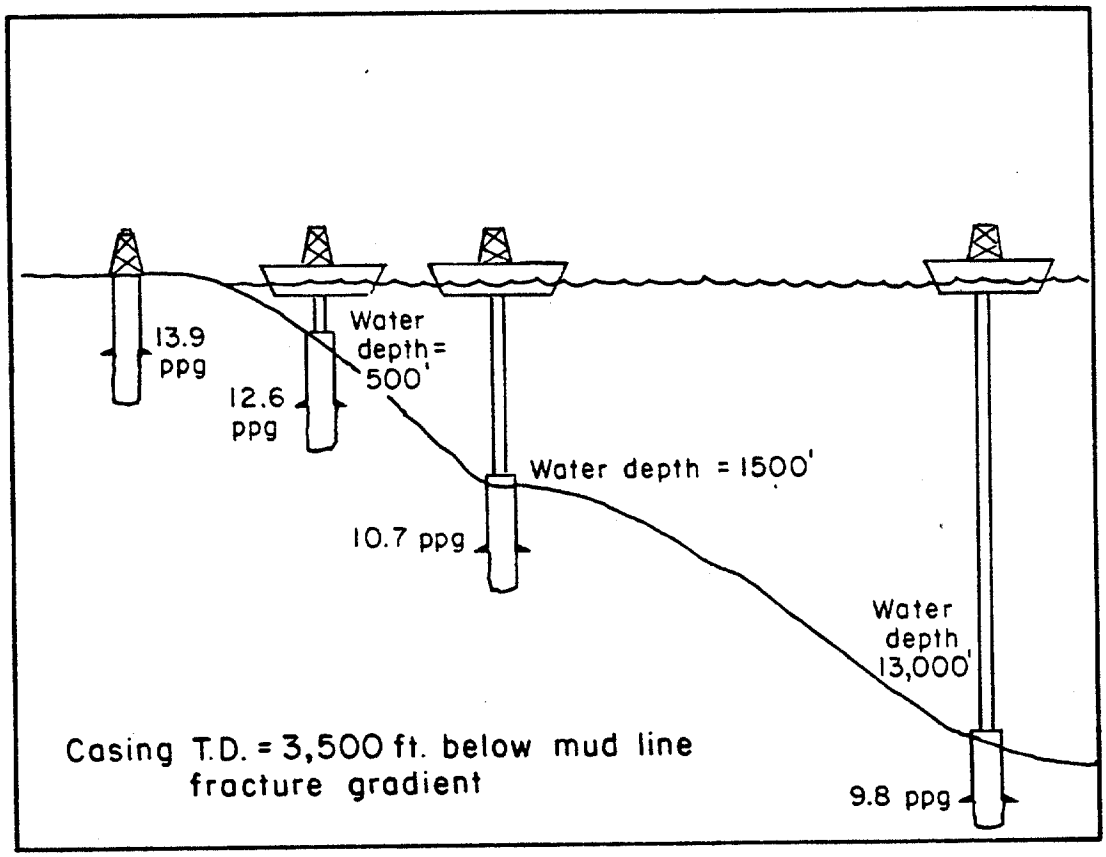

Figure 1.3 - Effect of Water Depth on Fracture Gradient (National Science Foundation, 1980)[36]

the maximum mud density decreases as the water depth increases.

Figure 1.1 shows the annual number of wells drilled in over 1,000 feet of water.[13]

This study is part of an experimental effort, on the subject of improving pressure control procedures in deep water depths, being conducted by the Petroleum Engineering Department at Louisiana State University. The purpose of this work is to develop improved calculation procedures for determining the change in pressure with depth in a subsea choke line during well control operations. The improved calculation procedure should allow for improved computer simulators for modeling well control operations on a floating drilling vessel. Well control simulators have been shown to be valuable in developing improved well control procedures and training drilling personnel in the use of these procedures.

In this work, the basic theoretical background is presented, an experimental procedure was established, and some experimental data was obtained. The theoretical background involves a discussion of the fluid rheology, a review of the more popular non-Newtonian and two-phase pressure loss correlations, and the use of computer models to describe these correlations. The experimental procedure includes suggested steps to be

followed in future work to furthe study the problem. The experimental work involves a study of pressure loss in 3000 feet of 2-3/8 inch subsurface choke line. The pressure losses of interest are the result of flow of different clay-water muds and nitrogen gas mixtures. The experimental work was conducted at Louisiana State University's new training and research well facility. This facility is centered around a 6,000 foot well, complete with surface and subsurface equipment, which allows essential full-scale modeling of the flow geometry present on a floating drilling vessel operating in 3,000 feet of water.

The results of this work are encouraging. They indicate that pressure losses in subsea choke lines can be predicted if proper mathematical models are considered.

CHAPTER II

FLUID RHEOLOGY AND FLOW REGIMES

It is the rheological characteristics of any drilling fluid that is most responsible for the pressure losses due to friction. This chapter will briefly discuss the fundamentals of fluid rheology and present the mathematical models commonly used to describe the drilling fluid's rheological behavior.

2.1 Fluid Rheology

In order to study the pressure loss associated with flow of any drilling fluid, it is essential to understand the fundamentals of fluid rheology. This fundamental is simply the shear stress-shear rate relationship, which is responsible for the frictional shear resistance that develops due to a velocity gradient in a liquid.

Figure 2.1, which can be used to illustrate the shear stress-shear rate relationship, consists of two parallel plates of area, A, separated by a distance, x, with the space between them filled with a fluid. A force, F, imposed on the upper plate will produce a shearing force, F/A, which in turn will develop a shearing rate, $d\bar{v}/dx$. For a Newtonian fluid flowing under laminar conditions, the shear stress-shear rate

relationship is linear. The constant of proportionality between shear rate and shear stress is called viscosity. For a non-Newtonian fluid, the relationship still exists, but is not necessarily linear.

2.1.1 Rheology Measurement

It is far from practical to build a rheology measuring device based on the relative movement of two flat parallel plates. However, laminar flow behavior can be well evaluated using cylindrical devices. The most common cylindrical viscometer is the rotational viscometer. The rotational viscometer[3, 33] consists of two cylinders, an outer rotating cylinder, called a rotor sleeve, and an inner stationary cylinder, called a bob. When running the viscometer, the portion of the liquid filling the space between the sleeve and the bob, is sheared. The developed torque, represented by angular displacement, is obtained directly from the viscometer. Accordingly, shear rate can be related to shear stress using the defining correlation of the Newtonian, the Bingham plastic or the Power law rheological models. The most popular rotational viscometer used in drilling operations is the model 35 Fann V-G meter.

2.1.2 Rheology Classification

Any material that moves under the influence of shear stress can be classified according to its shear

stress-shear rate relationship as either Newtonian or non-Newtonian. Figure 2.2 represents the shear diagram for various types of drilling fluids. The most common mathematical models used to describe the rheological behavior of these fluids are the Newtonian, the Bingham plastic, or the power law.

The simplest and most common type of fluid is one which follows the Newtonian model. Under laminar flowing conditions, a Newtonian fluid exhibits a direct proportionality between its shear stress and shear rate. This relation is described mathematically as follows:

$$\tau = \frac{\mu}{g_c} \left(\frac{-d\bar{v}}{dr}\right) \tag{2.1}$$

where τ is the shear stress, F/A, and $(-d\bar{v}/dr)$ is the shear rate, γ, within a circular pipe.

A non-Newtonian fluid is one which does not exhibit a direct proportionality between its shear stress and shear rate. Non-Newtonian fluids can be either time-dependent or time-independent. A time-dependent fluid is one whose rheological properties depend upon the amount as well as the duration of shear. A time-independent fluid is one whose rheological properties depend upon the amount, but not the duration of shear. Fluids of the latter type can be further classified as pseudoplastic or dilatant. Pseudoplastic fluids are characterized by the decrease of their apparent viscosity with

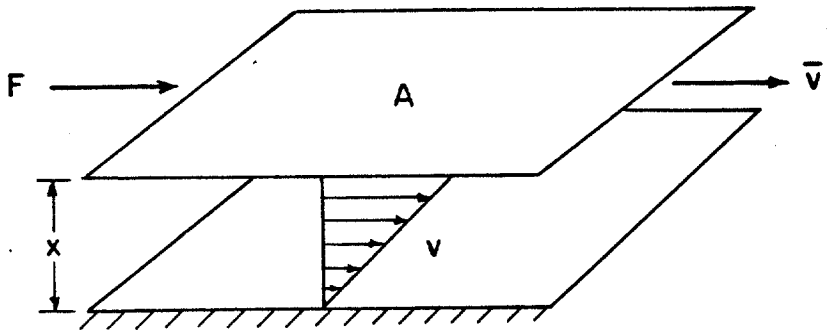

Figure 2.1 - Idealized Diagram Showing Relationship Between Shear Stress and Shear Rate

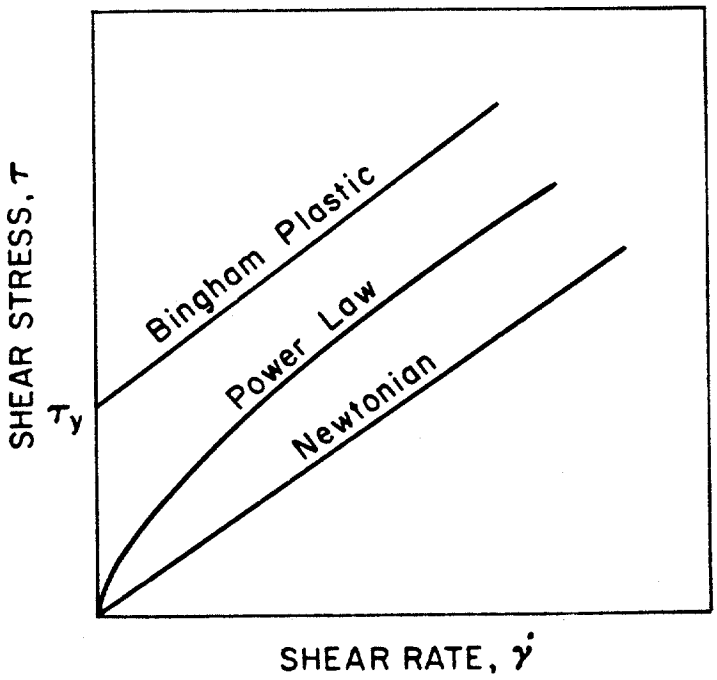

Figure 2.2 - Commonly Used Models to Approximate Flow Behavior of Drilling Fluids

shear rate; while dilatant fluids are characterized by the increase of apparent viscosity with shear rate. The apparent viscosity is defined as the viscosity at a given shear rate. Drilling fluids are generally pseudoplastic in nature. Two common rheological models are used to describe the behavior of pseudoplastic fluids. These models are the Bingham plastic and the power law. A pseudoplastic fluid that follows the Bingham plastic model will be called a Bingham plastic fluid. A Bingham plastic fluid is one with a linear shear stress-shear rate relationship, but sustains some finite shear stress before it begins to flow. Thus, a Bingham fluid will not move until the applied shear stress exceeds a certain minimum value known as the yield point, τ_y. Once the flow begins, the behavior of the fluid obeys a linear shear stress-shear rate proportionality. The Bingham plastic linear proportionality is called plastic viscosity, μ_p. Mathematically, the behavior of these fluids is defined as follows:[3, 10]

$$\dot{\gamma} = \frac{1}{\mu_p}(\tau - \frac{4}{3}\tau_y) \text{ for } \tau > \tau_y \qquad (2.2)$$

where $\dot{\gamma}$, the shear rate, is equal to $\frac{8\bar{v}}{g_c D}$, and, τ is the shear stress at the wall of the pipe.

A pseudoplastic fluid that follows the power law model will be called a power law fluid. The shear diagram of a power law fluid, Figure 2.2, shows a curve

which passes through the origin with a positive slopes range from zero to unity. This change in the slope indicates that the shear stress-shear rate relationship is not linear. The flow behavior of these fluids is described mathematically as follows:[5, 10]

$$\tau = k\left(\frac{-d\bar{v}}{dr}\right)^n \qquad (2.3)$$

where the deviation of the flow behavior index, n, from unity, characterizes the degree to which the fluid behavior is non-Newtonian.

2.2 Flow Regimes

In order to estimate the associate pressure loss with the movement of any fluid, it is as important to know the type of the fluid as it is to know under what conditions that fluid is flowing. Flow regimes are commonly classified as laminar or turbulent. A laminar flow is characterized by the movement of fluid particles in cylindrical layers parallel to the pipe axis. These layers move at different velocities ranging from zero at the pipe wall, to maximum at the center. At higher velocities, when the particles break down into random flocculation and the flow becomes unstable, the flow is characterized as turbulent.

An average velocity at any given point, devined as the steady state flow rate per unit area at that point, has been adopted to represent the fluid velocity.[5, 10] This average velocity, $\bar{v}$, is defined as follows:

$$\text{For pipe flow: } \bar{v} = \frac{Q}{\frac{\pi}{4}D^2} \tag{2.4}$$

$$\text{For annular flow: } \bar{v} = \frac{Q}{\frac{\pi}{4}(D_2^2 - D_1^2)} \tag{2.5}$$

where Q is the volumetric flow rate.

One hundred years ago, Osborn Reynolds showed experimentally that the type of fluid flow regime depends not only on velocity, but more generally, on the dimensionless group, $\frac{\rho D\bar{v}}{\mu}$, which is known as the Reynolds number, N_R. He also showed that if N_R is about 2100 or less, the flow is laminar, and at higher N_R values, the flow is turbulent.

The viscosity term, μ, used in the Reynolds number depends on wheter the fluid is Newtonian or non-Newtonian. For a Newtonian fluid, the Reynolds number viscosity is the Newtonian viscosity defined by Equation 2.1. For a non-Newtonian fluid, a common criterion is to use an equivalent viscosity, μ_e, to define the Reynolds number viscosity term.[5, 10] This equivalent viscosity depends on the model used to describe the rheological behavior of the non-Newtonian fluid.

If the Bingham plastic model is used, the equivalent viscosity is defined as follows.[3, 9, 10]

$$\text{For pipe flow: } \mu_e = \mu_p + \tau_y \frac{g_c D}{6\bar{v}} \tag{2.6}$$

or

For annular flow: $$\mu_e = \mu_p + \tau_y \frac{g_c (D_2 - D_1)}{8\bar{v}} \qquad (2.7)$$

It should be noted that the above equivalent viscosity definitions are used only to define the flow regime. Another criterion based on the Hedstrom number, which is presented by Hanks,[19] is also used to define the Bingham plastic flow regime.

On the other hand, if the power law model is used to describe the fluid behavior, the equivalent viscosity is defined as follows.[5]

For pipe flow:

$$\mu_e = \frac{g_c \, k (\bar{v})^{n-1} \, 8^n}{8 \, D^{n-1}} \left(\frac{3n + 1}{4n}\right)^n \qquad (2.8)$$

or

For annular flow:

$$\mu_e = \frac{g_c \, k (\bar{v})^{n-1} \, 12^n}{12 (D_2 - D_1)^{n-1}} \left(\frac{2n + 1}{3n}\right)^n \qquad (2.9)$$

The above devinitions were derived from the generalized Reynolds number presented by Metzner and Reed.[26]

The diameter, D, used in the Reynolds number equation is the inside diameter for pipe flow and the equivalent diameter for annular flow. The definition of the equivalent diameter is presented in Chapter III.

CHAPTER III

FRICTIONAL PRESSURE LOSSES IN PIPES AND ANNULI

The purpose of this chapter is to present the mathematical correlations that can be used to predict the frictional pressure loss behavior of drilling fluids flowing in well annuli and choke lines.

3.1 Frictional Pressure Losses in Pipes

The mathematical definition used to describe the frictional pressure loss, due to the flow of a given type of fluid, depends upont the flow regime. Accordingly, pressure losses in pipes can be discussed as follows.

3.1.1 Laminar Flow-Pressure Losses in Pipes

When a Newtonian or non-Newtonian fluid is in laminar flow, the resultant frictional pressure loss is a result of the viscous shear produced by the slippage between fluid layers. The nature of this viscous force depends on the rheological properties of the fluid. However, as discussed in Chapter II, the definition of the rheological properties depends on the rheological model used to describe the fluid.

The Newtonian frictional pressure loss definition was developed independently by Hagen and Poiseuille. This definition is as follows:[5, 10]

$$\frac{\Delta p}{L} = \frac{32\ \mu \bar{v}}{g_c D^2} \tag{3.1}$$

where $\frac{p}{L}$ is the frictional pressure gradient.

The frictional pressure loss correlation which characterizes the Bingham plastic fluids was originally presented by Bingham, and can be written as[5, 10]

$$\frac{\Delta p}{L} = \frac{32\ \mu_p \bar{v}}{g_c D^2} + \frac{16\ \tau_y}{3D} \tag{3.2}$$

The final form of the frictional pressure loss correlation which characterizes the power law fluids was presented by Metzner and Reed[26] as

$$\frac{\Delta p}{L} = \frac{4k\ (8\bar{v})^n}{D^{1+n}} \left(\frac{3n + 1}{4n}\right) \tag{3.3}$$

3.1.2 Turbulent Flow-Pressure Losses in Pipes

Unfortunately, the nature and mechanism of the turbulent flow regime frictional pressure loss is not completely understood. Accordingly, its theoretical analysis is still not complete. However, the results of many experimental studies have been utilized by the aid of dimensional analysis techniques to develop an emperical friction factor correlation. One form of this correlation is the Fanning equation. The Fanning equation is in the following form:[5, 10, 27]

$$\frac{\Delta p}{L} = \frac{2f\ \rho(\bar{v})^2}{g_c D} \tag{3.4}$$

where

$$f = F(N_R,\ \varepsilon/D) \tag{3.5}$$

The dimensionless parameter, "f", is called the Fanning friction factor. As shown in Equation 3.5, this factor is afunction of the Reynolds number, N_R, and the relative pipe roughness, ε/D. The relative pipe roughness is the ratio between the absolute pipe roughness, ε, and the inside pipe diameter, D. The inside pipe surface is not smooth, and under turbulent flowing regimes could have a considerable effect on the frictional pressure losses. It has been shown that the effect of pipe roughness is not its absolute value, but rather its relative roughness.[6] The absolute roughness is defined as the equivalent roughness of tightly packed sand grains that would have the same pressure gradient as the actual pipe. Moody,[27] based on Nikuradse's famous sand-grain experiment, compared the pressure behavior of different common pipes with one that is sand-grained and presented values of pipe roughness. Cullender and Smith[12] and Smith et al.,[34] based on data obtained on clean steel pipes, sugested an average absolute roughness value of 0.00065 in.

The Fanning equation, as defined by Equation 3.4,

is a generalized formula that is applicable to all types of fluids (Newtonian or non-Newtonian) and all flow regimes (laminar or turbulent). However, estimation of the friction factor, f, depends upon both the type of fluid and the flow regime.

Nikurade's sand grain experiment formed the basis for most of the friction factor emperical correlations.[6, 27] VonKarman and Prandtle independently developed emperical correlations for the case of completely turbulent flow and for the case of perfectly smooth pipe.[14, 27] Colebrook presented a friction factor correlation for Newtonian fluids that gained widespread acceptance in the engineering industry.[5, 10, 27] The Colebrook function is in the following form.

$$\frac{1}{f^{\frac{1}{2}}} = -4 \log \left[\frac{1}{3.72}\frac{\varepsilon}{D} + \frac{1.225}{N_R f^{\frac{1}{2}}}\right] \qquad (3.6)$$

The friction factor, f, appears both inside and outside the log term of the Colebrook function, requiring an itterative solution technique. Computation can be shortened, however, by a graphical solution such as that shown in Figure 3.1, which is known as the Stanton Chart. Moody[27] developed a similar graphical solution in which the symbol, f, represents Moody's friction factor and is four times larger than the Fanning factor.

It should be remembered that the Reynolds number used in the Colebrook equation is slightly different

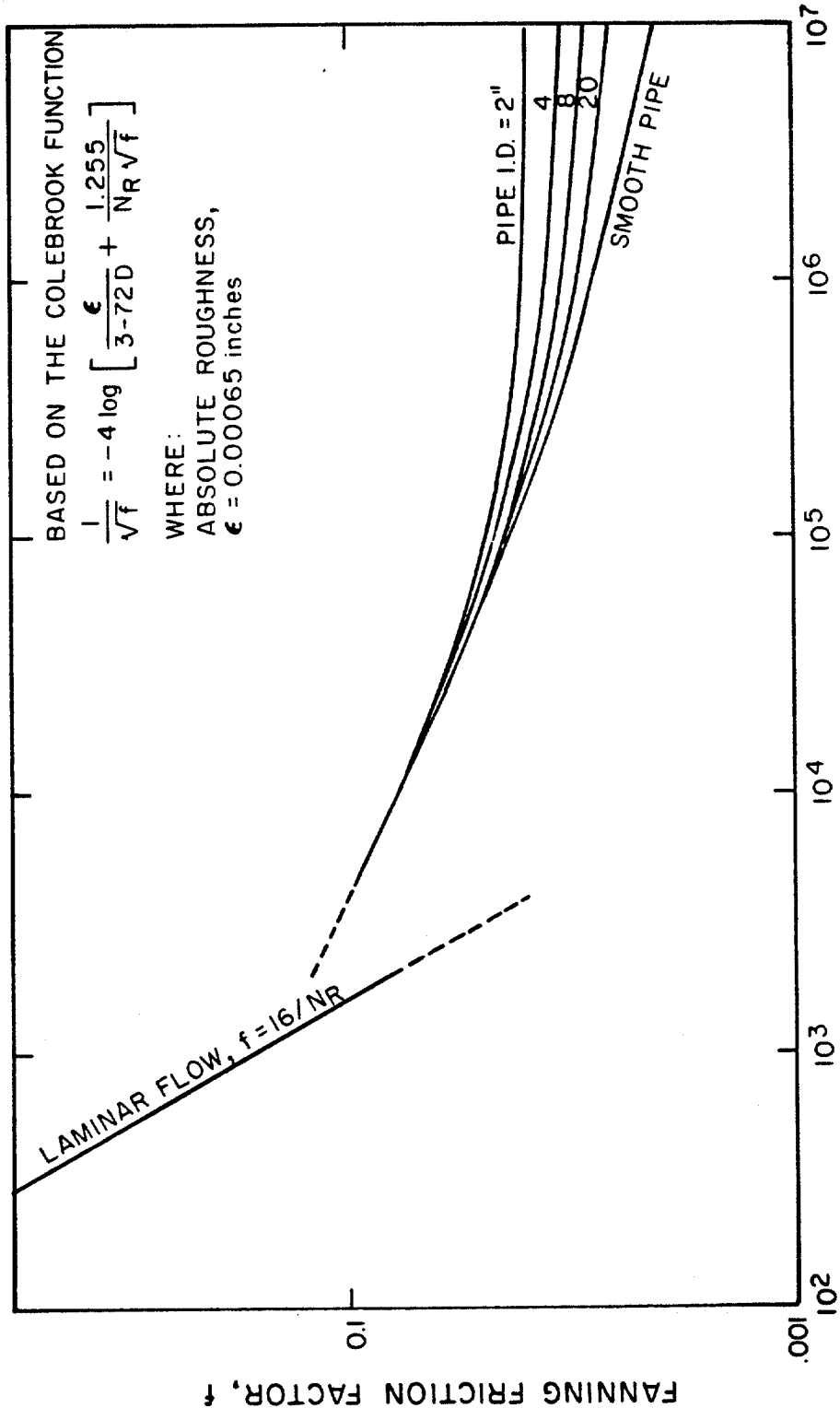

Figure 3.1 - Fanning Friction Factor for Newtonian Fluids[10]

than that used to evaluate the flow regime of non-Newtonian fluids.

For Bingham plastic fluids, Hedstrom[20] suggested that the Colebrook function can be used to estimate the corresponding friction factor if the Newtonian viscosity is replaced by the plastic viscosity in the Reynolds number equation. Accordingly, Reynolds number of this particular case can be written as:

$$N_R = \frac{\rho D\bar{v}}{\mu_p} \tag{3.7}$$

As a result of their experimental work, Dodge and Metzner, [14, 15] developed an emperical correlation to define the friction factor of the power law fluids. The correlation relates Fanning friction factor to the generalized Reynolds number and the flow behavior index, n. The Dodge and Metzner correlation is in the following form:

$$\frac{1}{f^{n/2}} = \frac{4}{n^{.75}} \log \left[N_{R_e} f^{1-n/2}\right] - \frac{0.4}{n^{1.2}} \tag{3.8}$$

where N_{Re} is the generalized Reynolds number defined by Metzner and Reed[26] as follows.

$$N_{R_e} = \frac{\rho D^n (\bar{v})^{2-n}}{g_c k 8^{n-1} (\frac{3n+1}{4n})^n} \tag{3.9}$$

Dodge and Metzner found that the Reynolds number

corresponding to the onset of turbulent flow increases with the flow behavior index. So they suggested that for any value of n, a critical Reynolds number above which the flow is turbulent is determined from the experimental chart shown in Figure 3.2. The critical number is then compared with the calculated Reynolds number using Equation 3.9. The Dodge and Metzner equation was developed for smooth pipes. However, this is not a severe limitation to its practical applicability.

3.2 Pressure Losses in Annuli

Basically the same discussion of frictional pressure losses in pipes applies to frictional pressure losses in annuli. In fact, pipe flow is considered as a limited case of annular flow. However, when the fluid flow is turbulent, the problem is slightly more complicated. Since no theoretical correlations are available to describe the frictional loss behavior in turbulent flow, the problem is choosing a diameter to describe the annular geometry. Fortunately, the relation between the friction factor and Reynolds number is practically independent on the shape of the cross section if the proper "equivalent diameter is used.[22]

3.2.1 Laminar Flow-Pressure Losses in Annuli

Lamb developed an analytical expression relating the Newtonian pressure losses to average fluid velocity as follows:[5, 10]

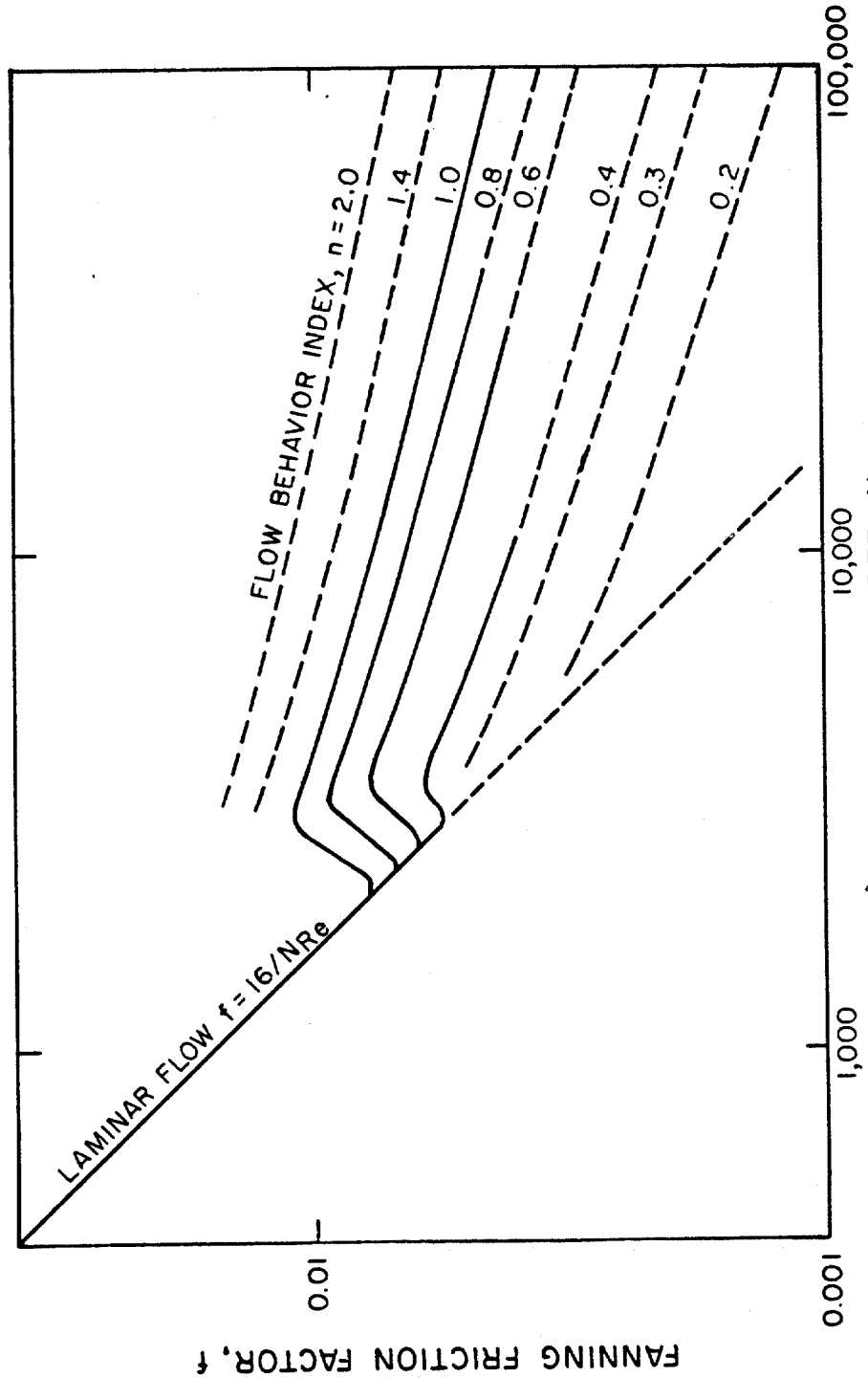

Figure 3.2 - Friction Factor Chart for Power Law Fluids
(After Dodge and Metzner)[14,15]

$$\frac{\Delta p}{L} = \frac{32 \mu \bar{v}}{g_c \left[D_2^2 + D_1^2 - \frac{D_2^2 - D_1^2}{\ln \frac{D_2}{D_1}} \right]} \tag{3.10}$$

Another correlation which describes the annular laminar flow of a Newtonian fluid is the rectangular slot equation.[10]

$$\frac{\Delta p}{L} = \frac{48 \mu \bar{v}}{g_c (D_2 - D_1)^2} \tag{3.11}$$

Analytical models for Bingham plastic fluids were developed by Larid[24] and by Fredrickson and Bird.[17] The complexity of these models, however, limited their practical application. Melrose et al.[25] suggested that a narrow slot approximation can be used to describe the flowing pressure losses for annular flow. This equation is as follows:

$$\frac{\Delta p}{L} = \frac{48 \mu_p \bar{v}}{g_c (D_2 - D_1)^2} + \frac{6 \tau_y}{(D_2 - D_1)} \tag{3.12}$$

The power law fluids correlation was derived analytically by Fredrickson and Bird.[17] Again, the complexity of their correlation limited its practical utility. Savis[32] presented a simplified correlation based on the slot flow equation in the following form.

$$\frac{\Delta p}{L} = \frac{4\ k(12\bar{v})^n}{(D_2 - D_1)^{1+n}} \left(\frac{2n + 1}{3n}\right)^n \qquad (3.13)$$

3.2.2 Turbulent Flow-Pressure Losses in Annuli

Annular pressure losses for turbulent flow can be approximated by the corresponding pipe flow correlations, (Section 3.1.2) if a proper equivalent diameter is used instead of the pipe diameter.

The equivalent diameter, D_e, is defined as a fictitious pipe diameter whose pressure loss-flow rate behavior duplicates that of a particular annulus. Four criteria are commonly used to define D_e as a function of the outer diameter of the inner pipe, D_1, and the inner diameter of the outer pipe, D_2. These criteria are as follows.

1. Hydraulic Radius Criterion[5, 10, 22, 27]

$$D_e = D_2 - D_1 \qquad (3.14)$$

2. Geometry Term Criterion[5]

$$D_e = \left[D_2^2 + D_1^2 - \frac{D_2^2 - D_1^2}{\ln \frac{D_2}{D_2}}\right]^{\frac{1}{2}} \qquad (3.15)$$

3. Slot Flow Criterion[5, 10]

$$D_e = 0.816\ (D_2 - D_1) \qquad (3.16)$$

4. Crittendon Emperical Criterion[11]

$$D_e = \frac{1}{2}[D_2^4 - D_1^4 - \frac{(D_2^2 - D_1^2)^2}{\ln \frac{D_2}{D_1}}]^{\frac{1}{4}} + \frac{1}{2}[D_2^2 - D_1^2]^{\frac{1}{2}} \quad (3.17)$$

It should be noted that when using the Crittendon Criterion, the average annular velocity is computed as follows.

$$\bar{v} = \frac{Q}{\frac{\pi}{4} D_e^2} \quad (3.18)$$

3.3 The Transition Flow Regime

For practical reasons it is usually assumed that the Reynolds number of 2100 is a critical value which distinguishes between laminar and turbulent flow regimes. Actually, the flow pattern does not change suddenly from laminar to turbulent at a particular Reynolds number; a transition region takes place between Reynolds numbers of about 2000 and 4000. During the transition region, neither the laminar nor the turbulent flow equations can be used to accurately predict the corresponding pressure losses. Also, the use of a Reynolds number of 2100 as a criterion for changing from the laminar flow equations to the turbulent flow equations causes a discontinuity in the relationship between pressure loss and average flow velocity. One way to avoid this discontinuity is to assume that the flow pattern deviates from laminar,

when laminar and turbulent equations yield the same value of pressure loss. Then, pressure loss, using both laminar and turbulent flow equations, is computed and the higher result is considered.

3.4 Non-Isothermal Flow

It is a well known phenomena that fluid properties change with temperature. During drilling operations, temperature changes with depth. Accordingly, fluid properties change with depth. Annis[1] and Bartlett[2] studied the effect of circulating temperature on the flow properties of drilling fluids. They concluded that, because fluid properties at surface conditions are different from those at conditions prevailing in the hole, surface fluid properties are not recommended when determining flow conditions at other elevated temperatures.

If the flowing temperature profile in a given system is known, the fluid properties at any point can be easily obtained. Practically, it is not possible to obtain a temperature profile during drilling operations. Hence, a mathematical correlation could be used of such temperature profiles are needed. In general, flowing fluid temperature is a function of circulating rate, overall heat transfer coefficient, formation temperature , pipe size, and fluid properties. Holmes and Swift[21] presented a practical solution to obtain drilling

fluid temperature profiles during circulation. Their model is a solution of the steady-state equation for heat transfer between the fluid and the formation. The correlation of Holmes and Swift is in the following mathematical form.

$$T_a = k_1 C_3 e^{Lc1} + k_2 C_4 e^{Lc1} + GL + T_s \tag{3.19}$$

and

$$T_b = k_1 e^{Lc1} + k_2 e^{Lc2} + GL + T_s - AG \tag{3.20}$$

where

$$A = mC_p/2\pi r_p h_p \tag{3.21}$$

$$B = r\mu/r_p h_p \tag{3.22}$$

$$C_1 = \frac{B}{2A}\left[1 + (1 + \frac{4}{B})^{\frac{1}{2}}\right] \tag{3.23}$$

$$C_2 = \frac{B}{2A}\left[1 - (1 + \frac{4}{B})^{\frac{1}{2}}\right] \tag{3.24}$$

$$C_3 = 1 + \frac{B}{2}\left[1 + (1 + \frac{4}{B})^{\frac{1}{2}}\right] \tag{3.25}$$

$$C_4 = 1 + \frac{B}{2}\left[1 - (1 + \frac{4}{B})^{\frac{1}{2}}\right] \tag{3.26}$$

$$k_1 = T_p - k_2 - T_s + AG \tag{3.27}$$

$$k_2 = \frac{AG - (T_p - T_s + AG)e^{HC1}(1 - C_3)}{e^{HC2}(1 - C_4) - e^{HC1}(1 - C_3)} \tag{3.28}$$

Two temperature profiles based on this correlation are shown in Figure 5.6. A computer program[8] which describes the Holmes and Swift correlation is shown as part of Appendix B.

A laboratory study on the effect of temperature on properties of three different clay-water muds showed that surface mud properties could be used as an average fluid property when drilling at relatively moderate depths. The result of this limited study conducted by the author is shown in Figures 5.7, 5.8 and 5.9.

CHAPTER IV

FLOW OF GAS-LIQUID MIXTURES IN VERTICAL PIPES

Pressure losses encountered in choke lines, as a result of the flow of formation gas and non-Newtonian drilling fluid mixtures, should be mathematically predictable. Unfortunately, such mathematical models are not available. However, many emperical correlations are available to analyze the two-phase flow of gas and Newtonian fluid mixtures. An attempt will be made to utilize such correlations to study the pressure behavior of gas and non-Newtonian drilling fluid mixtures. Before this step can be taken, however, it is essential to understand these two-phase correlations and their related variables and assumptions. The object of this chapter is to present the basic procedure to estimate the different properties that influence the two-phase flow problem and to briefly introduce some of those widely recognized vertical two-phase correlations. However, since most drilling fluids are water base and since the drilling fluids used in the experimental work of this research are water base, only gas-water two-phase flow will be considered in this discussion.

4.1 Fluid Properties

This section will briefly introduce the procedures

used to estimate the important liquid and gas properties and how they are related to the mixture properties. For more information about this subject the reader is referred to references 6, 7 and 23.

4.1.1 Liquid and Gas Hold Ups

Liquid and gas hold ups are the terms that relate liquid and gas properties to their mixture properties. Liquid hold up is a fraction of the total fluid in a pipe element, which varies from zero, for gas flow, to one, for liquid flow. It is defined as follows:

$$H_L = \frac{\text{Volume of liquid in pipe element}}{\text{Volume of pipe element}} \qquad (4.1)$$

Accordingly, gas hold up is defined as follows:

$$H_g = 1 - H_L \qquad (4.2)$$

Another term which is sometimes used is the no-slip hold up. It is defined as the ratio of the volume of liquid in a pipe element divided by the volume of the pipe element at zero slip velocity, or simply:

$$\lambda_L = \frac{q_L}{q_g + q_L} \qquad (4.3)$$

and

$$\lambda_g = 1 - \lambda_L$$

where the above terms are defined as follows:

H_g = gas hold up, fraction

H_L = liquid hold up, fraction

λ_g = no-slip gas hold up, fraction

λ_L = no-slip liquid hold up, fraction

q_g = in situ gas flow rate

q_L = in situ liquid flow rate

4.1.2 Velocity

Many two-phase flow correlations are based on a term called superficial velocity. The superficial velocity of a fluid is defined as the fluid velocity if it flows through the total cross sectional area of the pipe alone.[6] Accordingly,

$$V_{sg} = \frac{q_g}{A} \tag{4.4}$$

$$V_{sL} = \frac{q_L}{A} \tag{4.5}$$

$$V_m = \frac{q_{g+L}}{A} = V_{sg} + V_{sL} \tag{4.6}$$

where

V_{sg} = superficial gas velocity

Vs_L = superficial liquid velocity

V_m = superficial gas-liquid mixture velocity

q_g = gas flow rate

q_L = liquid flow rate

q_{g+L} = gas-liquid flow rate

A = cross-sectional area

$$\rho_L = \frac{350.4\ \gamma_L + 0.0764\ \gamma_g\ R}{5.615\ B_L} \tag{4.11}$$

The gas-liquid mixture density is calculated as follows:

$$\rho_m = \rho_L H_L + \rho_g H_g \tag{4.12}$$

or

$$\rho_m = \rho_L \lambda_L + \rho_g \lambda_g \tag{4.13}$$

or

$$\rho_m = \frac{\rho_L \lambda^2_L}{H_L} + \frac{\rho_g \lambda^2_g}{H_g} \tag{4.14}$$

Brill and Beggs[6] stated that Equation 4.12 is commonly used to determine the pressure gradient due to elevation changes, Equation 4.13 for no-slip two-phase flow correlations, and Equation 4.14 to define the mixture density used in the friction loss term and Reynolds number.

The variables used in the previous equations are defined as follows:

ρ_g = gas density, lbm/ft^3

P = pressure, psia

γ_g = gas gravity (air = 1.0)

Z = compressibility factor

T = absolute temperature, °R

ρ_L = liquid density, lbm/ft^3

γ_L = liquid gravity (water = 1.0)

R = dissolved gas-liquid ratio, SCF/STB

B_L = liquid formation volume factor, bbl/STB

ρ_m = gas-liquid mixture density, lbm/ft^3

4.1.4 Viscosity

Viscosity is another important property that affects the problem of gas-liquid flow in pipes. It is a control factor in the frictional pressure losses. Liquid viscous properties were discussed in detail in Chapter II. The gas viscosity is commonly calculated rather than measured. The two most widely used correlations to calculate the gas viscosity are those of Carr et al. and Lee et al. as recommended by Brown[7] and Brill and Beggs.[6] The Lee correlation is in the following form:

$$\mu_g = k \times 10^{-4} \, e^{X\rho_g^{\,y}} \tag{4.15}$$

$$k = \frac{(9.4 + 0.02\,M)T^{1.5}}{209 + 19M + T} \tag{4.16}$$

$$X = 3.5 + \frac{986}{T} + 0.01M \tag{4.17}$$

$$y = 2.4 = 0.2X \tag{4.18}$$

where

μ_g = gas viscosity, cp

ρ_g = gas density, gm/cc

M = molecular weight

T = absolute temperature, °R

The effect of the gas and liquid viscosities on the gas-liquid mixture viscosity is still not clear. Accordingly, the viscosity of the mixture still cannot be accurately predicted. One common method to determine mixture viscosity is to take an arithmetical average as shown below:

$$\mu_m = \mu_L H_L + \mu_g H_g \tag{4.19}$$

or

$$\mu_m = \mu_L \lambda_L + \mu_L \lambda_L \tag{4.20}$$

where Equation 4.20 defines the no-slip velocity. Brown[7] reported that the emperical correlation proposed by Arrhenius yields better results. The Arrhenius correlation is in the following form:

$$\mu_m = \mu_L^{H_L} \times \mu_g^{H_g} \tag{4.21}$$

4.1.5 Surface Tension

The influence of surface tension in gas-liquid flow problems is still not completely understood. Katz et al.[23] presented a combined chart of the gas-water surface tension based on emperical data of different investigators. The Katz diagram is commonly used to estimate a gas-water surface tension.

4.1.6 Gas Solubility

Gas is slightly soluble in water. Moreover, gas solubility in water decreases with the increas of gas molecular weight and the water salinity. In general, gas solubility in water ranges between 5 and 20 SCF/bbl.

4.1.7 Water Compressibility

For all practical purposes, water can be assumed completely incompressible. Hence, the change in water volume with pressure is neglected. However, many different correlations are available to estimabe the water compressibility.[6, 23]

4.1.8 Gas Compressibility Factor

The gas compressibility factor, z, is commonly obtained from the pseudo-reduced pressure and temperature chart. However, many different mathematical methods are available that can be used to estimate the gas compressibility factor. A list of these methods can be found in reference 6.

4.2 Flow of Gas-Liqiud Mixture in Vertical Pipes

The general energy equation is the basis of almost all the work done to solve the problem of fluid flow in pipes. The general energy equation expresses an energy balance between two points in a fluid flow system. It follows the law of conservation of energy, which states that the total energy input per unit time must equal

the total energy output. Assuming no work is done on or by the fluid, this equation can be written in the following simple pressure gradient form.

$$\left(\frac{dP}{dL}\right)_{total} = \left(\frac{dP}{dL}\right)_{elev} + \left(\frac{dP}{dL}\right)_{f} + \left(\frac{dP}{dL}\right)_{acc} \qquad (4.22)$$

The general energy equation in its pressure gradient form, Equation 4.22, indicates that the pressure gradient of the flow of fluids in vertical pipes, is the sum of the elevation pressure gradient, frictional pressure gradient, and acceleration pressure gradient.

As discussed in Chapter III, the frictional pressure loss of the fluids is commonly estimated from Fanning or Moody friction factor correlations. Accordingly, the frictional pressure gradient term could be defined as follows.

$$\left(\frac{dP}{dL}\right)_{f} = \frac{2\ f\rho v^2}{g_c D}, \text{ Fanning} \qquad (4.23)$$

or

$$\left(\frac{dP}{dL}\right)_{f} = \frac{f\rho v^2}{2g_c D}, \text{ Moody} \qquad (4.24)$$

Where the Moody friction factor is four times greater than that of Fanning.

The procedures used by most investigators to calculate the gas-liquid two-phase frictional pressure losses is basically the same as that which applies to

the single phase flow procedures, which were discussed in Chapter III. One major difference is that the gas-liquid mixture properties are to be used rather than the fluid properties. Accordingly, the Reynolds number can be re-defined as:

$$N_{R_m} = \frac{\rho_m D v_m}{\mu_m} \tag{4.25}$$

where the subscript, m, denotes the mixture properties. However, some investigators used their own correlating parameters to determine an energy loss factor.

The potential or elevation energy is related to the fluid density. It is also called hydrostatic energy, since it is the only energy component which would apply at conditions of no flow. Hydrostatic energy is a predominant term in vertical fluid flow. The elevation gradient is defined as follows.

$$\left(\frac{dP}{dL}\right)_{elev} = \frac{g}{g_c} \rho_m \tag{4.26}$$

The acceleration or kinetic energy is the energy that results from the change in the fluid velocity. The acceleration energy is usually small compared with the potential or the frictional energy in the flow of vertical pipes of constant diameters. The acceleration gradient is defined as follows:

$$\left(\frac{dP}{dL}\right)_{acc} = \frac{\rho_m v_m}{g_c} \frac{dv_m}{dL} \tag{4.27}$$

Accordingly, for any gas-liquid mixture flowing in a vertical pipe, the total pressure gradient can be defined as follows:

$$\left(\frac{dP}{dL}\right)_{total} = \frac{g}{g_c}\rho_m + \frac{2f_m\rho_m v_m^2}{g_c D} + \frac{\rho_m v_m dv_m}{g_c dL} \qquad (4.28)$$

where the frictional term is represented by the Fanning equation and D is the inside pipe diameter. Other variables are as previously defined.

Many emperical solutions are available to solve the problem of gas-liquid two-phase flow in vertical pipes. The remainder of this section wil introduce briefly some of those correlations which have gained wide recognition in dealing with the problem of two-phase flow. These correlations include those of Poettmann and Carpenter,[30] Hagedorn and Brown,[18] Orkiszewski,[29] and Beggs and Brill.[4]

As reported by Brill and Beggs,[6] the two-phase flow correlations can be classified into three main categories: a) correlations of no slip and no flow pattern consideration, b) correlations of slip consideration, but no flow pattern consideration, and c) correlations of slip and flow pattern consideration.

4.2.1 Correlations of No Slip and No Flow Pattern Consideration

Correlations of this category assume that the gas

and liquid flow at the same velocity and that the type of the flow pattern has no effect in the calculation of the pressure gradient. Methods of this category require correlations for friction factor only. One example of this category is the Poettmann and Carpenter correlation.

Poettmann and Carpenter[30] developed a Semi-emperical two-phase flow correlation. They simply related Fanning friction factor to the numerator of the Reynolds number for the fluid mixture, Figure 4.1. Their correlation ignores the acceleration term, the flow pattern and the fluid hold up. The correlation also assumes that frictional loss factor can be represented by an average value over the entire length of the pipe. The Poettmann and Carpenter correlation is in the following form:

$$\frac{dP}{dL} = \frac{1}{144}\left[\frac{g}{g_c}\rho_m + \frac{f_m w^2}{7.413 \times 10^{10} \rho_m D^5}\right] \tag{4.29}$$

$$\rho D v = 1.4737 \times 10^{-5} \frac{w}{D} \tag{4.30}$$

where

$\frac{dP}{dL}$ = total pressure gradient, psi/ft

ρ_m = no-slip density of mixture (Eq. 4.13), lbm/ft^3

w = mass flow rate of mixture, lbm/day

D = inside diameter of pipe, ft

f_m = Fanning friction factor of mixture

ρvD = the numerator of the Reynolds number

The mixture Fanning friction factor, f_m, can be obtained from the friction factor chart presented by Poettmann and Carpenter[30] as shown in Figure 4.1.

4.2.2 Correlations of Slip, But No Flow Pattern Consideration

Correlations of this category consider the slip velocity, but neglect the effect of different types of flow patterns. These correlations require methods to estimate fluid hold up and friction factor. An example of this category is the Hagedorn and Brown correlation.

Hagedorn and Brown[18] devleoped an emperical correlation from data obtained from a 1,500 feet experimental well. An average mixture density was used for calculating pressure losses caused by friction and acceleration. Liquid hold up was not measured, but was back calculated based on pressure loss data. The Hagedorn and Brown correlation is in the following form:

$$\frac{dP}{dL} = \frac{1}{144}\left[\frac{g}{g_c}\rho_m + \frac{f_m w^2}{7.413 \times 10^{10} \rho_m D^5} + \rho_m \frac{v_m^2}{2g_c dL}\right] \quad (4.31)$$

where ρ_m and v_m are as defined by Equations 4.12 and

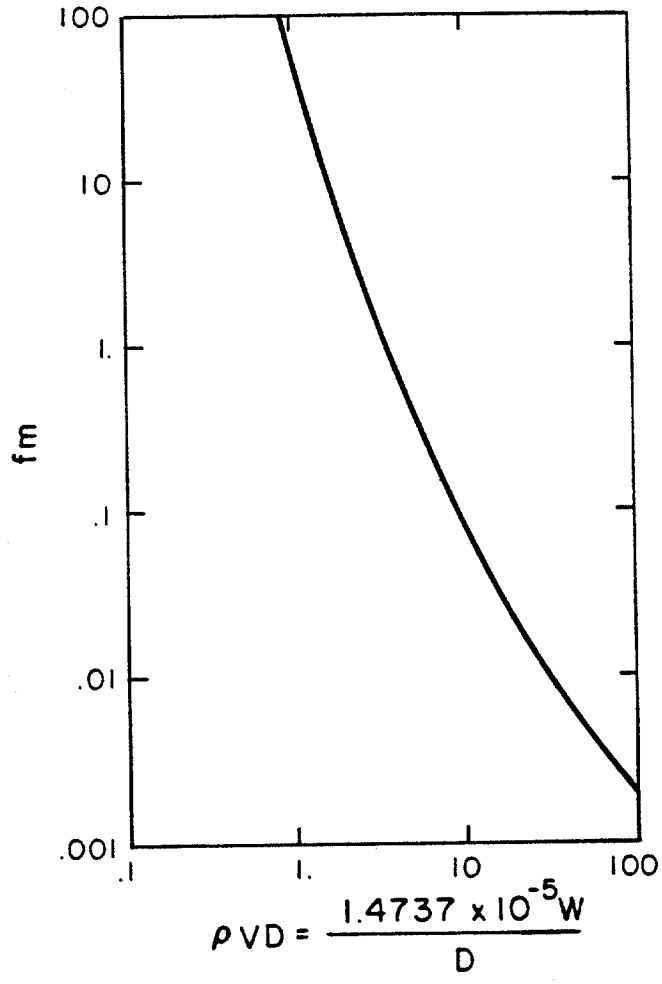

Figure 4.1 - Two-Phase Flow Fanning Friction Factor As Obtained by Poettmann and Carpenter[30]

4.6 respectively. The friction factor in the above equation is represented by the Fanning friction factor. The Fanning friction factor is determined using the gas-liquid mixture Reynolds number, N_{R_m}, defined by Equation 4.25, where ρ_m, v_m and μ_m are as defined by Equations 4.13, 4.6 and 4.21 respectively. Note that the density term used in Equation 4.31 is slightly different from that used in calculating Reynolds number. In calculating Reynolds number, the no-lsip density is used. Using methods similar to that of Ros,[31] Hagedorn and Brown showed that the liquid hold up, H_L, is related to the following four dimensionless groups.

$$N_{Lv} = 1.938\ v_{sL}\left(\frac{\rho_L}{\zeta_L}\right)^{1/4} \tag{4.32}$$

$$N_{gv} = 1.938\ v_{sg}\left(\frac{\rho_L}{\zeta_L}\right)^{1/4} \tag{4.33}$$

$$N_d = 120.872\ D\left(\frac{\rho_L}{\zeta_L}\right)^{1/2} \tag{4.34}$$

$$N_L = 0.15762\ \mu_L\left(\frac{1}{\rho_L \zeta_L^3}\right)^{1/4} \tag{4.35}$$

where

N_{Lv} = liquid velocity number

N_{gv} = gas velocity number

N_d = pipe diameter number

N_L = liquid viscosity number

V_{sL} = superficial liquid velocity (Eq. 4.5), ft/sec

V_{sg} = superficial gas velocity (Eq. 4.4), ft/sec

ρ_L = liquid density, lbm/ft^3

ζ_L = surface tension, dyne/cm

μ_L = liquid viscosity, cp

D = pipe diameter, ft

Hagedorn and Brown used a regression analysis technique to relate the four dimensionless groups and the pressure term. Their hold up correlation is shown in Figure 4.2. The term, C_{N_L}, was introduced to account for the viscosity of the liquid. C_{N_L} is obtained from a plot of N_L vs. C_{N_L} as the one shown in Figure 4.3. An additional factor was needed in the hold up correlation. The determination of this secondary correction factor, Ψ, is shown in Figure 4.4.

4.2.3 Correlations of Slip and Flow Pattern Consideration

Correlations of this category are the most general correlations. They consider the slip velocity as well as the different effect of different flow patterns. Accordingly, these correlations require methods to define the fluid hold up, friction factor and acceleration term which are all dependent upon the flow pattern. The most common flow patterns encountered in vertical two-phase flow, as described by Orkiszewski,[29] are bubble, slug, transition and mist flow. These four patterns are shown in Figure 4.5. Examples of correlations that can be listed under this category are that of Orkiszewski[29]

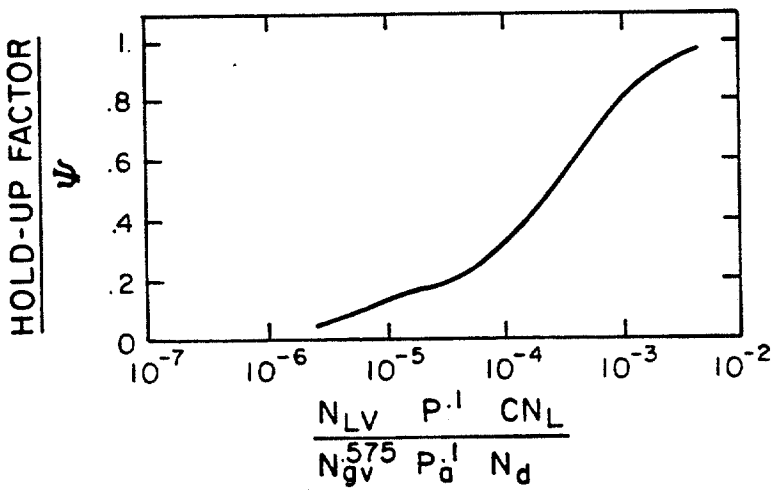

Figure 4.2 - Hold Up Factor Correlation[18]

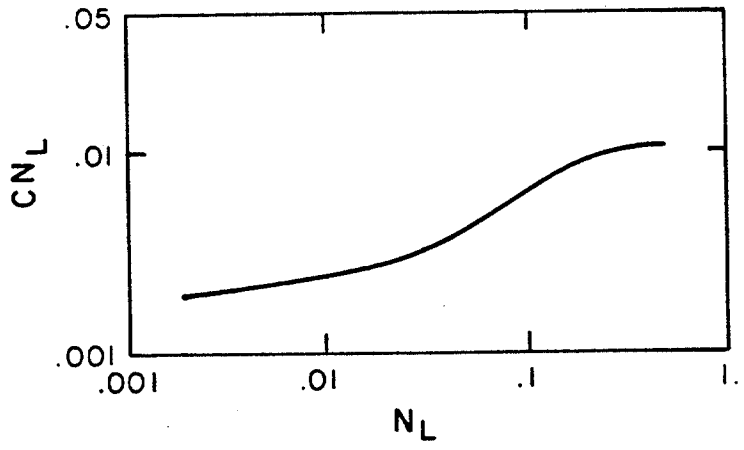

Figure 4.3 - Correlation For Viscosity Number Coefficient[18]

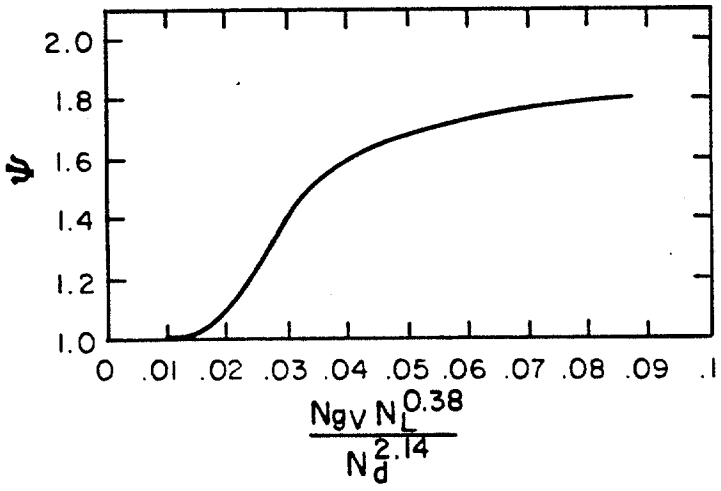

Figure 4.4 - Correlation For Secondary Correction Factor[18]

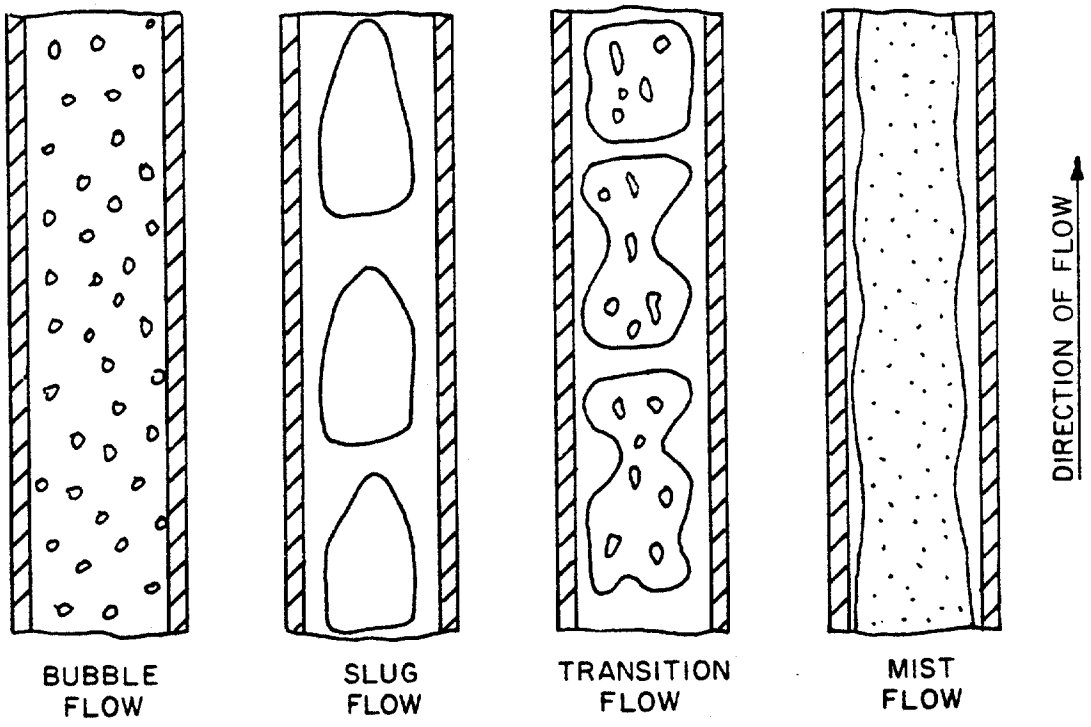

Figure 4.5 - Common Gas-Liquid Flow Patterns In Vertical Pipe Flow[29]

and Beggs and Brill.[4]

Orkiszewski[29] combined the work of several other investigators with some field data and proposed a composite correlation.

For the bubble flow pattern where $\frac{vsg}{vm} < L_B$ with the limit $L_B \geq 0.13$, he proposed the following equations.

$$L_B = 1.071 - \frac{.2218\ v_m^2}{D} \tag{4.36}$$

$$H_L = 1 - \frac{1}{2}[1 + \frac{v_m}{v_s} - (1 + \frac{v_m}{v_s})^2 - \frac{4v_{sg}}{.8})^{\frac{1}{2}}] \tag{4.37}$$

$$(\frac{dP}{dL})_f = \frac{2\ f\ \rho_L (v_{sL}/H_L)^2}{g_c\ D} \tag{4.38}$$

$$N_{R_m} = \frac{\rho_L\ D\ v_{sL}}{H_L \mu_L} \tag{4.39}$$

The acceleration term is negligible in the bubble flow.

For the slug flow pattern, where $\frac{Vsg}{Vm} > L_B$ and $N_{gv} < L_s$, Orkiszewski proposed the following equations:

$$\rho_m = \frac{\rho_L (v_{sL} + v_b) + \rho_g v_{sg}}{v_m + v_b} + \rho_L \zeta \tag{4.40}$$

$$v_b = C_1 C_2 (g\ D)^{\frac{1}{2}} \tag{4.41}$$

$$(\frac{dP}{dL})_f = \frac{2f\ \rho_L\ v_m^2}{g_c D}\ [\frac{v_{sL} + v_b}{v_m + v_b} + \delta] \tag{4.42}$$

where:

$$L_s = 50 + 36\ N_{Lv} \tag{4.43}$$

$$L_m = 75 + 84\ N_{Lv}^{.75} \tag{4.44}$$

$$N_{Rm} = \frac{\rho_L\ D\ v_m}{\mu_L} \tag{4.45}$$

$$\delta = \frac{.013 \log \mu_L}{D^{1.38}} - .681 + .232 \log v_m - .428 \log D \tag{4.46}$$

$$\delta = \frac{.045 \log \mu_L}{D^{.799}} - .709 - .162 \log v_m - .888 \log D \tag{4.47}$$

For $v_m < 10$, δ is calculated from Equation 4.46 with the limit $\delta \geq -.065\ v_m$. For $v_m > 10$, δ is calculated from Equation 4.47 with the limit

$$\delta \geq \frac{-v_b}{v_m + v_b}\left(1 - \frac{\rho_s}{\rho_L}\right)$$

where v_m is ft/sec.

The acceleration term is negligible in the slug flow pattern. C_1 and C_2 are given in Figures 4.6 and 4.7, respectively. For other values of C_1 and C_2 the reader is referred to the original work of Orkiszweski.[29] Other variables are as defined previously in this chapter.

For the transition flow pattern, where $L_m > N_{gv} > L_s$,

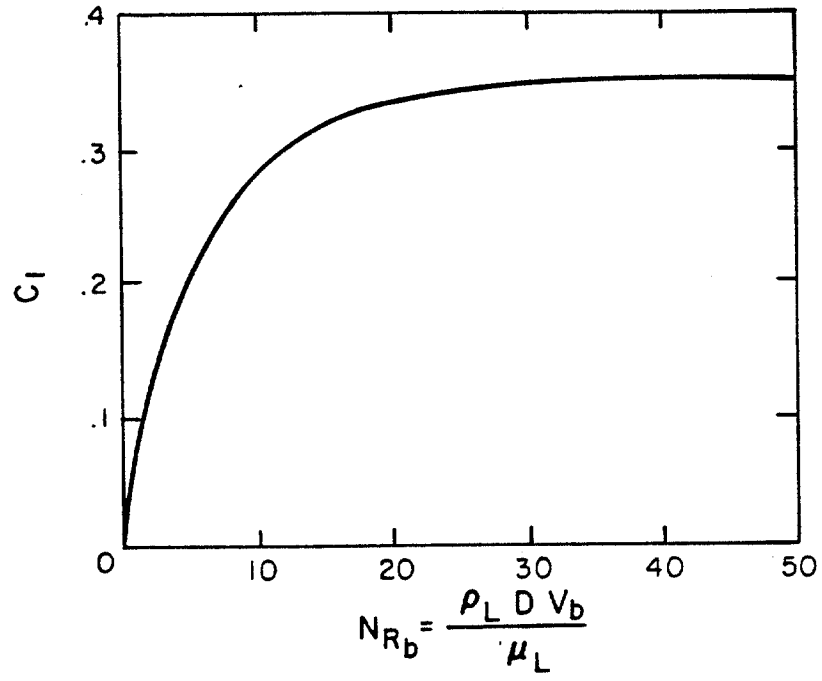

Figure 4.6 - C_1 vs. Bubble Reynolds Number[29]

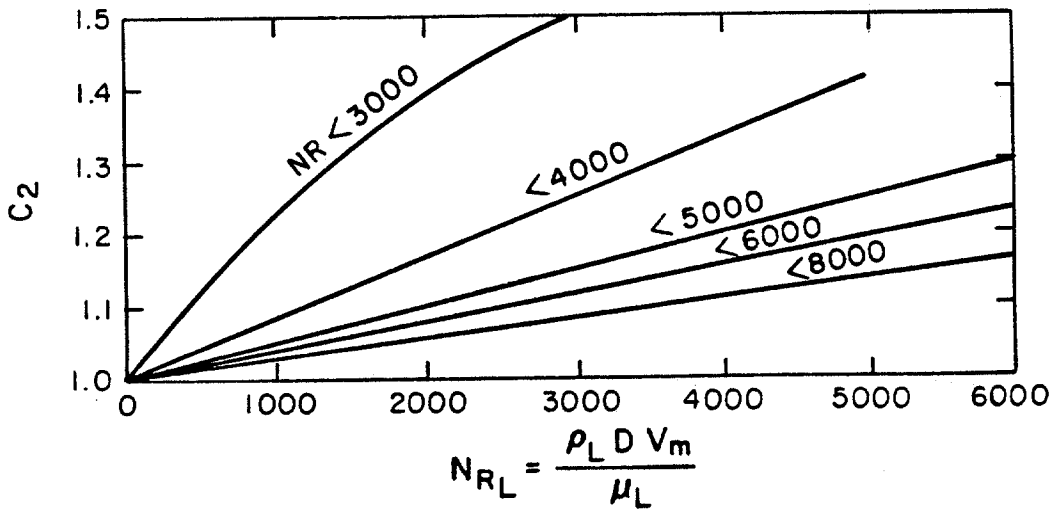

Figure 4.7 - C_2 vs. Liquid Reynolds Number[29]

and the mist flow, where $N_{gv} > L_m$, the pressure gradient is estimated using procedures suggested by Duns and Ros. These procedures are fully described in references 6 and 7.

Beggs and Brill[4] published an emperical correlation to compute pressure drops occuring during the flow of gas and liquid mixtures in pipes. Their correlation was originally developed using air-water mixtures flowing in pipes with different angles. The liquid hold up, which would exist if the pipe were horizontal, is first calculated and then corrected for the actual pipe inclination angle. They also defined a two-phase friction factor using equations which are independent of flow pattern, but depend on liquid hold up. For the full discussion of the Beggs and Brill correlation, the reader is referred to references 4, 6 and 7.

A computer program which describes the two-phase flow of nitrogen gas and non-Newtonian drilling fluid mixtures in pipes is shown in Appendix B. The two-phase flow subroutines used in this program were originally developed by Brill and Beggs.[6] The program was designed to include the following:

1) properties of the nitrogen gas.
2) solids content of drilling fluid.
3) the Bingham plastic rheological model and the Colebrook friction factor equation (Chapters II and III).

4) the power law rheological model and the Dodge and Metzner friction factor equation (Chapters II and III).

5) Holmes and Swift temperature correlations (Section 3.4).

6) The two-phase flow correlations previously described in this chapter.

CHAPTER V

EXPERIMENTAL MODEL AND PROCEDURE

The Petroleum Engineering Department of Louisiana State University operates two 6000 foot research and training well facilities. One was completed in 1971 and is used to simulate well-control operations for land rigs and bottom supported marine rigs. The other was completed in 1981 and is used to simulate well-control operations on floating drilling vessels in deep water. The new research and training facility, which is described in the next section, was utilized to conduct all the experimental phases of this study.

5.1 LSU New Research and Training Facility

A well-research facility was constructed and formally dedicated at Louisiana State University (LSU) by the Department of Petroleum Engineering on November 2, 1981. The facility is used to simulate well-control operations on a floating drilling vessel in deep water. Figure 5.1 shows a surface layout of this facility. The main features of this facility include: (1) a 6,000 foot well, (2) a choke manifold containing four 15,000 psi adjustable drilling chokes of varying design, (3) a 250 hp triplex pump and two 40 hp centrifugal pumps, (4) two mud tanks and a metering tank, (5) 10 hp air

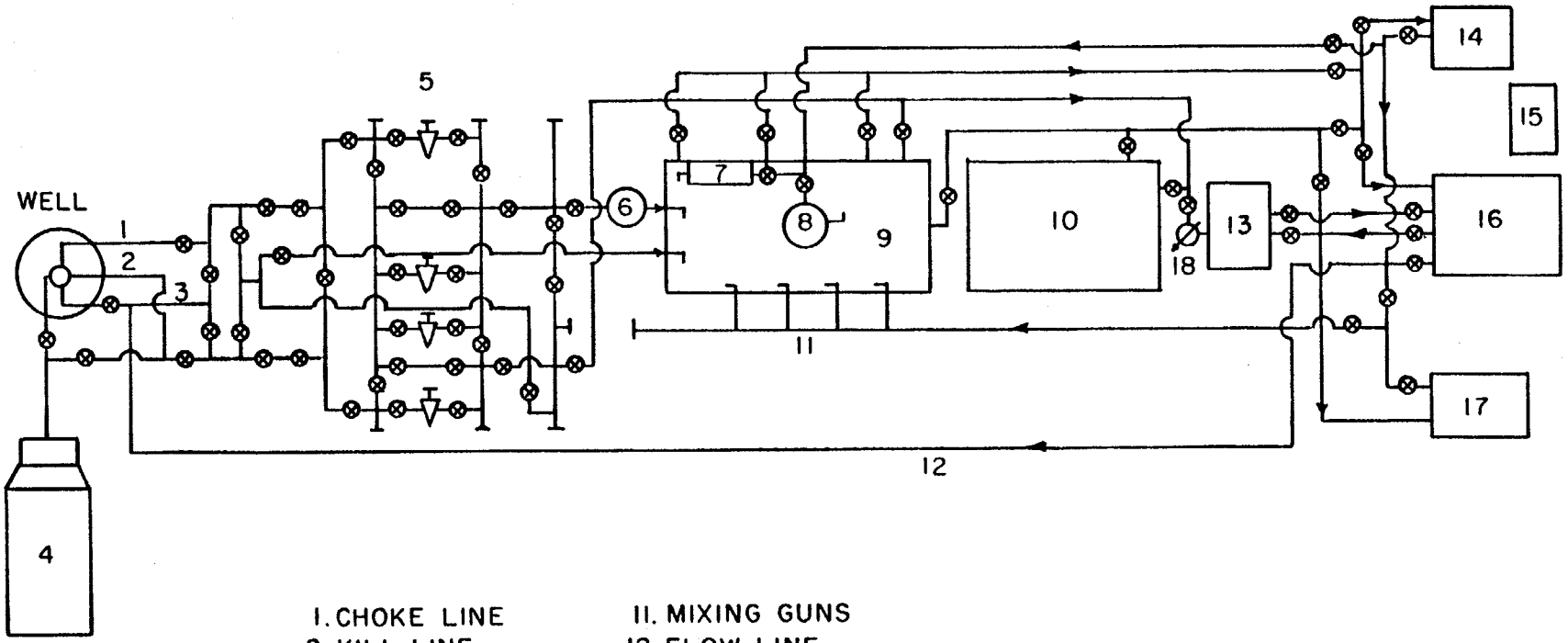

1. CHOKE LINE
2. KILL LINE
3. DRILL PIPE
4. NITROGEN UNIT
5. CHOKE MANIFOLD
6. GAS SEPARATOR
7. DEGASSING UNIT
8. MUD HOOPER
9., 10. MUD TANKS
11. MIXING GUNS
12. FLOW LINE
13. METER TANK
14. CENTRIFUGAL PUMP
15. AIR COMPRESSOR
16. TRIPLEX PUMP
17. CENTRIFUGAL PUMP
18. FLOW METER

Figure 5.1 - Surface Layout of LSU Research and Training Well Facility

compressor, (6) a mud-gas separator, (7) three mud degassers, (8) a mud mixing system, and (9) an instrumentation and control house.

As shown in Figure 5.2, the subsurface configuration of tubular members in the well was chosen so that the well would exhibit the same hydraulic behavior as a well drilled in 3,000 feet of water. The effect of the blowout preventor stack located on the seafloor is modeled in the well using a packer and triple parallel flow tube. Subsea choke and kill lines connecting the simulated BOP to the surface are modeled using two 2-3/8 inch tubings. The subsea kill line valve at 3,000 ft. is modeled using a surface-control subsurface safety valve. This control allows experiments to be conducted using only the choke line. The kill line can be isolated from the system as is often the case in well-control operations on floating drilling vessels. The drill pipe is simulated using 6,000 ft. of 2-7/8 in. tubing. Nitrogen gas is injected into the bottom of the well through a 1.315 in. tubing inserted inside the 2-7/8 in. pipe. A check valve located at the bottom of the nitrogen injection line allows the line to be isolated from the system after inducing the gas kick in the well. A pressure sensor system designed by Sperry-Sun is located at the bottom of the drill string to allow continuous surface monitoring of bottom-hole pressure. The pressure signal is transmitted to the surface through 6000 feet of

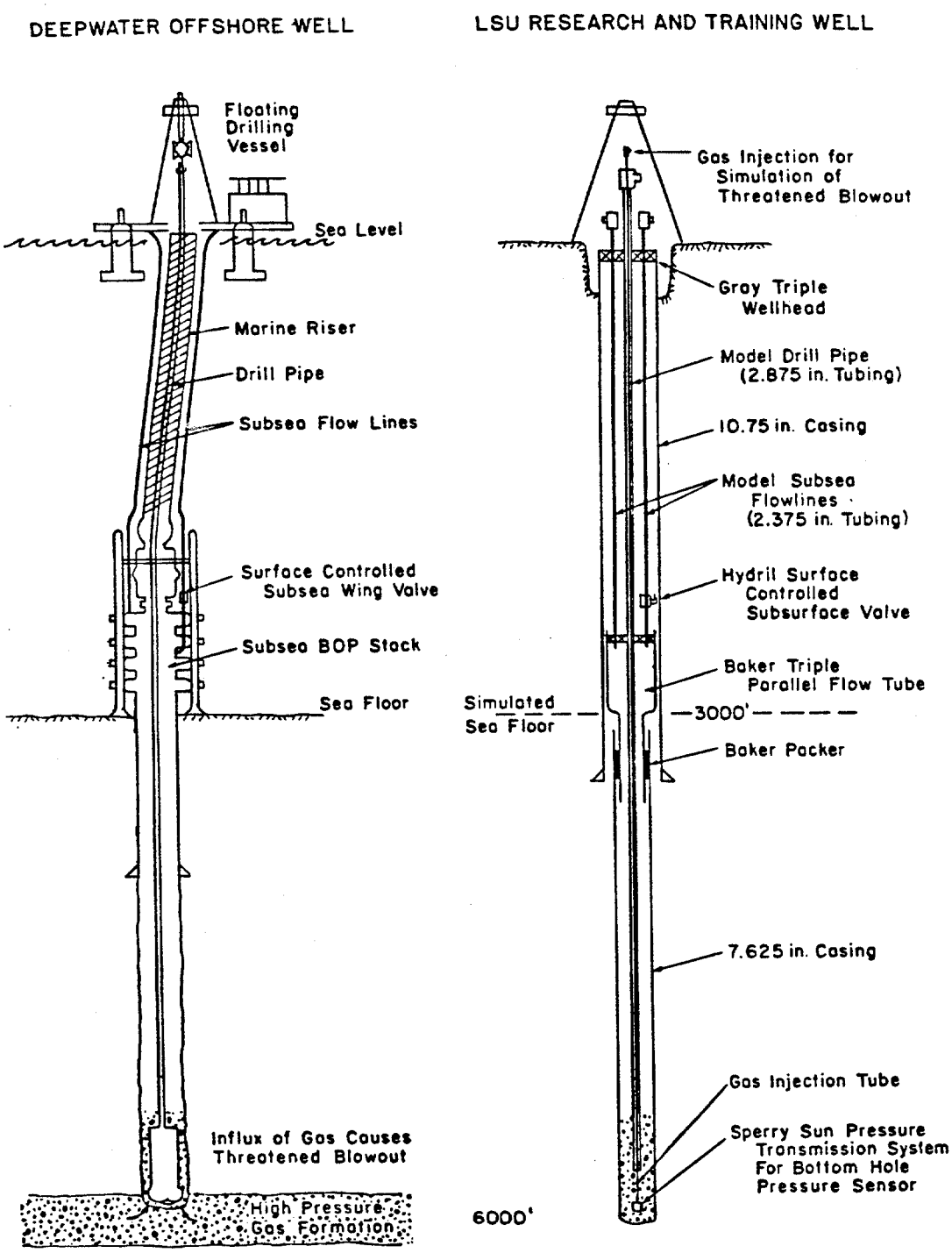

Figure 5.2 - Well Design for Modeling Well-Control Operations on Floating Drilling Vessels

0.069 in. ID capillary tube strapped to the 1.315 in. tubing. The capacity of the kill and choke lines is 11.6 bbls each and the capacity of the drill pipe annulus is 24.65 bbls. The capacity of the casing annulus is 113.65 bbls and the capacity of the 1.315 in. nitrogen injection line is 6.4 bbls. Table 5.1 shows the dimensions of the well-piping system.

The two centrifugal pumps are a 40 hp Swaco pump and a 40 hp Baroid pump. They are usually used to feed the triplex Halliburton pump and to mix and circulate mud through the surface equipment. The triplex pump is a 250 hp Halliburton model HT-400. It is a single acting pump with three plungers of 4 in. diameter with a stroke length of 8 in. The discharge from the triplex pump is tied-in to a kill line manifold which allows pumping down the drill pipe, the kill line, or the choke line. Circulation can also by-pass the well to the surface equipment.

The outlet flow stream from the well passes through either the kill manifold or the choke manifold. The choke manifold consists of four 15,000 psi adjustable chokes, which are three remote-control chokes designed by Swaco, Cameron and Shaffer, and one hand-control designed by Cameron. The fluid then either flows through a Swaco gas separator or by-passes the separator into a mud tank. There are two three-section mud tanks; one

PIPE	GRADE	Weight (lb/ft)	OD (in.)	ID (in.)	Length Ft.
Nitrogen Line	J-55 (integral)	1.72	1.315	1.049	6010
Kill Line	J-55	4.7	2 3/8	1.995	2962
Choke Line	J-55	4.7	2 3/8	1.995	2962
Drill pipe (Outer pipe)	J-55	6.5	2 7/8	2.441	5994
Casing	N-80	26.4	7 5/8	6.969	6100
Capillary Tube	316L Stainless Steel	ASTM A-269	.125	0.069	6010

Table 5.1 - Dimensions Of The Well Piping System

tank measures 8 ft. wide, 30 ft. long and 6 ft. high with 1.187 bbl/in./section or 256 bbls tank capacity, and the other measures 8 ft. wide, 36 ft. long and 6 ft. high with 1.426 bbl/in./section or 309 bbls tank capacity. A two-section 30 bbl metering (trip) tank is available to meter the flow rate and evaluate the pump efficiency.

The instrumentation and control house contains all the operating and control panels. These panels include Swaco, Cameron and Shaffer choke-control panels, kill line hydraulic control valves, Halliburton pump-control panel, and Sperry-Sun bottom hole pressure monitoring and recording systems. A mini computerized unit designed by Totco is also available, which is equipped with multi-pen recorder, printer and TV screens to provide and display all needed information for each experimental run.

Drill pipe pressure is the pressure at the well inlet flow line which represents the total pressure loss in the system, or the pump pressure. The casing pressure or the choke line pressure is the pressure measured at the outlet flow line upstream of the choke manifold. The kill line pressure is the pressure measured downstream of the kill line. Drill pipe and casing pressures are measured through four sets of pressure-monitoring systems designed by Swaco, Cameron, Shaffer and Totco. The kill line pressure is measured with two

pressure-monitoring systems designed by Swaco and Totco.

The well bottom hole pressure, at 6,000 feet , is measured through the Sperry-Sun pressure transmission system. This system consists of a down-hole chamber connected to a surface pressure monitoring device through 6000 ft. of 0.125 by 0.69 inch diameter capillary tube filled with water. The surface pressure reading is corrected to bottom hole value by adding the hydrostatic head due to the water column.

The Nitrogen unit,[28] shown in Figure 5.3, consists of a Nowsco truck which carries a liquid Nitrogen "vacuum bottle" storage vessel, pumping, gasifier, metering system, pressure monitoring system and all appropriate controls and instruments for operation. The liquid nitrogen at -320°F is stored under atmospheric pressure. It is continually boiling away to a small extent as heat seeps in, the accumulated pressure being relieved through a safety valve.

5.2 Procedure

The experimental work of this study consisted of two parts. The first part was to measure frictional pressure losses in the choke line and casing annulus due to the flow of different clay-water muds. The second part involved the study of pressure drop in the choke line as a result of flow of clay-water muds and nitrogen gas mixtures.

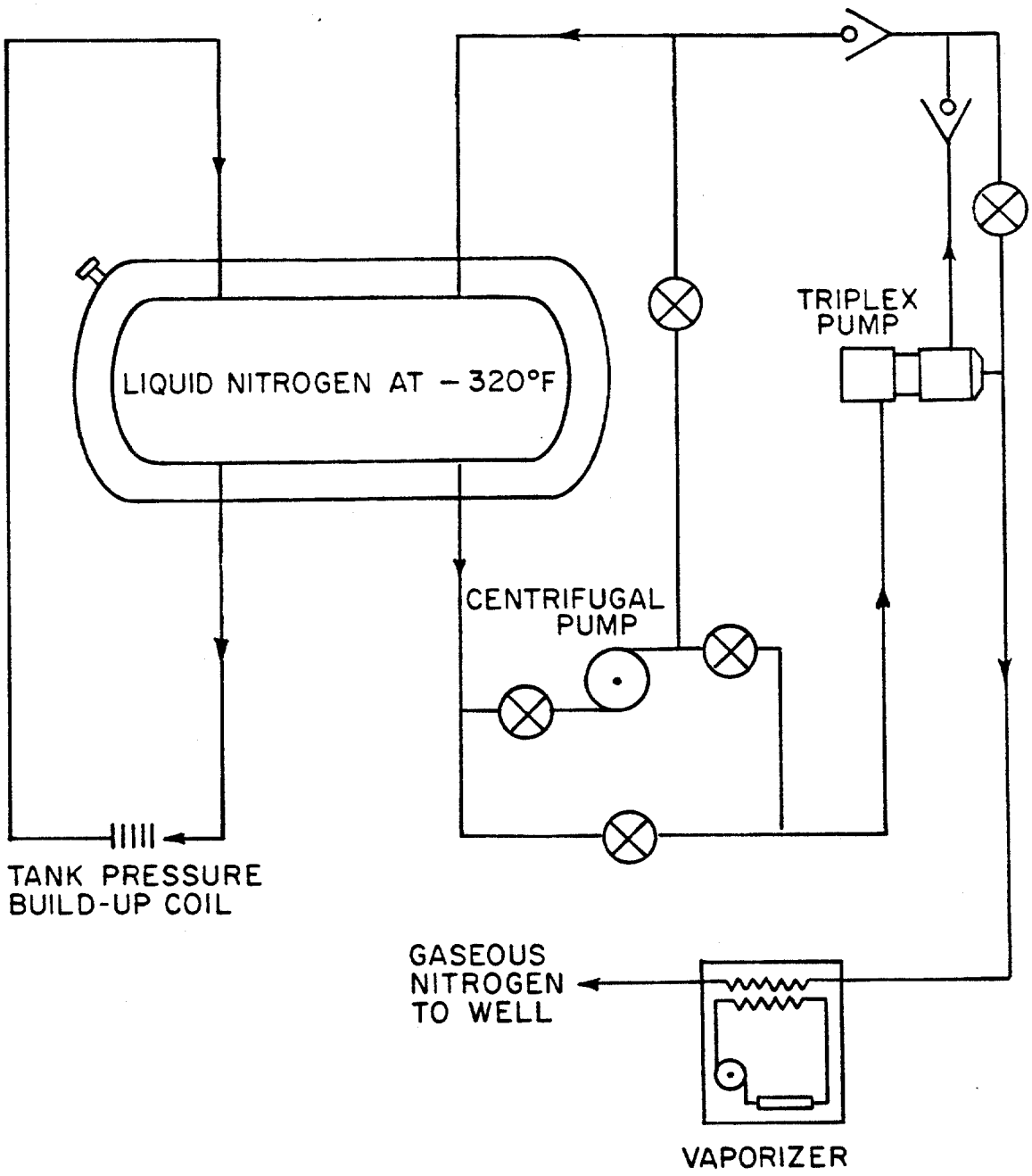

Figure 5.3 - The Nitrogen Unit[28]

The first part of the experimental work was performed by pumping a clay water mud down the drill pipe annulus and up the choke line while the kill line is shut-in. The kill line was shut-in to utilize its pressure monitoring system in measuring the frictional pressure losses in the choke line. The flow diagram of this part is shown in Figure 5.4. The experimental procedure of this part is as follows:

1. Bring pump to desired speed. Let well reach stabilized conditions of pressure, temperature, and flow rate.
2. Determine pump efficiency.
3. Measure and record following data:
    a. Drill Pipe Pressure
    b. Bottom Hole Pressure
    c. Kill Line Pressure
    d. Choke Line Pressure
    e. Mud Temperature, Properties and Flow Rate
4. Change mud rate and repeat measurement.

The flow diagram of the clay-water muds and nitrogen mixtures is shown in Figure 5.5. This part of the experiment was performed by injecting nitrogen gas down the kill line and pumping de-gassed mud down the drill pipe. Both mud and gas were then flowed up the choke line to the choke line manifold and finally to the degassing system before the mud was re-circulated.

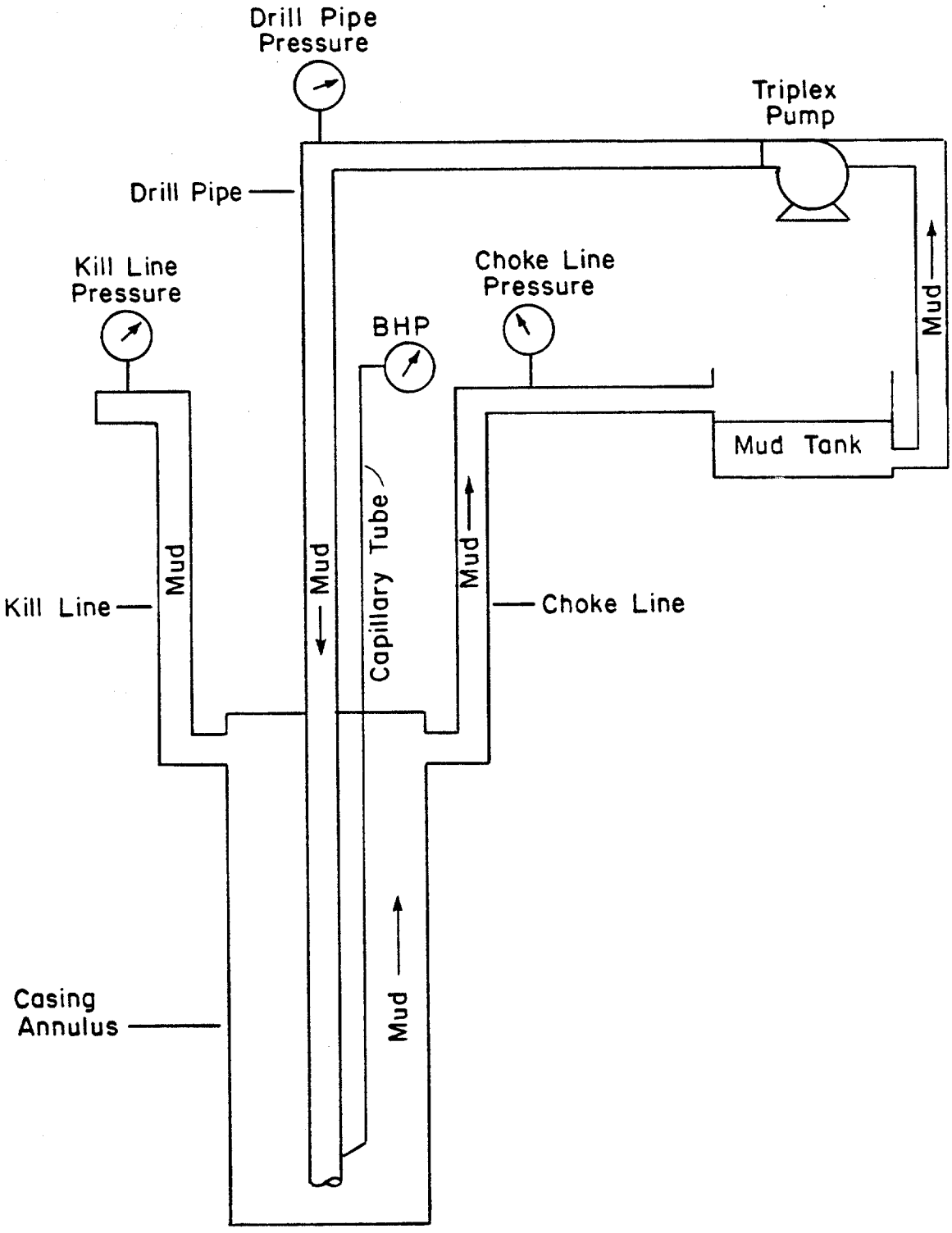

Figure 5.4 - Flow of the Clay-Water Muds In the Well

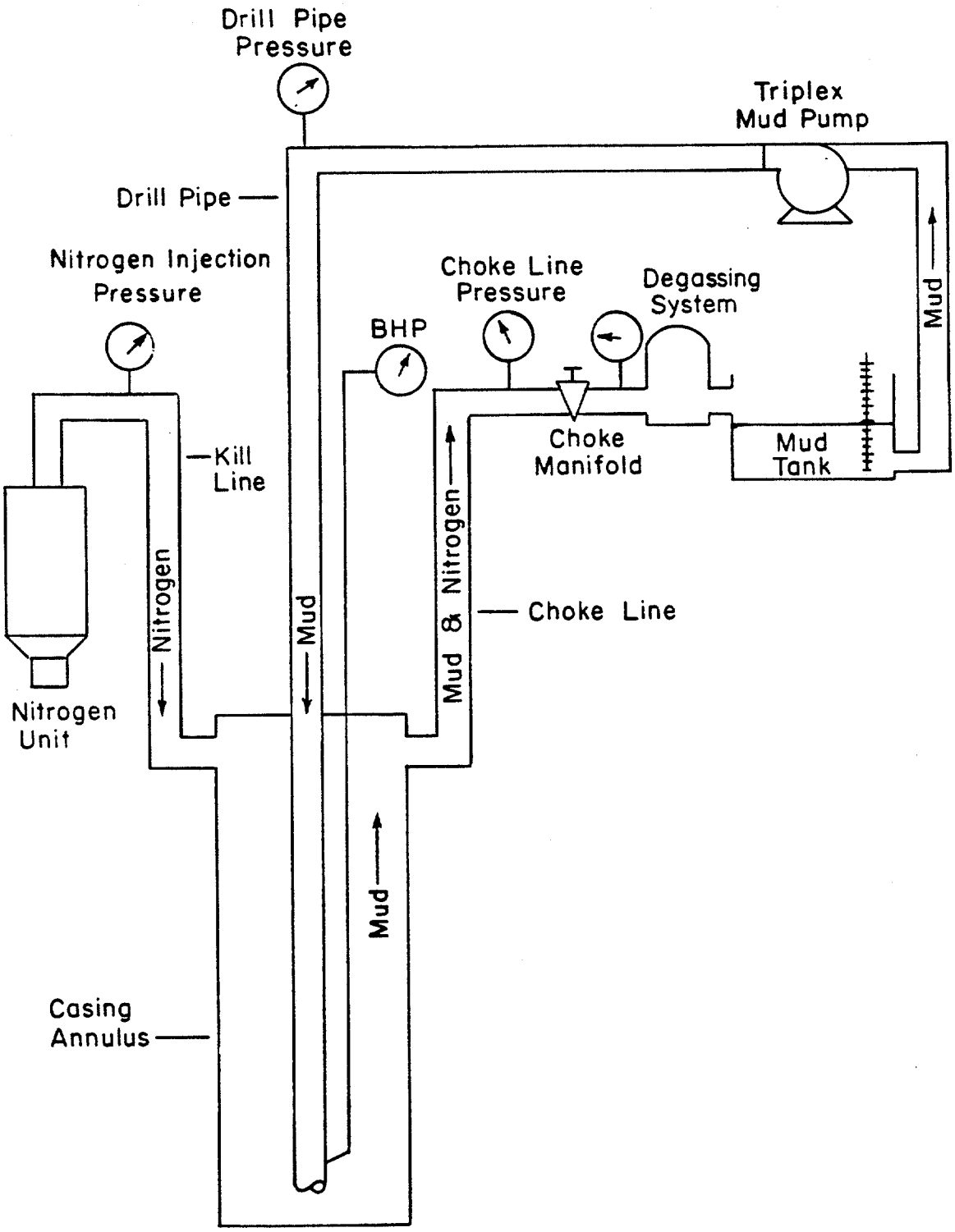

Figure 5.5 - Flow of the Nitrogen-Mud Mixtures in the Well

The experimental procedure of this part is as follows:

1. Bring mud pump to desired speed and set choke at desired initial pressure. Let system reach stabilized conditions of pressure, temperature, and flow rate.
2. Measure mud level in tank.
3. Start nitrogen injection at desired rate. Observe mud level in tank. Let system stabilize.
4. Measure and record following data:
   a. Drill Pipe Pressure
   b. Bottom Hole Pressure
   c. Nitrogen Injection Pressure
   d. Choke Pressure and Position
   e. Mud Temperature, Properties and Flow Rate.
   f. Nitrogen Temperature and Injection Rate.
5. Change choke pressure and repeat measurements.
6. Change mud rate and repeat measurements.

5.2.1 Pressure Measurement

Pressure data were obtained using a set of monitoring devices checked and calibrated with a dead weight tester. Bottom hole pressures at the bottom of the casing annulus were measured at the surface using the Sperry-Sun capillary tube system. The surface reading at no flow conditions indicates the difference in hydrostatic pressure between mud in the well and water in the capillary tube. This reading was always checked before

and after each run. A maximum difference of about 15 psi was detected. This difference was believed to be due to the temperature effect. An arithmetic average of the two values was adopted.

Drill pipe pressure, choke pressure, and nitrogen injection pressure were measured and recorded with the Totco monitoring system. However, pressure data provided by Swaco, Cameron and Shaffer systems were used to double check Totco data.

Preliminary data, obtained with the clay-water muds, indicated that frictional pressure losses in the casing annulus are too small to be detected. Also calculated data showed that these pressures are very small. Accordingly, the Sperry-Sun capillary tube readings were utilized to obtain the pressure drop data in the choke line for all phases of this experimental work. However, when circulating mud only, the kill line was also used to monitor pressure losses in the choke line. In this latter case, data obtained from the kill line pressure monitoring system and data obtained from the capillary tube system were almost identical. As would be expected, a maximum of about 25 psi difference was detected with the high viscosity mud no. 3.

5.2.2 Flow Rate Measurement

The mud flow rates were measured by counting the pump strokes per minute and then multiplying by the

pump factor to obtain the volumetric flow rate. The pump strokes per minute were measured with four different monitoring systems designed by Swaco, Totco, Cameron and Shaffer. The accuracy of these systems was periodically checked by direct measurement. The pump factor was determined by evaulating the pump efficiency through the two-section 30 bbl metering tank. In order to improve the efficiency of the triplex pump, one of the centrifugal pumps was used to supercharge the pump suction. The actual triplex pump efficiency was determined for various pressures and flow rates and an average of 99% was found. Accordingly, the flow rates were determined as follows:

$$Q = PF \times SPM \tag{5.1}$$

$$PF = \frac{S \times D^2}{98.03} \times \text{pump efficiency} \tag{5.2}$$

or

$$Q = 1.2927 \times SPM \tag{5.3}$$

where

Q = flow rate, gal/minute

PF = pump factor, gal/stroke

SPM = strokes per minute

S = stroke length, in.

D = liner diameter, in.

When taking nitrogen-mud data, the nitrogen

injection rate was kept as constant as possible during each run. Different hold ups and gas-mud ratios were obtained by changing the choke position or the mud flow rate. The nitrogen rate was determined from the liquid nitrogen pump speed as read from the pump rate - pump speed tacometer and by monitoring the change in the liquid nitrogen level in the tank.

5.2.3 Temperature Consideration

Surface flowing mud temperatures were measured with a thermometer mounted at the end of the mud return flow line. Injected nitrogen temperatures were measured by the nitrogen truck monitors. Downhole flowing temperature profiles were not measured, but were estimated based on the Holmes and Swift Correlation (Section 3.4). Figure 5.6 shows flowing temperature profiles at two different flow rates of mud no. 1. The figure, also, shows the static temperature profile of the well. The constants used in constructing the flowing profiles are the overall heat transfer coefficient across the pipe, hp, the overall heat transfer coefficient across the wellbore, U, and the mud heat capacity, cp. The static profile was obtained from a temperature log which was run in the well. Table 5.2 shows these data and their sources.

Figure 5.6 indicated that the temperature changes with depth were not too significant. However, the

Table 5.2 - Additional Data Used In Study

	Data	Source
1.	Geothermal gradient, °F/100 ft = 1.1	Temperature log
2.	Ambient surfact temperature, °F = 75	Extrapolated from the log
3.	Mud Heat capacity, BTU/lb-°F = 0.8	References No. 8 & 20
4.	Heat transfer coefficient across pipe, BTU/ft^2-°F-hr = 30	References No. 8 & 20
5.	Heat transfer coefficient across wellbore BTU/ft^2-°F-hr = 1.3	References No. 8 & 20
6.	Mud-gas surface tension	Correlation of water-gas surface tension[6]
7.	Mud compressibility	Correlation of water compressibility[6]
8.	Nitrogen viscosity	Correlation based on published data[16]
9.	Nitrogen solubility	Correlation based on published data[16]
10.	Nitrogen z factor	Correlation[35]

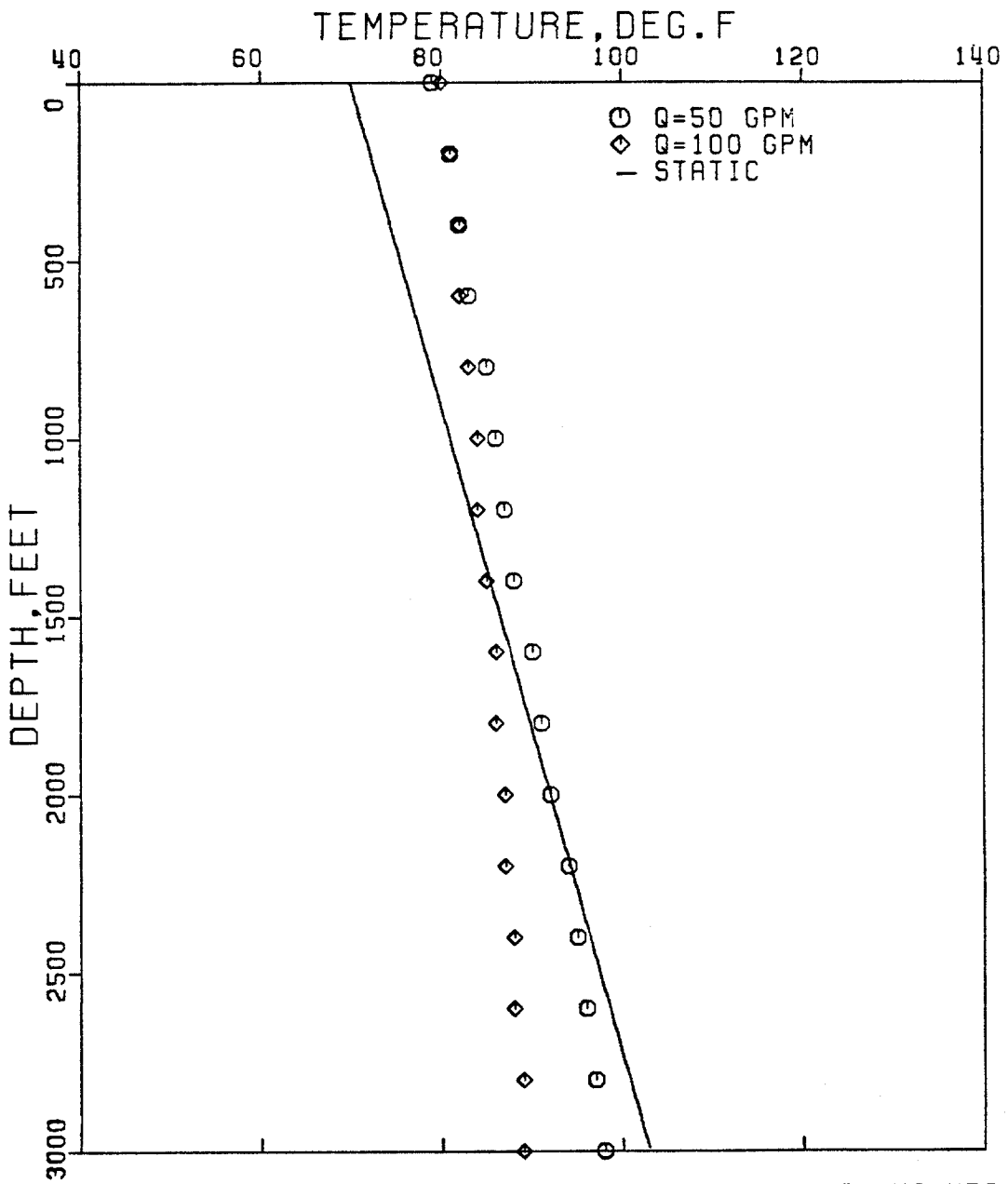

FIG.5.6-FLOWING TEMPERATURE PROFILE BASED ON HOLMES AND SWIFT CORRELATION-MUD NO.1

effect of temperature on mud properties was investigated in the laboratory as shown in Figures 5.7, 5.8, and 5.9. The result of the laboratory study showed that surface mud properties can be used to represent the average mud properties in the system. The same conclusion was also proven to be valid since calculated bottom hole pressure, based on surface mud density, agreed very well with the measured data.

5.2.4 Fluid Properties

Mud properties were checked before and after the pressure-drop flow-rate data were taken. No significant changes in the mud properties were detected which might offset the quality of the data. The mud properties which were measured are density and viscous properties. The mud density was measured with a mud balance and periodically checked with a specific gravity balance. The viscous properties were measured with a V-G meter Model 35 as follows:

$$\mu_p = \theta 600 - \theta 300 \tag{5.4}$$

$$\tau_y = \theta 300 - \mu_p \tag{5.5}$$

$$n = 3.322 \log \frac{\theta 600}{\theta 300} \tag{5.6}$$

$$k = \frac{510\ \theta 300}{(511)^n} \tag{5.7}$$

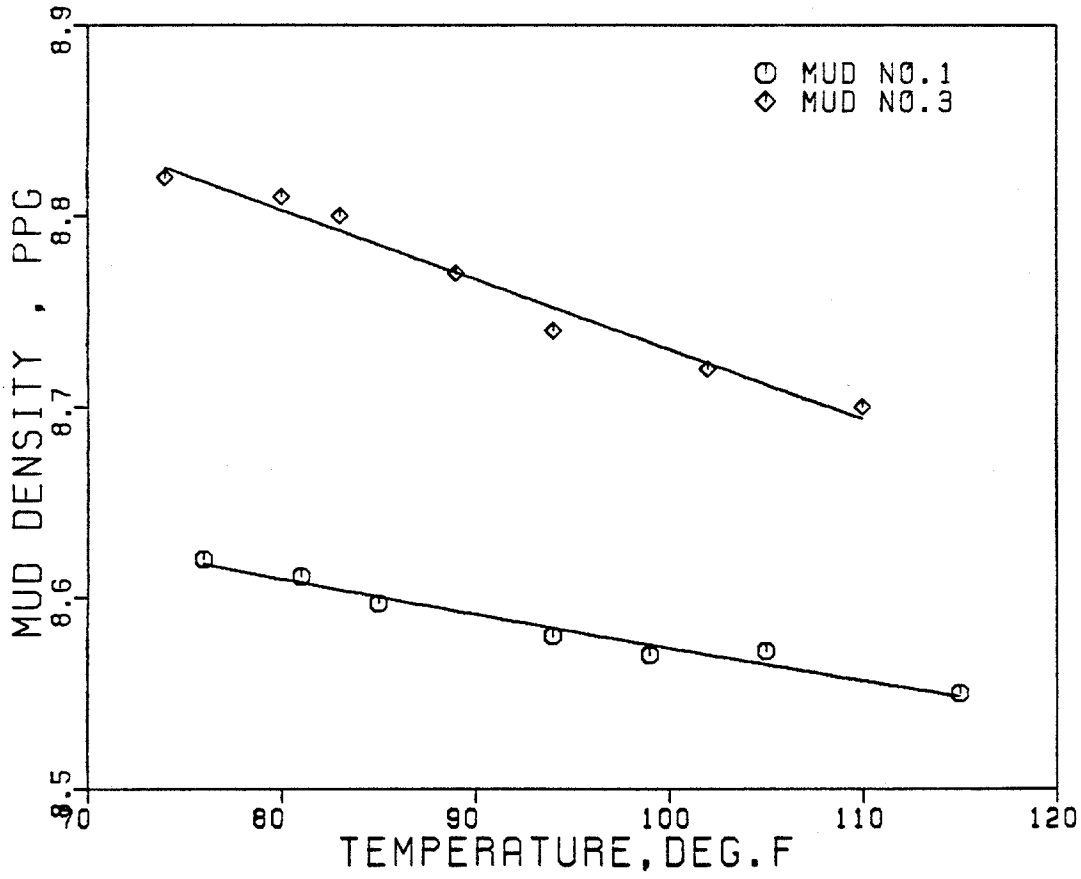

FIG.5.7-DENSITY VS.TEMPERATURE FOR MUD(1) & MUD(3)

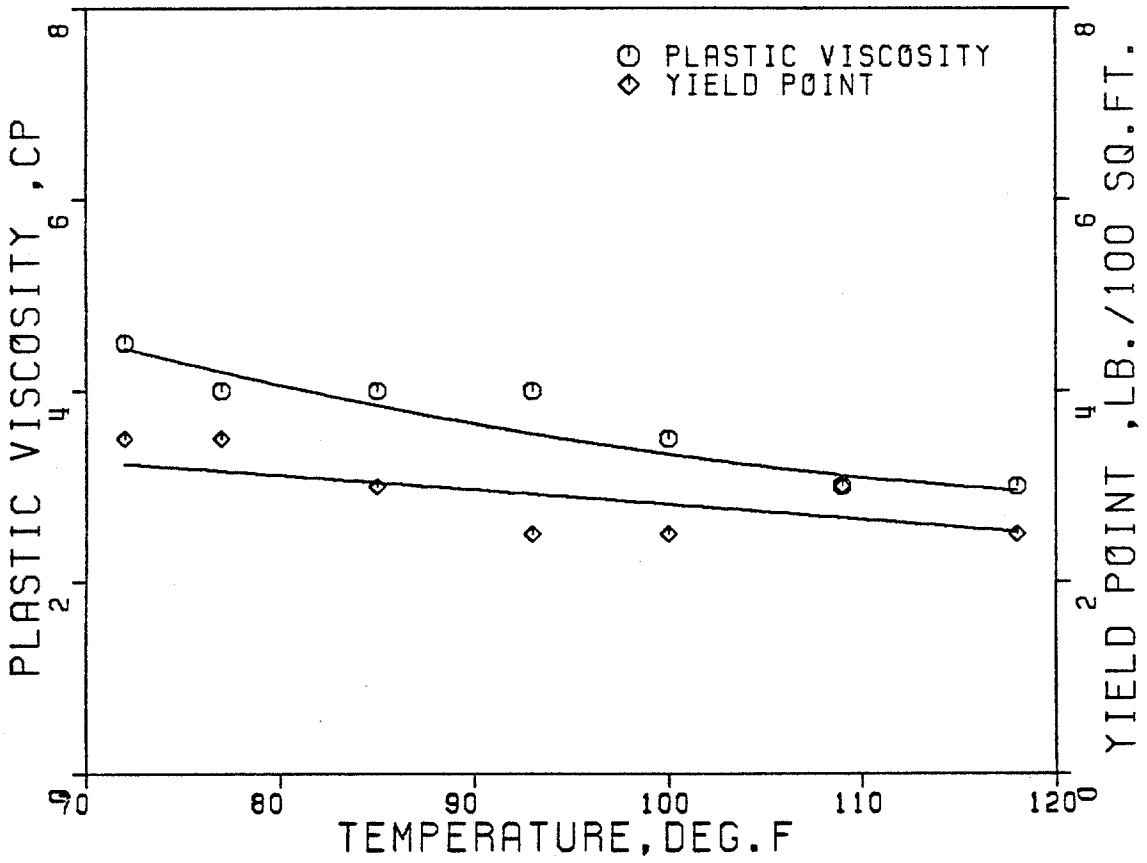

FIG.5.8-VISCOUS PROPERTIES VS.TEMPERATURE FOR MUD NO.1

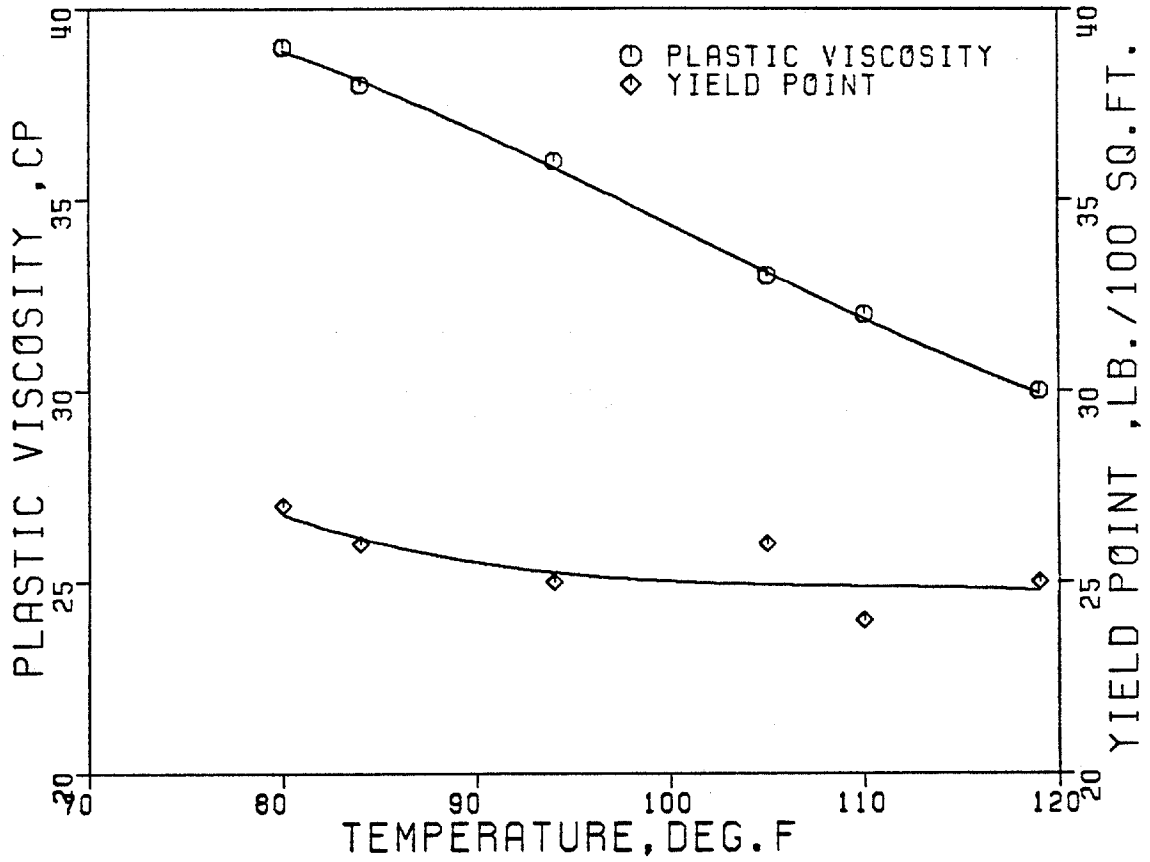

FIG.5.9-VISCOUS PROPERTIES VS.TEMPERATURE FOR MUD NO.3

where

μ_p = plastic viscosity, cp

τ_y = yield point, lb/100 sq ft

n = flow behavior index, dimensionless

k = consistency index, equivalent cp

$\theta 600$ = viscometer dial reading at 600 rpm

$\theta 300$ = viscometer dial reading at 300 rpm

Other mud properties, such as surface tension and compressibility, and nitrogen properties such as viscosity, solubility, specific gravity and compressibility factor were estimated from published data or correlations. However, when mud data were not available, the water properties were used. Flowing temperatures as estimated from Holmes and Swift correlation (Secion 3.4) were used to obtain these data. Table 5.2 shows a list of these properties.

5.2.5 Gas-Liquid Ratio and Hold Up

The nitrogen to mud flowing ratio, NMR, and the nitrogen to liquid ratio, NLR, in SCF/bbl were calculated as follows:

$$NMR = \frac{\text{Nitrogen rate, SCF/min}}{\text{Mud rate, gpm}} \times 42 \qquad (5.8)$$

and

$$NLR = \frac{NMR}{f_w^v} \qquad (5.9)$$

where f_w^v is the water fraction by volume in the mud.

Nitrogen and mud hold ups, H_N and H_M, were estimated as follows:

$$H_N = \frac{\text{Displaced mud from the choke line}}{\text{Choke line capacity}} \qquad (5.10)$$

and

$$H_m = 1 - H_N \qquad (5.11)$$

CHAPTER VI

RESULTS

Two computer programs were used to obtain the calculated pressure loss data of this study. These programs, which are listed in Appendices A and B, were developed based upon the theoretical discussion presented in Chapters II, III and IV. Mud viscous properties, as shown in Chapter V, were determined based upon viscometer dial readings measured at 600 and 300 rpm. Measured data were obtained using the well-facility and procedure described in Chapter V. The discussion of the results will be presented in the following sections.

6.1 Clay-Water Muds Pressure Data

Three different unweighted clay-water muds were used in the experiment. Table 6.1 shows the properties of these muds. Mud No. 1 was characterized by its low viscosity, Mud No. 2 by its intermediate viscosity, and Mud No. 3 by its high viscosity. The desired viscosity of Mud No. 1 and Mud No. 2 was obtained by adding bentonite clay to the mud. Mud No. 3 was Mud No. 2 treated with caustic soda.

The rheological models used to describe the behavior of these fluids are: 1) the Bingham plastic model, and 2) the power law model. The discussion of these

Table 6.1 - Properties of Clay-Water Muds

MUD PROPERTY	MUD NO. 1	MUD NO. 2	MUD NO. 3
Specific Gravity (Water = 1.0)	1.031	1.055	1.056
Density, ppg	8.6	8.8	8.8
Plastic Viscosity, cp	4	20	38
Yield Point, Lb/100 ft^2	3	8	27
Flow Behavior Index, n	0.65	0.78	0.66
Consistency Index, eq. cp	61	112	527
Bentonite Content, % by volume	2	3	3
pH	7.5	7.5	11
Average Flowing Temperature, °F	79	84	82

two models was presented in Chapter II. The frictional pressure loss correlation used to describe the Bingham plastic model frictional pressure loss-flow rate behavior was based on the Colebrook function as discussed in Chapter III. The frictional pressure equation used to describe the power law behavior was based on the Dodge and Metzner equation, also as discussed in Chapter III. The Reynolds number for the two correlations was calculated based on the discussion presented in Chapters II and III.

For simplicity, the definition of a Bingham plastic model as used in this chapter will refer to the rheological Bingham plastic model as well as its corresponding friction factor correlation, the Colebrook function. Similarly, the power law model will refer to the power law rheological model as well as the Dodge and Metzner equation for friction factors.

The measured and calculated frictional pressure data of the three muds at different flow rates are listed in Tables 6.2 through 6.4 and displayed in Figures 6.1 through 6.5. The tables also show the percent deviations of calculated pressures from measured values. The pressure losses shown in the tables and the figures are the frictional pressure losses for the total length of the choke line. The calculated data were obtained from the computer program "PRESS" which is listed in Appendix A. The Bingham model pressure data listed in

the Tables and Figures 6.1, 6.3 and 6.5 were based upon an absolute pipe roughness of 0.00065 inches. However, since the power law model correlation was developed for smooth pipes, the Bingham model data shown in Figure 6.2 were prepared with zero pipe roughness. The results of each mud will be discussed separately as follows.

6.1.1 Mud No. 1

Figures 6.1 and 6.2 display the pressure data of Mud No. 1. Figure 6.1 is a plot of pressure data listed in Table 6.2. The Bingham model data based on an absolute pipe rouhness of 0.00065 inches are presented in Figure 6.1 and Table 6.2., while those calculated with zero roughness are shown in Figure 6.2.

Both the Bingham and the power law models indicated that the data were taken under a fully turbulent flow regime. The Bingham model indicated that Reynolds numbers ranged from 5,400 to 30,000; while the power law showed a range of about 6,800 to 30,000. Each model, as shown in the figures, predicted a similar pressure loss-flow rate behavior (trend) as the measured data. However, the two models predicted slightly different pressure values. The Bingham model data calculated with the 0.00065 in. roughness was very close to the measured data, while those calculated with 0.0 roughness showed some deviation, with the majority of them below the measured data line. This behavior,

Table 6.2 - Choke Line Frictional Pressure Losses For Mud No. 1

Data No.	Mud Rate gpm	Measured Data psi	Bingham Plastic Model psi	Bingham Plastic Model %Deviation	Power Law Model psi	Power Law Model %Deviation
14	87	236	235	0.42	199	15.68
15	81	206	207	-0.48	177	14.08
16	80	196	202	-3.06	173	11.73
17	79	193	198	-2.59	170	11.92
18	70	156	159	-1.92	140	10.26
19	69	148	155	-4.73	136	8.10
20	67	141	147	-4.26	130	7.80
21	62	122	128	-4.92	115	5.74
22	59	116	117	-0.86	106	8.62
23	58	110	114	-3.64	103	6.36
24	54	96	100	-4.17	92	4.17
25	53	88	97	-10.23	89	-1.14
26	48	75	81	-8.00	76	-1.33
27	43	68	67	1.47	64	5.88

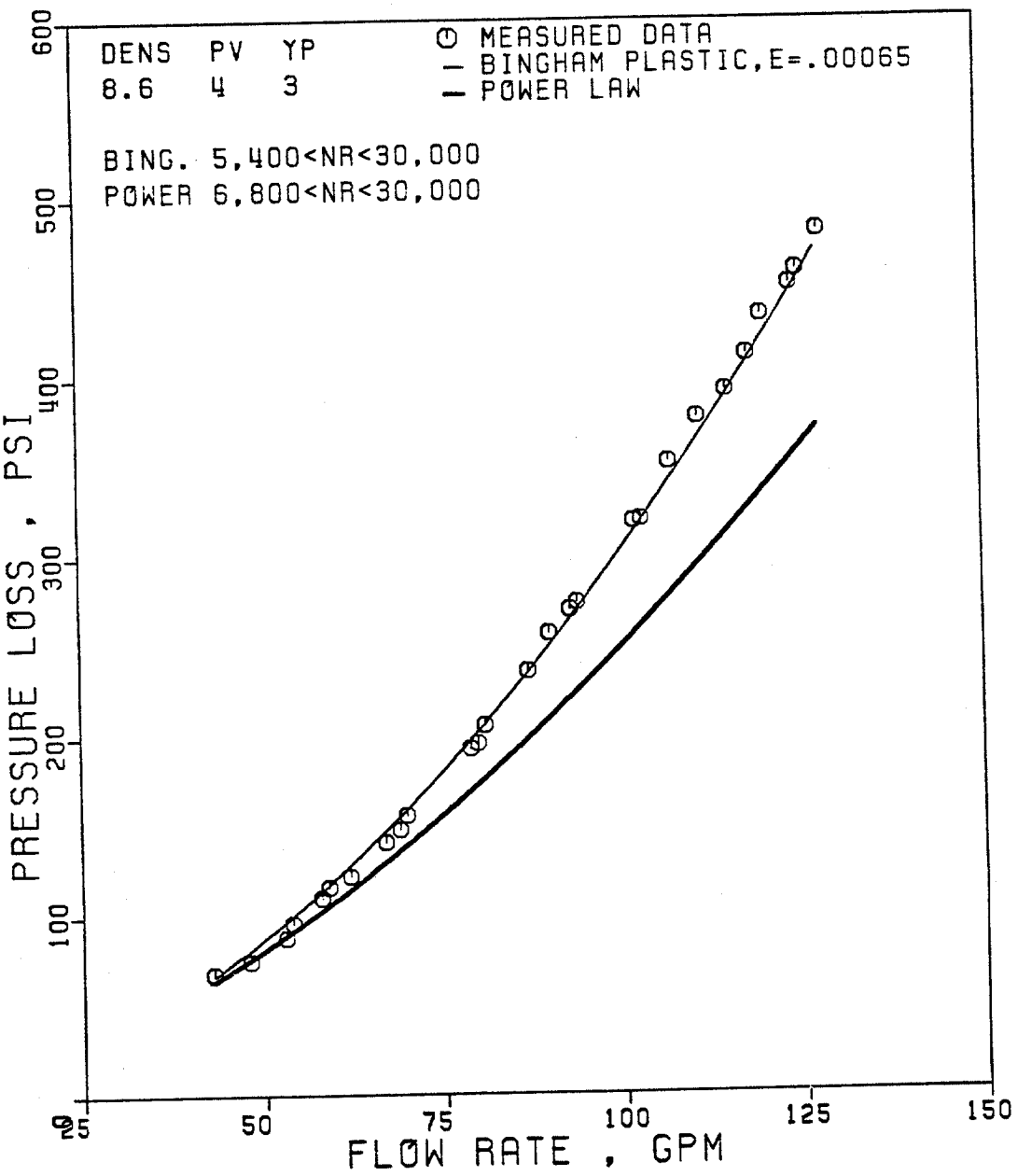

FIG.6.1-MEASURED AND CALCULATED CHOKE LINE FRICTIONAL PRESSURE DROP VS.FLOW RATE FOR MUD NO.1

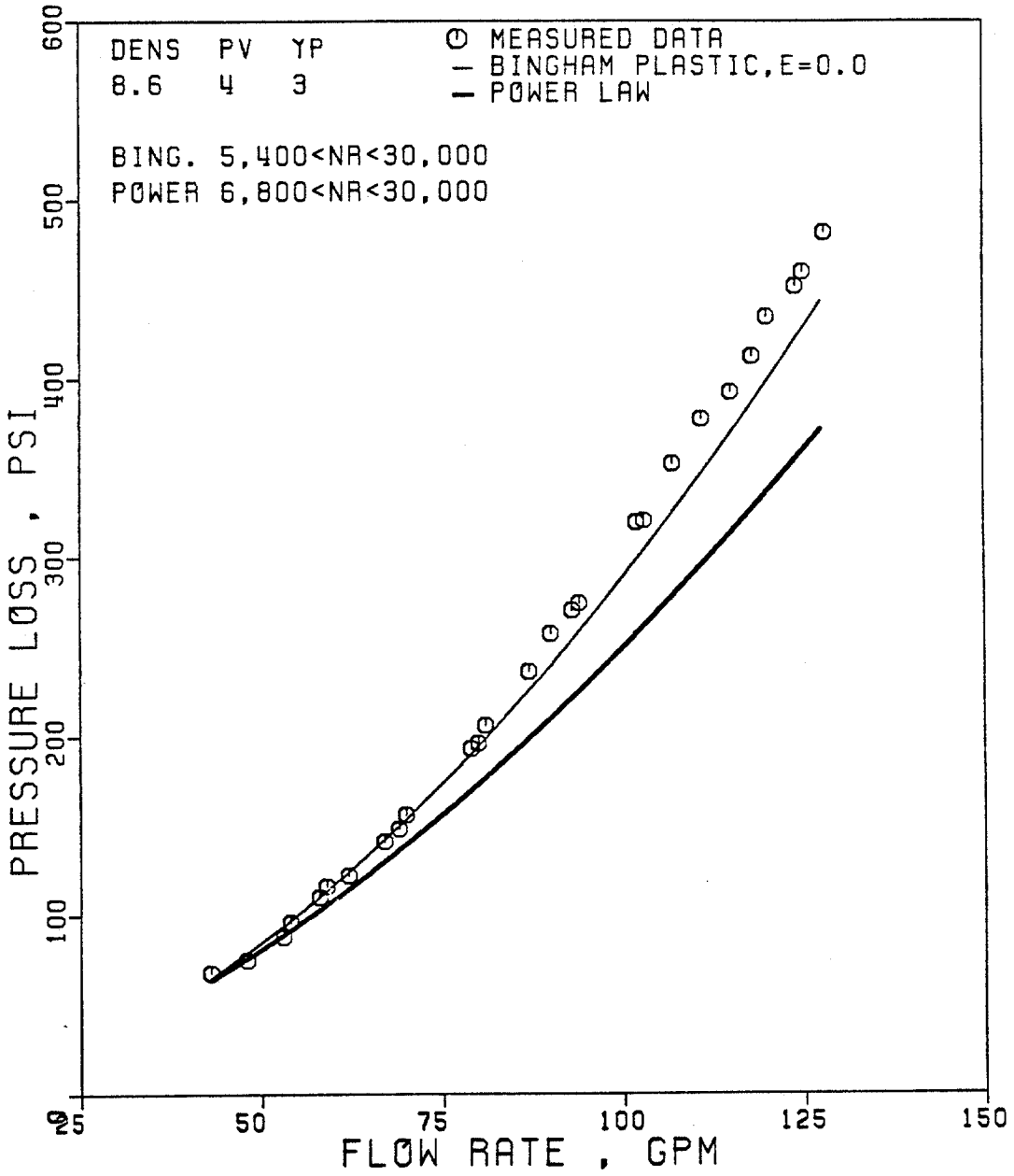

FIG.6.2-MEASURED AND CALCULATED CHOKE LINE FRICTIONAL PRESSURE DROP VS.FLOW RATE FOR MUD NO.1

which showed that the effect of pipe roughness on predicted data was relatively significant, was expected as discussed in Section 1.2 of Chapter III. On the other hand, predictions based upon the power law model were below both the measured data and the Bingham data. Moreover, the discrepancy between the power law and the measured data increased with Reynolds number. Again, this could indicate that the effect of pipe roughness was related to the degree of turbulence.

A summary of pressure statistical analysis is shown in Figure 6.18. This analysis shows that the Bingham model with ε = 0.0065" had an arithematic mean deviation of -0.8%, an average absolute deviation of 2.8% and an estimated standard deviation of 3.5%, while the power law was found to have values of 13.71%, 13.9%, and 7.4%, respectively.

6.1.2 Mud No. 2

The frictional pressure loss data of Mud No. 2 is shown in Table 6.3 and Figures 6.3 and 6.4. The Bingham model data shown in the table and Figure 6.3 were based upon the 0.00065" absolute roughness. As was found with the other muds, the Bingham and the power law models agreed on the values of the Reynolds number. The range of Reynolds numbers obtained with the Bingham model was between about 1,600 and 6,700; while that obtained with the power law was between 2,000 and 6,700. The lower

Table 6.3 - Choke Line Frictional Pressure Losses For Mud No. 2

Data No.	Mud Rate gpm	Measured Data psi	Bingham Plastic Model psi	Bingham Plastic Model %Deviation	Power Law Model psi	Power Law Model %Deviation
1	116	533	575	-7.88	535	-0.36
2	112	498	541	-8.64	405	-1.41
3	107	471	499	-5.94	468	0.64
4	103	439	467	-6.38	440	-0.23
5	98	401	429	-6.98	406	-1.25
6	97	386	421	-9.07	399	-3.37
7	94	381	398	-4.46	379	0.52
8	89	347	362	-4.32	347	0.00
9	87	322	348	-8.07	334	-3.73
10	83	306	321	-4.90	310	-1.31
11	76	277	276	0.36	269	2.89
12	72	250	251	-0.40	246	1.60
13	71	226	245	-8.41	241	-6.64

Table 6.3 - Choke Line Frictional Pressure Losses For Mud No. 2

Data No.	Mud Rate gpm	Measured Data psi	Bingham Plastic Model psi	Bingham Plastic Model %Deviation	Power Law Model psi	Power Law Model %Deviation
14	67	215	222	-3.26	219	-1.86
15	63	192	200	-4.20	199	-3.65
16	58	163	173	-6.14	174	-6.75
17	55	151	158	-4.64	160	-5.96
18	52	120	144	-20.00	146	-21.67
19	49	116	130	-12.07	133	-14.66
20	43	102	104	-1.96	108	-5.88

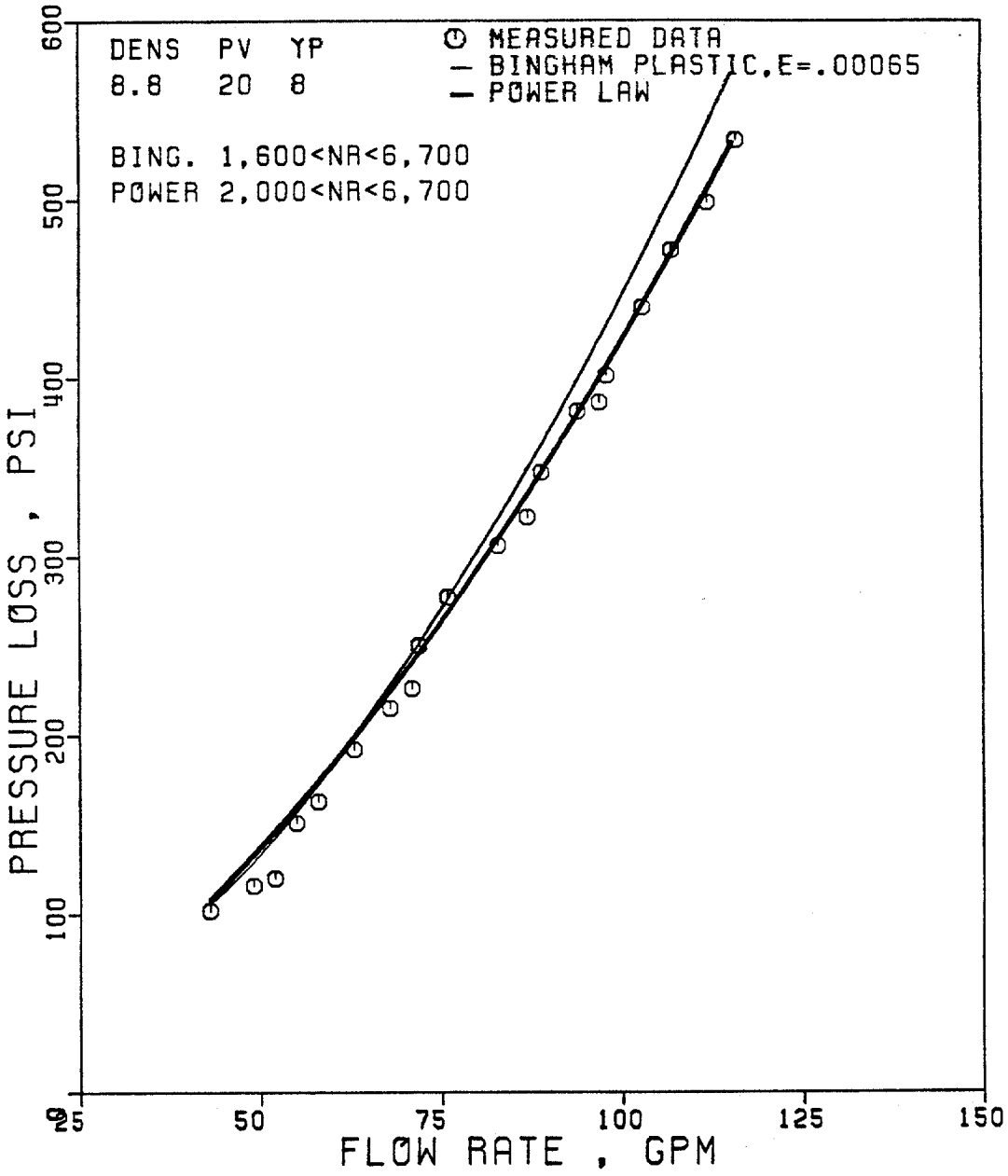

FIG.6.3-MEASURED AND CALCULATED CHOKE LINE FRICTIONAL PRESSURE DROP VS.FLOW RATE FOR MUD NO.2

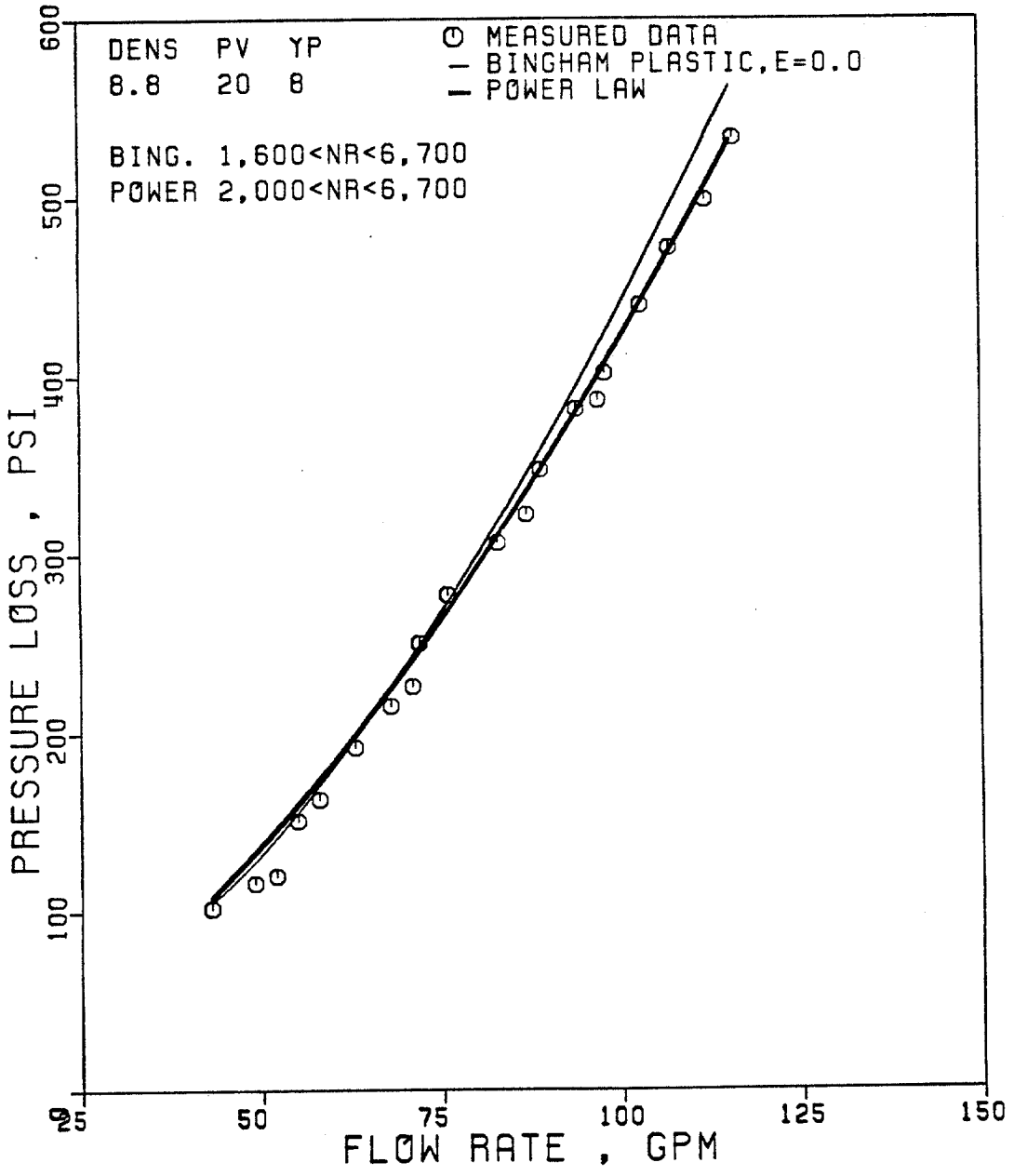

FIG.6.4-MEASURED AND CALCULATED CHOKE LINE FRICTIONAL PRESSURE DROP VS.FLOW RATE FOR MUD NO.2

values of Reynolds number suggested that some of the data points were within the transition flow regime. Also, the measured data showed that the last 3 data points, corresponding to flow rate of 52 gpm and lower, followed a slightly different behavior which could indicate a different flow regime. This difference in the behavior was not shown by either of the theoretical models, since the technique of treating the transition flow regime, which is presented in Section 3 of Chapter III, is used.

Similar to the other two muds, the two models again showed similar pressure-flow rate behavior, but with different values. However, unlike Mud No. 1, the power law model showed a better performance than the Bingham model. Two possible reasons for the good performance of the power law are the low effect of pipe roughness and the low yield point of the mud. As expected, Figures 6.3 and 6.4 indicated that the pipe roughness was not a significant factor on the predicted pressure values. However, as shown in the statistical analysis of Table 6.18, the Bingham model was found to have an arithematic mead deviation of -6.4%, an average absolute deviation of 6.4%, and an estimated standard deviation of 4.4%, compared with -3.7%, 4.2% and 5.8%, respectively, for the power law.

6.1.3 Mud No. 3

Figure 6.5, which is a plot of Tabl3 6.4, displays the pressure data of the high yield point Mud No. 3. Again, both the Bingham and the power law models indicated similar values of Reynolds number. The predicted pressure loss-flow rate behavior of both models showed a close behavior to the measured data. Reynolds numbers and the behavior of the measured data points, clearly indicate different flow regimes. As can be seen from Figure 6.5, the behavior of the last 12 points, corresponding to flow rates of 75 gpm and lower, is linear. This linear behavior suggested that the flow regime of these data points was laminar. The rest of the data were probably in the transition flow regime. The approximate Reynolds number at which the flow behavior of the measured data starts to deviate from laminar was about 1500. Since no correlations are available to estimate the frictional pressure losses of the transition flow regime, the technique discussed in Section 3 of Chapter III was used. In summary, this technique assumes that the flow regime deviates from laminar when both the laminar and turbulent equations yield the same value of pressure loss. Then, pressure loss, using both laminar and turbulent flow equations, is computed and the higher result is considered. The Bingham model showed that the point at which the laminar and turbulent equations yielded the same pressure loss was at a

Table 6.4 - Choke Line Frictional Pressure Losses For Mud No. 3

Data No.	Mud Rate gpm	Measured Data psi	Bingham Plastic Model psi	Bingham Plastic Model %Deviation	Power Law Model psi	Power Law Model %Deviation
1	105	501	574	-14.57	547	-9.18
2	98	432	511	-18.28	484	-12.03
3	93	406	467	-15.02	459	-13.05
4	88	381	424	-11.28	417	-9.45
5	83	362	384	-6.08	381	-5.25
6	79	343	353	-2.92	354	-3.21
7	75	329	327	0.61	327	0.61
8	71	319	319	0.0	302	5.33
9	67	308	311	-0.97	282	8.44
10	63	292	303	-3.77	270	7.58
11	59	286	296	-3.5	258	9.8
12	54	274	286	-4.38	244	10.9
13	48	255	274	-7.45	226	11.37

Table 6.4 - Choke Line Frictional Pressure Losses For Mud No. 3

Data No.	Mud Rate gpm	Measured Data psi	Bingham Plastic Model psi	%Deviation	Power Law Model psi	%Deviation
14	44	245	266	-8.57	214	12.65
15	41	236	260	-10.17	204	13.56
16	36	225	251	-11.56	187	16.9
17	32	216	243	-12.5	173	19.9
18	30	210	238	-13.33	165	21.43

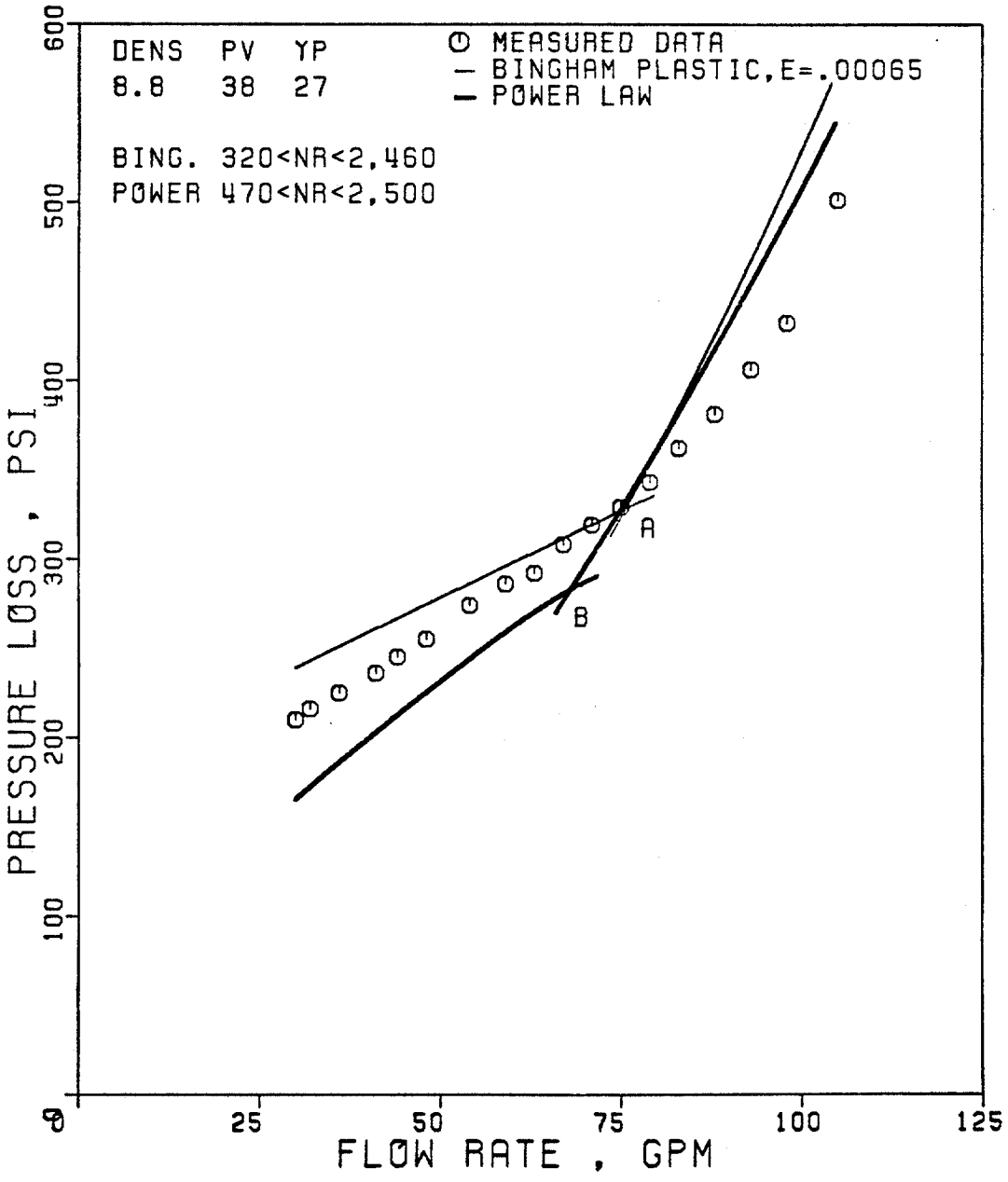

FIG.6.5-MEASURED AND CALCULATED CHOKE LINE FRICTIONAL PRESSURE DROP VS.FLOW RATE FOR MUD NO.3

Reynolds number of about 1400 (Point A in Figure 5.6); while the power law indicated that they were equal at a Reynolds number of about 1300 (Point B in Figure 5.6).

In predicting the data of the laminar flow regime, the laminar equation of the Bingham model provided a better performance than that of the power law. In this case, the majority of the Bingham model data were above the measured pressure line, while the power law model predicted consistently lower values than the measured data. However, as shown in Chapter II, the power law rheological model does not consider the mud yield point. Accordingly, it is believed that the performance of the power law model was affected by the high yiled point of this particular mud. On the other hand, above the flow rate at which the flow regime changed from laminar, the performance of the turbulent equation of the power law was better than that of the Bingham. However, in this case, the predictions of both models were consistently higher than the measured data. The statistical analysis of the pressure data is shown in Figure 6.18.

6.2 Gas-Mud Mixtures Pressure Data

The same three muds used to obtain the clay-water muds data were used to obtain the nitrogen-mud mixtures data. The physical properties of the nitrogen are listed in Table 6.5. The characteristics of the nitrogen-mud mixtures are shown in Table 6.6.

Table 6.5 - Physical Properties of Nitrogen[28]

LIQUID NITROGEN:

Specific Gravity = 0.809

Weight Density = 6.8 lb. liquid/gal. liquid

Boiling Point = -320°F

GASEOUS NITROGEN:

Weight Density = 0.0724 Lb/SCF

SCF of Gallon of Liquid = 93.0

Critical Pressure = 492.2 psia

Critical Temperature = -232.8°F

Specific Heat Ratio, k = 1.4 @ 68°F and 14.7 psia

Table 6.6 - Properties of Gas-Mud Mixtures

Property	Run No. 1	Run No. 2	Run No. 3
Type of Mud	Mud No. 1	Mud No. 2	Mud No. 3
Gas Injection Rate, SCF/min	650	625	650
Average Gas Injection Temperature, °F	120	110	115
Average Mud Outlet Temperature °F	82	85	82

The two-phase flow correlations used in the study are: 1) Poettmann and Carpenter, 2) Hagedorn and Brown, 3) Orkiszewski, and 4) Beggs and Brill. The discussion of these correlations is presented in Chapter IV. A summary of the conditions under which each correlation was developed is shown in Table 6.7.

Measured data, which included choke line upstream pressures (bottom hole choke line pressure), choke line downstream pressure (choke manifold pressure), nitrogen injection pressure, and surface average liquid hold up are listed in Tables 6.8, 6.9 and 6.10.

Measured and calculated choke line pressure drop data are listed in Tables 6.11 through 6.16 and displayed in Figures 6.6 through 6.11. Pressure drop data shown in these tables and figures is the total pressure losses, including frictional, potential and acceleration terms for the total length of the choke line. Calculated data was obtained using the computer program "TWPHAS", which is listed in Appendix B. In this program, the upstream choke line pressure value is given as part of the input data, and the total pressure drop is calculated. The total pressure drop is computed by dividing the choke line into 20 foot intervals. The pressure drop of each interval is calculated, and then the total choke line pressure drop is computed as the sum of the interval pressure drops.

Two sets of pressure drop data were prepared. One

Table 6.7 - Summary of Conditions Under Which The Two-Phase Flow Correlations Were Developed As Compared With This Work

Correlation	Pipe Size Inches	Length Feet	Fluid Tested	Comments
Poetmann and Carpenter	2, 2 3/8, 2 7/8 OD		oil, water, gas	Field data.
Hagedorn and Brown	1, 1 1/4, 1 1/2 Nominal	1500	oil, water, gas	Experimental well using different viscosities.
Orkiszewski	General		oil, water, gas	Combination and modification of different correlations.
Beggs and Brill	1, 1 1/2 Nominal	90	air, water	Laboratory work developed for inclined pipes.
Data of this work	1.995 ID (2 3/8 OD)	3000	Nitrogen, clay-water muds	Experimental well.

Table 6.10 - Measured Choke Line Pressure Data For Gas-Mud Mixtures - Run No. 3

Data No.	Mud Rate gpm	Upstream Pressure, psig	Downstream Pressure, psig	Gas Injection Pressure, psig	Average Liquid Holdup, %
1	79	2294	500	1975	77.2
2	81	2137	315	1900	77.2
3	73	2048	350	1830	69.2
4	67	1914	325	1695	64.4
5	61	1840	290	1595	64.4
6	56	1760	285	1555	58.0
7	51	1680	275	1485	54.0
8	45	1586	265	1405	49.0
9	40	1477	240	1300	46.5
10	34	1324	210	1160	41.4
11	32	2276	1000	1955	60.6
12	38	1741	540	1535	72.1
13	57	2095	545	1825	72.1
14	66	2123	470	1810	78.5

Table 6.8 - Measured Choke Line Pressure Data For Gas-Mud Mixtures - Run No. 1

Data No.	Mud Rate gpm	Upstream Pressure, psig	Downstream Pressure, psig	Gas Injection Pressure, psig	Average Liquid Holdup, %
1	70	3060	1785	2730	81.0
2	70	3086	1805	2735	84.1
3	72	2905	1615	2600	78.9
4	72	2750	1460	2505	78.9
5	78	2488	1180	2285	76.9
6	80	2314	1010	2105	74.8
7	84	2051	745	1805	81.0
8	105	2437	920	2150	84.1
9	44	2546	1510	2355	64.5
10	54	2112	1070	1855	64.5

Table 6.9 - Measured Chokeline Pressure Data For Gas-Mud Mixtures - Run No. 2

Data No.	Mud Rate gpm	Upstream Pressure, psig	Downstream Pressure, psig	Gas Injection Pressure, psig	Average Liquid Holdup, %
1	71	2177	825	1975	61.9
2	81	2337	895	2105	65.7
3	89	2460	940	2175	72.1
4	97	2572	955	2275	75.9
5	100	2584	945	2285	75.9
6	59	2372	1060	2095	68.3
7	52	2187	940	2015	59.3
8	47	2053	860	1885	52.9
9	40	1868	760	1720	50.3
10	61	2386	1040	2105	70.8

by defining the mud viscosity with the Bingham model plastic viscosity and the friction factor by the Colebrook equation. In this case, the plastic viscosity was used to calculate the Reynolds number for both the friction factor, as well as the type of flow regime. The Bingham model data were based on a pipe roughness of 0.00065 inches.

The second set of data was prepared by defining the mud viscosity with the power law model equivalent viscosity and the friction factor by the Dodge and Metzner equation. The power law equivalent viscosity was calculated based upon the nitrogen-mud mixture velocity, v_m (Equation 4.6).

The pressure drop data calculated with the Bingham model is shown in Tables 6.11, 6.12 and 6.13, and Figure 6.10, while those based upon the power law model are shown in Tables 6.14, 6.15 and 6.16, and Figure 6.11. The performance of each correlation will be discussed separately as follows.

6.2.1 Poettmann and Carpenter

Figure 6.6 displays the pressure data of the three runs as predicted by the Poettmann and Carpenter correlation. As mentioned in Chapter IV, this correlation relates the friction factor to the numerator of the Reynolds number; that is, it does not consider the viscosity term. It should also be mentioned that no

Table 6.11 - Choke Line Pressure Drop Data For Gas-Mud Mixtures - Run No. 1

(Bingham Plastic Model)

Mud Rate gpm	P_D psig	Measured Δp	Poettmann & Carpenter Δp	%Deviation	Hagedorn & Brown Δp	%Deviation	Orkiszewski Δp	%Deviation	Beggs & Brill Δp	%Deviation
70	1785	1275	1062	16.71	1295	-1.57	1197	6.12	1349	-5.80
70	1805	1281	1065	16.86	1297	-1.25	1199	6.40	1350	-5.39
72	1615	1290	1048	18.76	1297	-.54	1193	7.52	1355	-5.04
72	1460	1290	1024	20.62	1282	.62	1173	9.07	1345	-4.26
78	1180	1308	1000	23.55	1303	.38	1188	9.17	1381	-5.58
80	1010	1304	973	25.38	1300	.01	1180	9.50	1389	-6.52
84	745	1306	921	29.48	1297	.69	1172	10.26	1413	-8.19
105	920	1517	1045	31.11	1506	.73	1404	7.44	1659	-9.36
44	1510	1036	876	15.44	1030	.58	954	7.92	1052	-1.54
54	1070	1042	854	18.04	1069	-2.60	944	9.41	1104	-5.95

P_D = Downstream Choke Line Pressure, psig

Δp = Total Pressure Drop Across Choke Line, psi

Table 6.12 - Choke Line Pressure Drop Data For Gas-Mud Mixtures - Run No. 2

(Bingham Plastic Model)

Mud Rate gpm	P_D psig	Measured Δp	Poettmann & Carpenter Δp	%Deviation	Hagedorn & Brown Δp	%Deviation	Orkiszewski Δp	%Deviation	Beggs & Brill Δp	%Deviation
71	825	1352	906	32.99	1441	-6.58	1407	-4.07	1480	-9.47
81	895	1442	973	32.52	1544	-7.07	1525	-5.76	1620	-12.34
89	940	1520	1017	33.09	1622	-6.71	1616	-6.32	1731	-13.88
97	955	1617	1050	35.06	1699	-5.07	1703	-5.32	1849	-14.35
100	945	1639	1058	35.45	1726	-5.31	1735	-5.86	1893	-12.20
59	1060	1312	902	31.25	1356	-3.35	1325	-0.99	1331	-1.45
52	940	1247	827	33.68	1267	-1.60	1226	1.68	1212	2.81
47	860	1193	769	35.54	1196	-0.25	1151	3.52	1141	4.36
40	760	1108	684	38.27	1091	1.53	1041	6.05	1039	6.23
61	1040	1346	909	32.47	1373	-2.0	1341	0.37	1358	-0.89

P_D = Downstream Choke Line Pressure, psig

Δp = Total Pressure Drop Across Choke Line, psi

Table 6.13 - Choke Line Pressure Drop Data For Gas-Mud Mixtures - Run No. 3

(Bingham Plastic Model)

Mud Rate gpm	P_D psig	Measured Δp	Poettmann & Carpenter Δp	%Deviation	Hagedorn & Brown Δp	%Deviation	Orkiszewski Δp	%Deviation	Beggs & Brill Δp	%Deviation
79	500	1794	834	53.51	1612	10.14	1672	6.80	1711	4.63
81	315	1822	763	58.12	1633	10.37	1689	7.30	1762	3.29
73	350	1698	742	56.30	1544	9.07	1579	7.01	1623	4.42
67	325	1589	702	55.82	1481	6.80	1493	6.04	1523	4.15
61	290	1550	658	57.55	1418	8.52	1406	9.29	1420	8.39
56	285	1475	631	57.15	1360	7.80	1333	9.63	1336	9.42
51	275	1405	604	57.01	1302	7.33	1260	10.32	1256	10.61
45	265	1321	569	56.93	1225	7.27	1171	11.36	1156	12.49
40	240	1237	539	56.43	1157	6.47	1093	11.64	1072	13.34
34	210	1114	507	54.49	1069	4.04	999	10.32	967	13.20
32	1000	1276	674	47.18	1168	8.46	1096	14.11	1001	21.55
38	540	1201	600	50.04	1160	3.41	1114	7.24	1043	13.16
57	545	1550	734	52.65	1389	10.39	1382	10.84	1341	13.48
66	470	1653	756	54.27	1475	10.77	1493	9.68	1497	9.44

P_D = Downstream Choke Line Pressure, psig

Δp = Total Pressure Drop Across Choke Line, psi

Table 6.14 - Choke Line Pressure Drop Data For Gas-Mud Mixtures - Run No. 1

(Power Law Model)

Mud Rate gpm	P_D psig	Measured Δp	Poettmann & Carpenter Δp	%Deviation	Hagedorn & Brown Δp	%Deviation	Orkiszewski Δp	%Deviation	Beggs & Brill Δp	%Deviation
70	1785	1275	1062	16.71	1289	-1.1	1198	6.04	1287	-0.94
70	1805	1281	1065	16.86	1290	-0.7	1201	6.25	1288	-0.55
72	1615	1290	1048	18.76	1287	0.23	1182	8.37	1288	-0.16
72	1460	1290	1024	20.62	1271	1.47	1159	10.16	1274	1.24
78	1180	1308	1000	23.55	1278	2.29	1144	12.54	1292	1.22
80	1010	1304	973	25.38	1268	2.76	1124	13.80	1290	1.07
84	745	1306	921	29.48	1251	4.21	1096	16.08	1292	1.07
105	920	1517	1045	31.11	1425	6.06	1301	14.24	1495	1.45
44	1510	1036	876	15.44	1057	-2.03	1011	2.41	1022	1.35
54	1070	1042	854	18.04	1076	-3.26	979	6.05	1052	-0.96

P_D = Downstream Choke Line Pressure, psig

Δp = Total Pressure Drop Across Choke Line, psi

Table 6.15 - Choke Line Pressure Drop Data For Gas-Mud Mixtures - Mud No. 2

(Power Law Model)

Mud Rate gpm	P_D psig	Measured Δp	Poettmann & Carpenter Δp	Poettmann & Carpenter %Deviation	Hagedorn & Brown Δp	Hagedorn & Brown %Deviation	Orkiszewski Δp	Orkiszewski %Deviation	Beggs & Brill Δp	Beggs & Brill %Deviation
71	825	1352	906	32.99	1460	-7.99	1428	-5.6	1434	-6.07
81	895	1442	973	32.52	1548	-7.35	1539	-6.73	1564	-8.46
89	940	1520	1017	33.09	1617	-6.38	1623	-6.78	1666	-9.61
97	955	1617	1050	35.06	1684	-4.14	1701	-5.20	1771	-9.52
100	945	1639	1058	35.45	1708	-4.21	1729	-5.50	1811	-10.50
59	1060	1312	902	31.25	1391	-6.02	1359	-3.58	1302	0.76
52	940	1247	827	33.68	1316	-5.53	1262	-1.20	1188	4.73
47	860	1193	769	35.54	1254	-5.11	1188	.42	1119	6.20
40	760	1108	684	38.27	1157	-4.42	1080	2.53	1019	8.03
61	1040	1346	909	32.47	1405	-4.38	1374	-2.08	1327	1.41

P_D = Downstream Choke Line Pressure, psig

Δp = Total Pressure Drop Across Choke Line, psi

Table 6.16 - Choke Line Pressure Drop Data For Gas-Mud Mixtures - Run No. 3

(Power Law Model)

Mud Rate gpm	P_D psig	Measured Δp	Poettmann & Carpenter Δp	Poettmann & Carpenter %Deviation	Hagedorn & Brown Δp	Hagedorn & Brown %Deviation	Orkiszewski Δp	Orkiszewski %Deviation	Beggs & Brill Δp	Beggs & Brill %Deviation
79	500	1794	834	53.51	1634	8.92	1692	5.69	1623	9.53
81	315	1822	763	58.12	1657	9.06	1685	7.52	1652	9.33
73	350	1698	742	56.30	1586	6.60	1591	6.30	1531	9.84
67	325	1589	702	55.82	1535	3.40	1511	4.91	1438	9.50
61	290	1550	658	57.55	1484	4.26	1426	8.0	1340	13.55
56	285	1475	632	57.15	1439	2.44	1358	7.93	1265	14.24
51	275	1405	604	57.01	1393	0.85	1289	8.26	1188	15.44
45	265	1321	569	56.93	1331	-0.76	1203	8.93	1094	17.18
40	240	1237	539	56.43	1274	-2.99	1126	8.97	1012	18.19
34	210	1114	507	54.49	1195	7.27	1032	7.36	908	18.49
32	1000	1276	674	47.18	1264	0.94	1164	8.78	995	22.02
38	540	1201	600	50.04	1260	-4.91	1173	2.33	1015	15.49
59	545	1550	734	52.65	1445	6.77	1432	7.61	1292	16.65
66	470	1653	756	54.27	1520	8.05	1528	7.56	1428	13.61

P_D = Downstream Choke Line Pressure, psig

Δp = Total Pressure Drop Across Choke Line, psi

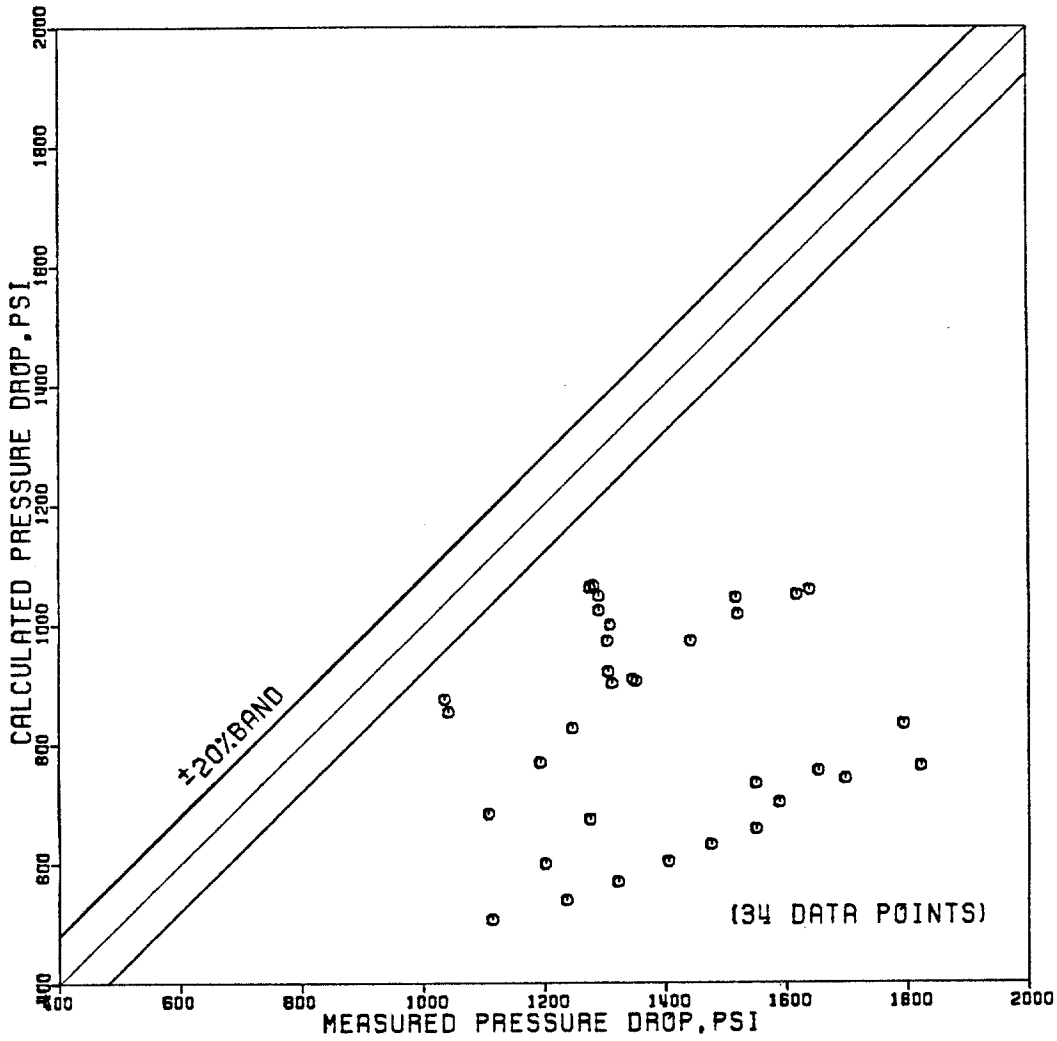

FIG.6.6-COMPARISON OF THE GAS-MUD MIXTURES PRESSURE DROP DATA.POETTMANN AND CARPENTER CORRELATION

attempt was made by the correlation to account for the liquid hold up and the type of flow regime. Accordingly, as expected, the correlation predictions had the highest deviation from measured data. However, as can be noted from the data or the statistical analysis of Table 6.19 or 6.20, the correlation performance was better with the lower mud viscosity. The correlation, with the low viscosity Mud No. 1, had an arithmetic mean deviation and average absolute deviation of 21.6% with an estimated standard deviation of 5.5%, as compared with 54.8% and 3.1% for the high viscosity Mud No. 3. One obvious reason for this behavior is that as the viscosity was increased, the friction factor became more significant in determining the total pressure drop.

6.2.2 Hagedorn and Brown

As shown in Figures 6.7, 6.10 and 6.11, most of the Hagedorn and Brown predictions fell within the $\pm$ 20% band. The statistical analysis of Tables 6.19 and 6.20 indicates that the correlation had the least deviation from the measured data. The correlation predictions, using the Bingham model, was found to have an overall arithmetic mean deviation of 2.1%, an average absolute deviation of 4.7%, and an estimated standard deviation of 5.6%; while the correlation predictions based on the power law was found to have values of -0.3%, 4.3%, and 5.1%, respectively.

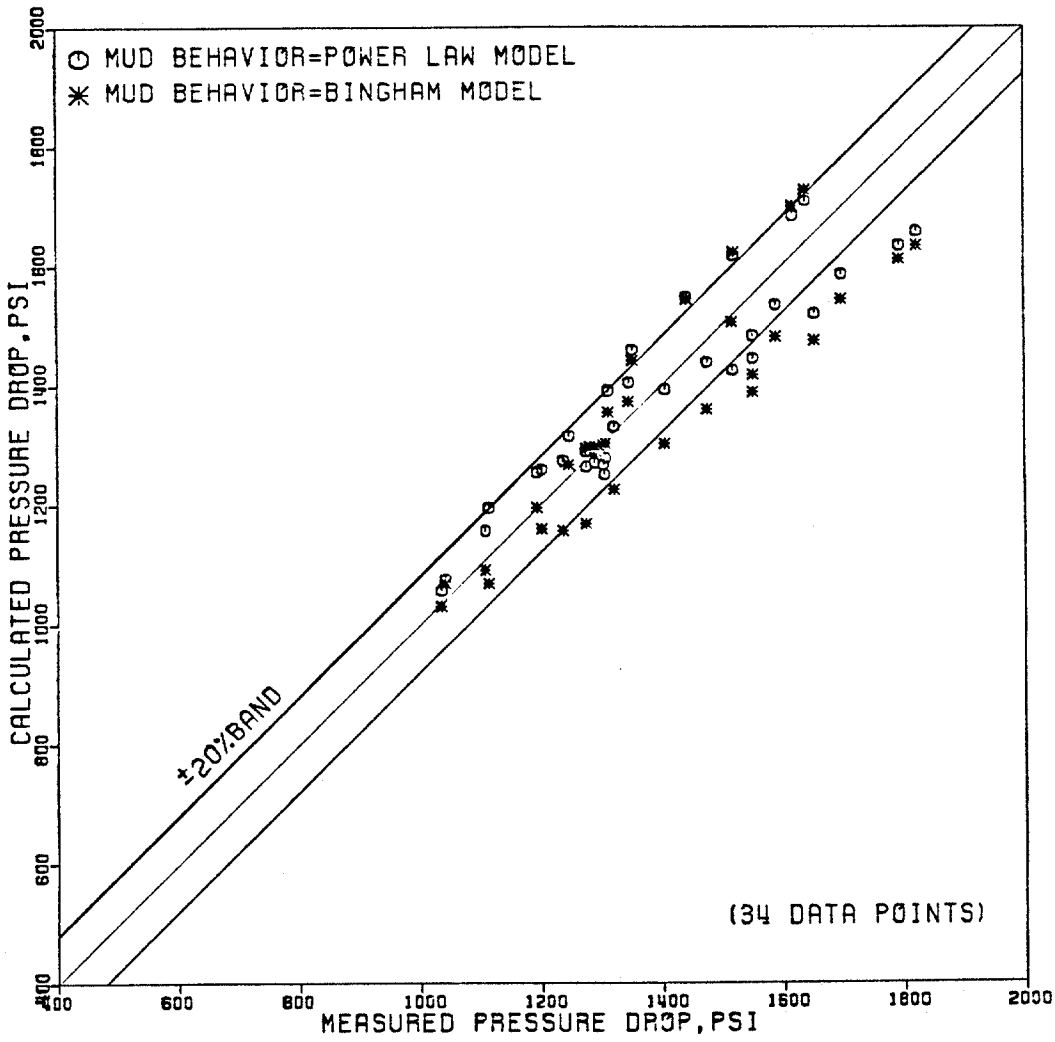

FIG.6.7-COMPARISON OF THE GAS-MUD MIXTURES PRESSURE DROP DATA. HAGEDORN AND BROWN CORRELATION

It was interesting to learn that the Hagedorn and Brown correlation, which does not consider the type of flow regime, showed better performance than those which do. However, as shown in Table 6.7, the experimental conditions under which the Hagedorn and Brown correlation was developed correspond more closely to this experimental procedure.

6.2.3 Orkiszewski

Figure 6.8 represents a plot of the data by Orkiszewski's correlation. The figure displays the correlation data listed in Tables 6.11 through 6.16. As is the case with the other correlations, the results of the Orkiszewski correlation based upon the Bingham model and the power law model were very close. When the correlation was used with the Bingham model, it was found to have an overall arithmetic mean deviation of 5.8%, an average absolute deviation of 7.5%, and an estimated standard deviation of 5.7%, while with the power law model, it had values of 4.8%, 6.9%, and 6.3%, respectively. Compared with the other correlations, the performance of the Orkiszewski correlation was the second best after Hagedorn and Brown.

6.2.4 Beggs and Brill

Figure 6.9 shows the pressure data as predicted by the correlation of Beggs and Brill. The overall

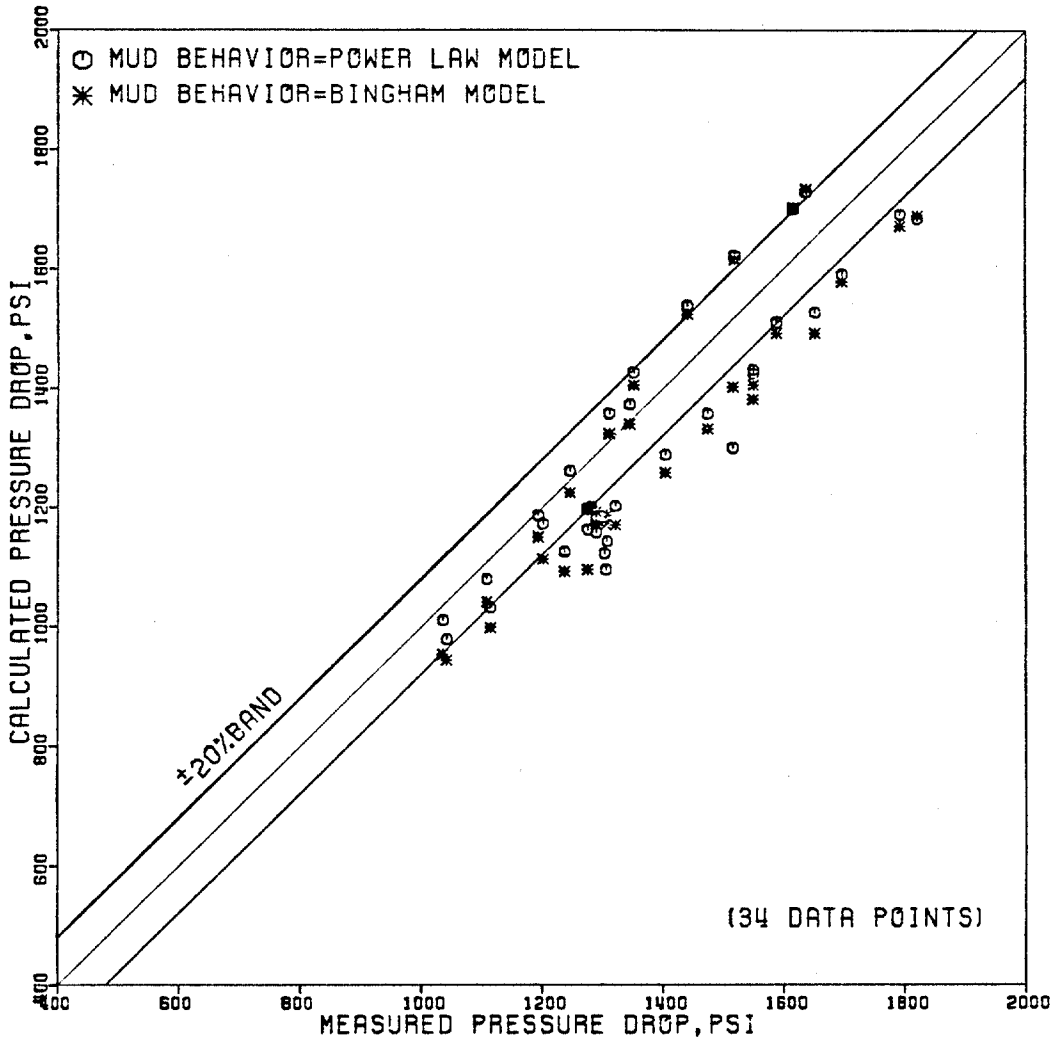

FIG.6.8-COMPARISON OF THE GAS-MUD MIXTURES PRESSURE DROP DATA. ORKISZEWSKI CORRELATION

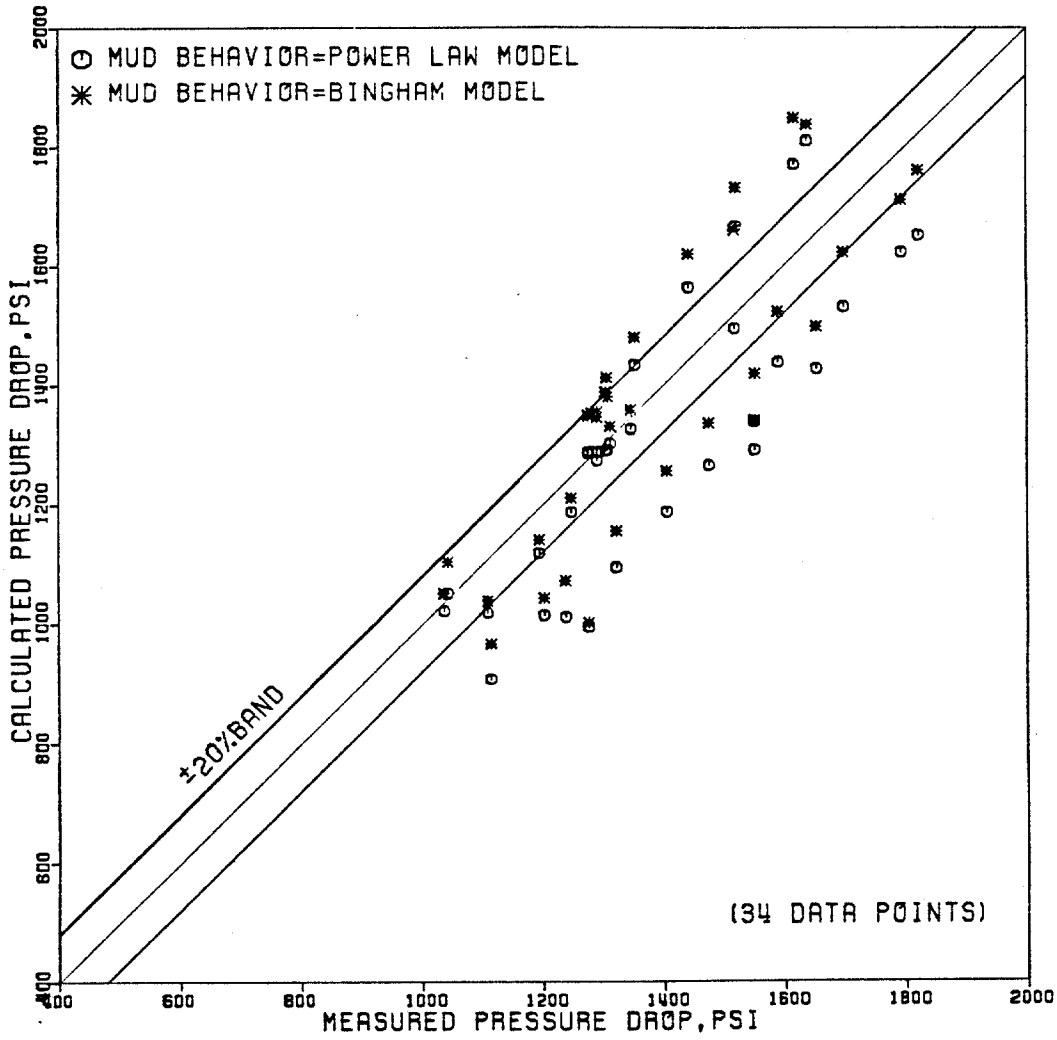

FIG.6.9-COMPARISON OF THE GAS-MUD MIXTURES PRESSURE DROP DATA. BEGGS AND BRILL CORRELATION

deviation of the Beggs and Brill correlation from the measured data is only exceeded by that of Poettmann and Carpenter. This correlation, with the Bingham model, was found to have an average arithmetic deviation of 1.0%, overall average absolute deviation of 8.2%, with an estimated standard deviation of 9.5%; while, with the power law it had values of 5.4%, 8.2% and 9.0% respectively. However, it should be mentioned, as shown in Table 6.7, that the correlation was originally developed based upon experimental data using water and air. This could explain the excellent performance of the correlation when the low viscosity Mud No. 1 (mostly water) was used. With this mud, using the power law model, the Beggs and Brill correlation reproduced the measured data to an arithmetic mean deviation of 0.5%, an average absolute deviation of 1.0%, and an estimated standard deviation of 1.0%.

Figures 6.10 and 6.11 were prepared to provide an easy visual comparison between the correlations. Based upon these figures as well as the tabulated data of Tables 6.8 through 6.16 and the statistical analysis of Tables 6.18 and 6.19, the following general observations can be made:

1. The data measured did not allow any significant discussions of the effect of other variables such as liquid hold up, gas-liquid ratio and

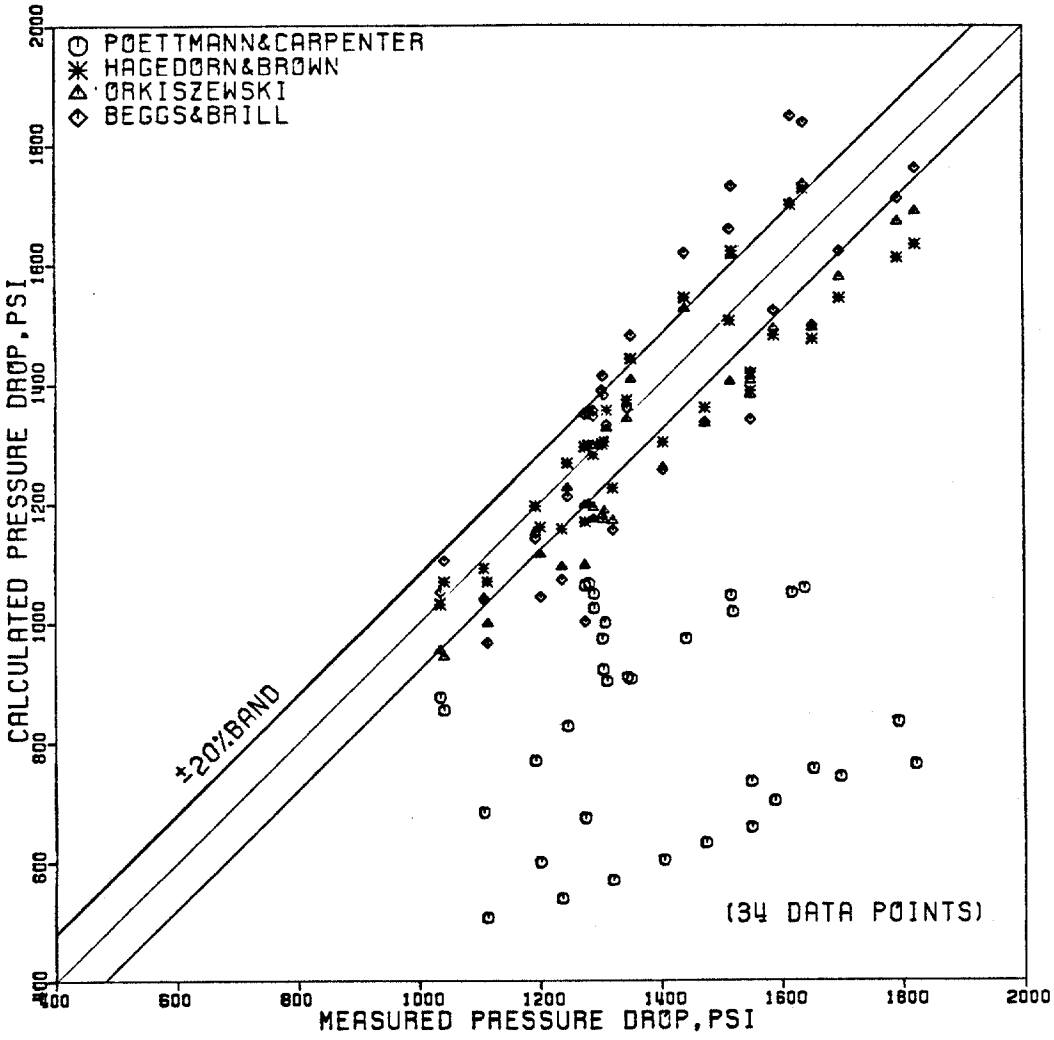

FIG.6.10-COMPARISON OF THE GAS-MUD MIXTURES PRESSURE DROP DATA. MUD BEHAVIOR IS DEFINED BY THE BINGHAM MODEL

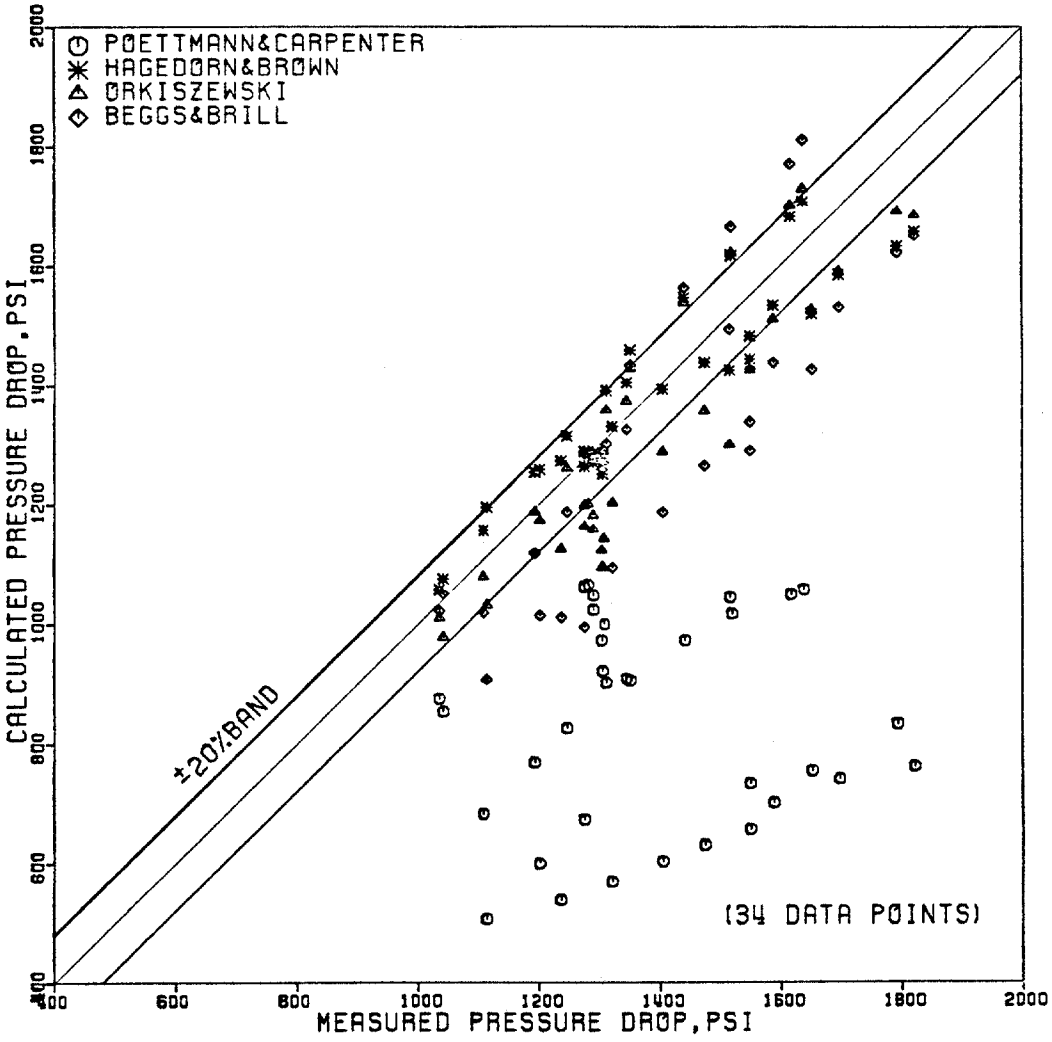

FIG.6.11-COMPARISON OF THE GAS-MUD MIXTURES PRESSURE DROP DATA. MUD BEHAVIOR IS DEFINED BY THE POWER LAW MODEL

type of flow regime on pressure drops. It was impractical to determine these variables at various depths.

2. All correlations, except that of Poettmann and Carpenter, showed acceptable performance. However, the correlations of Hagedorn and Brown seemed to have the best agreement with measured data.
3. Each correlation showed excellent performance when the measured data were taken under similar experimental conditions to those used to develop the particular correlation.
4. All correlations were found to have low values of estimated standard deviation. This showed that the calculated data had similar trends or behaviors as the measured data.
5. The majority of predicted data for Run No. 2 were higher than the measured data, while those of Runs No. 1 and 3 were lower.
6. In general, the deviation of calculated data from measured data was increased with the increase in viscosity.

6.3 Annular Flow Pressure Losses

Frictional pressure losses in the 2-7/8" x 7-5/8" casing annulus due to the flow of the clay water muds were very small, and impractical to measure. However,

Table 6.17 - Measured Drill Pipe Annulus Frictional Pressure Losses

Mud No. 1 Flow Rate gpm	Mud No. 1 Δp psi	Mud No. 2 Flow Rate gpm	Mud No. 2 Δp psi	Mud No. 3 Flow Rate gpm	Mud No. 3 Δp psi
125	1956	116	2182	105	2479
120	1831	112	2052	98	2318
118	1763	107	1934	93	2189
115	1683	103	1841	88	2044
111	1588	98	1669	83	1913
107	1533	94	1604	79	1792
103	1375	89	1453	75	1681
94	1186	87	1403	71	1575
90	1108	83	1294	67	1477
87	1029	76	1148	63	1383
80	859	72	1100	59	1304
69	667	67	965	54	1196
67	649	63	853	48	1050
62	578	58	782	44	955
59	519	55	709	41	895
54	465	52	675	36	815
48	380	49	664	32	744
43	312	43	533	30	700

since the drill pipe is actually a 2-7/" x 1.315" annulus, this annulus was utilized to obtain some annular flow data. Table 6.17 tabulates the annular data obtained with each mud.

The computer program "PRESS" was designed to allow the prediction of the annular flow frictional pressure losses. The technique which is used to treat the annular flow is presented in Section 2 of Chapter III.

6.4 Statistical Analysis

Pressure drop data obtained from different correlations as well as those actually measured were statistically analyzed to qualitatively measure the degree of accuracy and to evaluate the field applicability of the correlations. The statistical parameters used in this analysis are as follows.

1. Percent Deviation

Percent deviation, PD_i, is a measure of the deviation of each calculated pressure drop from the corresponding measured value. It is defined as follows:

$$PD_i = \frac{P_m - P_c}{P_m} \tag{6.1}$$

where

P_m = measured value of pressure drop as obtained from experiment

P_c = calculated value of pressure drop

A negative percent deviation indicates that calculated pressure drop is greater than the measured value. Percent deviations are shown in Tables 6.2 through 6.4 and 6.11 through 6.16.

2. Arithmetic Mean Deviation

The arithmetic mean deviation, AMD, is defined as follows:

$$AMD = \frac{\Sigma PD_i}{n} \tag{6.2}$$

where

n = number of data points.

A positive arithmetic mean deviation indicates that the correlation consistently predicts pressure drops greater than those actually measured, while a negative arithmetic mean deviation indicates that the correlation consistently predicts pressure drops greater than those actually measured.

3. Average Absolute Deviation

The average absolute deviation AAD, is used to evaluate the degree of accuracy of each correlation. It is defined as follows:

$$AAD = \frac{\Sigma |PD_i|}{n} \tag{6.3}$$

As indicated from Equation 6.3, the average absolute deviation is always positive. However, a high average

absolute deviation indicates that correlation pressure drops deviate greatly from measured data.

4. Estimated Standard Deviation

The estimated standard deviation, ESD, is used to measure the spread of each correlation data about the arithmetic mean deviation. It is defined as follows:

$$ESD = \left[\frac{\Sigma (PD_i - AMD)^2}{n}\right]^{\frac{1}{2}} \qquad (6.4)$$

A low estimated standard deviation indicates that calculated pressure drops have a relatively similar deviation from measured values, or in other words, it indicates that the calculated data are consistantly near, higher than or lower than measured data. A high estimated standard deviation indicates that calculated pressure drops are randomly scattered around the measured data.

Pressure loss arithmetic mean deviations, average absolute deviations, and estimated standard deviations are listed in Tables 6.18 through 6.20.

Table 6.18 - Summary of Statistical Analysis For Clay-Water Muds

Model	Mud No. 1 (27 data points)	Mud No. 2 (20 data points)	Mud No. 3 (18 data points)		Overall (65 data points)
		A. Arithmetic Mean Deviation			
			Laminar	Turbulent	
Bingham	-0.8	-6.4	-6.3	11.4	-4.5
Power Law	13.7	-3.7	13.3	-5.8	5.9
		B. Average Absolute Percent Deviation			
Bingham	2.8	6.4	6.4	-11.4	5.4
Power Law	13.9	4.2	13.3	7.3	10.0
		C. Estimated Standard Deviation			
Bingham	3.5	4.4	5.0	5.8	5.4
Power Law	7.4	5.8	4.7	6.4	10.9

Table 6.19 - Summary Of Statistical Analysis For The Gas-Mud Mixtures (The Bingham Plastic Model)

Correlation	Run No. 1 (10 data points)	Run No. 2 (10 data points)	Run No. 3 (14 data points)	Overall (34 data points)
	A. Arithmetic Mean Deviation			
Poettmann and Carpenter	21.6	34.0	54.8	38.9
Hagedorn and Brown	-0.3	-3.6	7.9	2.1
Orkiszewski	8.3	-1.7	9.4	5.8
Beggs and Brill	-5.8	-5.1	10.11	1.0
	B. Average Absolute Percent Deviation			
Poettmann and Carpenter	21.6	34.0	54.8	38.9
Hagedorn and Brown	0.9	3.9	7.9	4.7
Orkiszewski	8.3	4.0	9.4	7.5
Beggs and Brill	5.8	7.8	10.11	8.2
	C. Estimated Standard Deviation			
Poettmann and Carpenter	5.5	2.1	3.1	14.8
Hagedorn and Brown	1.2	3.0	2.3	5.6
Orkiszewski	1.4	4.4	2.3	5.7
Beggs and Brill	2.1	8.1	5.0	9.5

Table 6.20 - Summary Of Statistical Analysis For The Gas-Mud Mixtures (Power Law Model)

Correlation	Run No. 1 (10 data points)	Run No. 2 (10 data points)	Run No. 3 (14 data points)	Overall (34 data points)
	A. Arithmetic Mean Deviation			
Poettmann and Carpenter	21.6	34.0	54.8	38.9
Hagedorn and Brown	1.0	-5.6	2.5	-0.3
Orkiszewski	9.6	-3.4	7.2	4.8
Beggs and Brill	0.5	-2.3	14.5	5.4
	B. Average Absolute Percent Deviation			
Poettmann and Carpenter	21.6	34.0	54.8	38.9
Hagedorn and Brown	2.4	5.6	4.8	4.3
Orkiszewski	9.6	4.0	7.2	6.9
Beggs and Brill	1.0	6.5	14.5	8.2
	C. Estimated Standard Deviation			
Poettman and Carpenter	5.5	2.1	3.1	14.8
Hagedorn and Brown	2.9	1.4	5.2	5.1
Orkiszewski	4.5	3.2	1.8	6.3
Beggs and Brill	1.0	7.3	3.9	9.0

CHAPTER VII

CONCLUSIONS AND RECOMMENDATIONS

Based on the experimental results of this study, the following conclusions and recommendations can be made.

1. Flow behavior of non-Newtonian drilling fluids can be well defined by either the Bingham plastic or the power law model.
2. Available vertical two-phase correlations originally developed for gas and Newtonian fluid mixtures can be utilized to include the gas and non-Newtonian drilling fluid mixtures. This allows the predictions of subsea choke line pressure losses during gas kick well control operations.
3. Combined with either the Bingham plastic or the power law model, all the two-phase flow correlations except that of Poettmann and Carpenter provided acceptable results. However, the correlation of Hagedorn and Brown was found to have the least deviation from measured data.
4. The practical applicability of any correlation is highly influenced by the similarity between the conditions under which the correlation is

to be used and those under which it was developed.

5. It is suggested that the experimental work be continued to cover the following:
   a) Other mud types and mud properties.
   b) Other gas and mud rates.
   c) Annular flow.

NOMENCLATURE

A	Cross sectional area, ft^2
B_L	Liquid formation volume factor, bbl/STB
CN_L	Viscosity correction term, dimensionless
C_p	Heat capacity, $BTU/L_{bm}-°F$
D	Inside pipe diameter, ft.
D_1	Annulus outside diameter of inner pipe, ft.
D_2	Annulus inside diameter of outer pipe, ft.
De	Equivalent annulus diameter, ft.
f	Fanning Friction factor, dimensionless
f_m	Mixture Fanning friction factor, dimensionless
G	Geothermal gradient, °F/ft.
g	Acceleration of gravity, 32.17 ft/sec^2
g_c	Gravitational constant, 32.2 lbm-ft/lbf - sec^2
H	Total depth, ft
H_L	Liquid hold up, fraction
H_M	Mud hold up, fraction
H_N	Nitrogen holdup, fraction
H_g	Gas hold up, fraction
h_p	Overall heat transfer coefficient across pipe, $BTU/(ft^2-°F-hr)$
k	Consistency index, Lbf - sec^n/ft^2
L	Length, ft.
M	Gas Molecular weight
n	Flow behavior index, dimensionless
N_d	Pipe diameter number, dimensionless

N_L	Liquid viscosity number, dimensionless
NLR	Nitrogen - Liquid ratio, SCF/bbl
N_{Lv}	Liquid velocity number, dimensionless
NMR	Nitrogen - Mud ratio, SCF/bbl
N_{gv}	Gas velocity number, dimensionless
N_R	Reynolds number, dimensionless
N_{Rm}	Reynolds number of mixture, dimensionless
N_{Re}	Generalized Reynolds number, dimensionless
N_μ	Viscosity number, dimensionless
P	Pressure lbf/ft^2
p	Absolute pressure, psia
Q	Volumetric flow rate, ft^3/sec
Qa	Heat flow in annulus, BTU/hr
Qap	Heat flow across pipe, BTU/hr
Q_f	Heat flux to formation, BTU/hr
Qp	Heat flow in pipe, BTU/hr
q_L	Liquid flow rate, ft^3/sec
q_g	Gas flow rate, ft^3/sec
R	Radius, ft.
R	Dissolved gas-liquid ratio, SCF/STB
r	Radius of well, ft.
ra	Radius of casing, ft.
r_p	Radius of pipe, ft.
S	Dimensionless slip velocity
T	Absolute temperature, °R
T_a	Fluid temperature in annulus, °F
T_f	Formation temperature, °F

T_p	Fluid temperature in pipe, °F
Ts	Surface temperature, °F
U	Overall heat transfer coefficient across well-bore, BTU/(ft^2-°F-hr)
$\bar{v}$	Average fluid velocity, ft/sec
V_L	Actual liquid velocity, ft/sec
V_g	Actual gas velocity, ft/sec
V_m	Mixture superficial velocity, ft/sec
V_s	Slip velocity, ft/sec
V_{sg}	Gas superficial velocity, ft/sec
V_{sL}	Liquid superficial velocity, ft/sec
W	Mass flow rate, lbm/day
X	Distance, ft.
Z	Gas compressibility factor, dimensionless
γ_g	Gas gravity (air = 1)
γ_L	Liquid specific gravity (water = 1)
ε	Absolute pipe roughness, ft.
$\frac{\varepsilon}{D}$	Relative pipe roughness, dimensionless
λ_g	No-slip gas hold up, fraction
λ_L	No-slip liquid hold up, fraction
μ	Absolute viscosity, lbm/ft-sec
μ_a	Apparent viscosity, lbm/ft-sec
μ_e	Equivalent viscosity, lbm/ft-sec
μ_g	Gas viscosity, cp
μ_L	Liquid viscosity, cp
μ_m	Mixture viscosity, cp
μ_n	No-slip viscosity, cp

μ_p	Plastic viscosity, lbm/ft-sec
μ_s	Slip viscosity, cp
ρ	Density, lbm/ft^3
ρ_g	Gas density, lbm/ft^3
ρ_L	Liquid density, lbm/ft^3
ρ_m	Mixture density, lbm/ft^3
ρ_n	No-slip density, lbm/ft^3
ρ_s	Slip density, lbm/ft^3
ζ	Surface tension, dyne/cm
ζ_L	Gas-liquid interfacial tension, dyne/cm
τ	Shear stress, lbf/ft^2
τ_y	Yield point, lbf/ft^2
ψ	Secondary holdup correction factor, dimensionless
acc	Acceleration
e	Exponential
elev	Elevation
f	Friction

REFERENCES

1. Annis, M. R., "High-Temperature Flow Properties of Water-Base Drilling Fluids," Jour. Pet. Tech., (August, 1967).

2. Bartlett, L. E., "Effect of Temperature on the Flow Properties of Drilling Fluids," Paper Number SPE 1861, (1967).

3. Beck, R. W., et al., "The Flow Properties of Drilling Muds," Drilling and Production Practices, (1947).

4. Beggs, H. D. and Brill, J. P., "A Study of Two-Phase Flow in Inclined Pipes," Jour. Pet. Tech., (May, 1973).

5. Bourgoyne, A. T., et al., Applied Drilling Engineering, Louisiana State University, Petroleum Engineering Department.

6. Brill, J. P. and Beggs, H. D., Two-Phase Flow in Pipes, The University of Tulsa, (1978).

7. Brown, K. E., The Technology of Artificial Lift Methods, Vol. 1, Tulsa, PPC, (1977).

8. Butts, H. B., "The Effect of Temperature on Pressure Losses During Drilling," M.S. Thesis, Louisiana State University, (May, 1972).

9. Caldwell, D. H. and Babbitt, H. E., "Flow of Muds, Sludges, and Suspensions in Circular Pipe," Ind. Eng. Chem., Vol. 33, (February, 1941).

10. Craft, B. C., Holden, W. R., and Gravis, E. D., Jr., Well Design: Drilling and Production, Prentice-Hall, (1962).

11. Crittendon, B. C., "The Mechanics of Design and Interpretation of Hydraulic Fracture Treatments," Jour. Pet. Tech., (October, 1959).

12. Cullender, M. H. and Smith, R. V., "Practical Solution of Gas-Flow Equations for Wells and Pipelines with Large Temperature Gradients," Trans. AIME, Vol. 207, (1956).

13. "Deep Water Report," Offshore Tech., Vol. 41, (June, 1981).

14. Dodge, D. W., "Turbulent Flow of Non-Newtonian Fluids in Smooth Round Tubes," Ph.D. Thesis, University of Delaware, Newark, Delaware, (1958).

15. Dodge, D. W. and Metzner, A. B., "Turbulent Flow of Non-Newtonian Systems," AIChE Jour., Vol. 5, (June, 1959).

16. Encyclopedie Des Gas, L'air Liquide, Division Scientifique, Elsevier: Amsterdam, (1976).

17. Fredrickson, A. G. and Bird, R. B., "Non-Newtonian Flow in Annuli," Ind. Eng. Chem., Vol. 50, (March, 1958).

18. Hagedorn, A. R. and Brown, K. E., "Experimental Study of Pressure Gradients Occuring During Continuous Two-Phase Flow in Small-Diameter Vertical Conduits," Jour. Pet. Tech., (April, 1965).

19. Hanks, R. W., "On the Flow of Bingham Plastic Slurries in Pipes and Between Parallel Plates," SPE Jour., (December, 1967).

20. Hedstrom, B. O. A., "Flow of Plastic Materials in Pipes," Ind. Eng. Chem., Vol. 44, (March, 1952).

21. Holmes, C. S. and Swift, S. C., "Calculation of Circulating Mud Temperatures," Jour. Pet. Tech., (June, 1970).

22. Hunsker, J. C. and Rightmire, B. C., Engineering Applications of Fluid Mechanics, McGraw-Hill, (1947).

23. Katz, D. L., et al., Handbook of Natural Gas Engineering, McGraw-Hill, (1959).

24. Larid, W. M., "Slurry and Suspension Transport," Ind. Eng. Chem., Vol. 49 (January, 1957).

25. Melrose, J. C. et al., "A Practical Utilization of the Theory of Bingham Plastic Flow in Stationary Pipes and Annuli," Trans. AIME, Vol. 213, (1958).

26. Metzner, A. B. and Reed, J. C., "Flow of Non-Newtonian Fluid - Correlation of the Laminar, Transition, and Turbulent-Flow Regimes," AIChE Jour., Vol. 1, (December, 1955).

27. Moody, L. F., "Friction Factor for Pipe Flow," Trans. AIME, Vol. 66, (1944).

28. Nitrogen Oil Wells Supplier Company, Lafayette, Louisiana

29. Orkiszewski, J., "Predicting Two-Phase Pressure Drops in Vertical Pipe," Jour. Pet. Tech., (June, 1967).

30. Poettmann, F. H. and Carpenter, P. G., "The Multiphase Flow of Gas, Oil, and Water Through Vertical Flow Strings with Application to the Design of Gas-Lift Installations," Drill. and Prod. Prac., (1952).

31. Ros, N. C. J., "Simultaneous Flow of Gas and Liquid as Encountered in Well Tubing," Jour. Pet. Tech., (October, 1961).

32. Savins, J. G., "Generalized Newtonian (Pseudoplastic) Flow in Stationary Pipes and Annuli," Trans. AIME, Vol. 213, (1958).

33. Savins, J. G. and Roper, W. F., "A Direct-Indicating Viscometer for Drilling Fluids," Drill. Prod. Prac., Vol. 7, (1955).

34. Smith, R. V., et al., "Measurement of Resistance to Flow of Fluids in Natural Gas Wells," Trans. AIME, Vol. 201, (1954).

35. Sperry-Sun, Inc., Houston, Texas.

36. Ocean Margin Drilling Program: Final Report, "National Science Foundation," 1980.

APPENDIX A

The Fortran computer program "PRESS" calculates frictional pressure losses of Newtonian, Bingham plastic, or Power law fluids flowing in pipes or annuli. Nomenclature and units are provided in the main program or subroutines. The following is a list of subroutines used in the program. Variables in the argument lists with an asterisk are calculated in the subroutines.

A-1) VIS (T600, T300, PV*, YP*, UA*, N*, K*)

A-2) FFAN (IR, DE, XN, RN, RNR, F*)

A-3) VEL (NT, D1, D2, Q, DE*, V*)

A-4) EQVIS (IR, D1, D2, V, XN, XK, PV, YP, EU*, EUR*)

A-5) RYNOLD (W, EU, DE, V, RN*, EUR, RNR*)

A-6) PGRAD (IR, D1, D2, DE, F, W, V, YP, EU, GF*)

A-7) PL (IR, DENS, T600, T300, DEPTH, D1, D2, NT, DE
Q, V, P*, NR, NRR)

```
$JOB PRESS
C
C      COMPUTER PROGRAM "PRESS" CALCULATES THE FRICTIONAL PRESSUR LOSSES
C      USING THE BINGHAM PLASTIC CORRLATION (COLEBROOK EQUATION WITH
C      PLASTIC VISCOSITY) WHEN IR=1 AND THE POWER LAW MODEL (DODGE AND
C      METZNER CORRELATION) WHEN IR=2.
C
C      ABSOLUTE PIPE ROUGHNESS,E=0.00065 IN. (BINGHAM PLASTIC MODEL)
C      ABSOLUTE PIPE ROUGHNESS,E=0.0(POWER LAW MODEL)
C
C      THE ANNULUR GEOMETRIES ARE TREATED AS PIPES WITH EQUIVALENT DIAMETERS
C      AS CALCULATED BY SUBROUTINE "VEL".
C
C    THE FOLLOWING IS A LIST OF THE VARIABLES USED IN THE PROGRAM LISTED
C    IN ALPHABETICAL ORDER:
C      D1=OUTSIDE DIAMETER OF THE INNER PIPE (ANNULUS),IN.
C      D2=INSIDE DIAMETER OF OUTER PIPE (ANNULUS),IN.
C      DD=LENGTH ,FT.
C      DE= EQUIVALENT DIAMETER (INCHES)
C      DENS=FLUID DENSITY (PPG)
C      DEPB=LENGTH OF DRILL PIPE INCLUDES EQUIVALENT LENGTH OF SURFACE
C      EQUIPMENT.
C      DEPC=LENGTH OF CHOKE LINE INCLUDES EQUIVALENT LENGTH OF SURFACE
C      EQUIPMENT.
C      DEPD=LENGTH OF CASING ANNULUS
C      E=ABSOLUTE PIPE ROUGHNESS ,IN.
C      EU=EQUIVALENT VISCOSITY,CP
C      EUR=BINGHAM FLOW REGIME EQ.VISCOSITY,CP
C      F=FANNING FRICTION FACTOR
C      FLUID=TYPE OF FLUID
C      GF=FRICTIONAL PRESSURE GRADIENT ,PSI/FT.
C      ID1=INSIDE DIAMETER=1.049 IN. (1.315 IN.PIPE)
C      ID2=INSIDE DIAMETER=2.441 IN. (27/8 IN.PIPE)
C      ID3=INSIDE DIAMETER=1.995 IN. (23/8 IN.PIPE)
C      IDC=CASING INSID DIAMETER=6.969 IN.(75/8 IN.CASING)
C      IR=1 , BINGHAM PLASTIC MODEL
C      IR=2 , POWER LAW MODEL
C      K=CONSISTENCY INDEX,EQ.CP
C      N=FLOW BEHAVIOR INDEX,DIMENSIONLESS
C      NO=NUMBER OF DATA POINTS
C      NR=REYNOLDS NO.
C      NRR=BINGHAM FLOW REGIME REYNOLDS NUMBER
C      NT=1,DE IS CALCULATED USING CRITTENDON CRITERIA(JPT PP21,OCT.1959)
C      NT=2,DE IS CALCULATED USING HYDRAULIC RADIC CRITERIA
C      NT=3,DE IS CALCULATED USING SLOT FLOW CRITERIA
C      NT=4,DE IS CALCULATED USING GEOMETRY TERM CRITERIA
C      OD1=OUTSIDE DIAMETER=1.315 IN.(1.315 IN.PIPE)
C      OD2=OUTSIDE DIAMETER=2.875 IN.(27/8 IN.PIPE)
C      OD3=OUTSIDE DIAMETER=2.375 IN.(23/8 IN.PIPE)
C      P1=FRICTIONAL PRESSURE LOSS IN THE DRILL PIPE ANNULUS , PSI
C      P2=FRICTIONAL PRESSURE LOSS IN THE CASING ANNULUS , PSI
C      P3=FRICTIONAL PRESSURE LOSS IN THE CHOKE LINE , PSI
C      PHP=PUMP HORSEPOWER
C      PV=PLASTIC VISCOMETER,CP
C      Q=PUMP FLOW RATE (GPM)
C      RN=REYNOLDS NO.
C      RNR=BINGHAM FLOW REGIME REYNOLDS NUMBER
C      SR=8V/D OR THE NEWTONIAN SHEAR RATE AT PIPE WALL ,1/SEC
```

```
C     T300=VISCOMETER DIAL READING AT 300 RPM
C     T600=VISCOMETER DIAL READING AT 600 RPM
C     TPL=TOTAL PRESSURE LOSS ,PSI
C     UA=APPERANT VISCOSITY ,CP
C     V=AVERAGE FLUID VELOCITY,FT./SEC
C     W=FLUID DENSITY,PPG
C     XK=CONSISTENCY INDEX
C     XN=FLOW BEHAVIOR INDEX
C     YP=YIELD POINT ,LB/100 SQ.FT.
C
      DIMENSION Q(50),V1(50),V2(50),V3(50),NR1(50),NR2(50),NR3(50),SR1(5
     10),SR2(50),SR3(50),P1(50),P2(50),P3(50),TPL(50),PHP(50),DD(50)
     1,NER1(50),NER2(50),NER3(50)
      DIMENSION LABELX(50),LABELY(50)
      REAL N,K
      CHARACTER FLUID*11
      REAL ID1,ID2,ID3,IDC
      INTEGER DEPB,DEPC,DEPD,DD,Q
      DATA OD1,ID1,OD2,ID2,OD3,ID3,IDC/1.315,1.0419,2.875,2.441,2.375,1.
     1995,6.969/
      READ(5,90) (LABELX(I),I=1,10)
      READ(5,90) (LABELY(I),I=1,10)
   90 FORMAT(10A4)
      READ(5,*)DEPB,DEPC,DEPD
      READ(5,*)FLUID,DEBS,T600,T300,NO
      READ(5,*) (Q(I),I=1,NO)
      CALL VIS(T600,T300,PV,YP,UA,N,K)
      DO 10 IR=1,2
      DO 329 NT=1,4
C
C     CALCULATION OF EQUIVALENT DIAMETERS BY CALLING SUBROUTINE "VEL"
      CALL VEL(NT,OD1,ID2,0.0,DE1,VA)
      CALL VEL(NT,OD2,IDC,0.0,DE2,VB)
      CALL VEL(NT,0.0,ID3,0.0,DE3,VC)
C
      WRITE(6,55)
      WRITE(6,111)
  111 FORMAT(20X,'LSU NEW RESEARCH AND TRAINING FACILITY'/20X,38(1H-))
      WRITE(6,324)FLUID
  324 FORMAT( 20X,'PREDICTED PRESSURE LOSS DATA(',A11,')'/20X,41(1H-))
      IF(IR.EQ.1)GO TO 673
      WRITE(6,674)
  674 FORMAT(20X,'DATA ARE BASED ON DODGE AND METZNER CORRELATION'/20X,
     147(1H-))
      GO TO 91
  673 WRITE(6,675)
  675 FORMAT(20X,'DATA ARE BASED ON BINGHAM PLASTIC CORRELATION'/20X,
     145(1H-))
   91 CONTINUE
      IF(NT.EQ.1)WRITE(6,15)
   15  FORMAT( 20X,'EQUIVALENT DIAMETER IS BASED ON CRITTENDON CRITERIA'/
     120X,51(1H-))
      IF(NT.EQ.2)WRITE(6,16)
   16  FORMAT( 20X,'EQUIVALENT DIAMETER IS BASED ON HYDRAULIC RADIUS CRIT
     1ERIA'/20X,56(1H-))
```

```
      IF(MT.EQ.3)WRITE(6,17)
   17 FORMAT( 20X,'EQUIVALENT DIAMETER BASED ON SLOT FLOW CRITERIA'/20X,4
     116(1H-))
      IF(MT.EQ.4)WRITE(6,18)
   18 FORMAT( 20X,'EQUIVALENT DIAMETER BASED ON GEOMETRY TERM CRITERIA'/
     120X,51(1H-))
      IF(FLUID.EQ.'WATER')GO TO 280
      WRITE(6,68)DENS,PV,YP,N,K
   68 FORMAT(20X,'MUD DENSITY=',F4.2,'PPG,PV=',F3.0,
     1'CP,YP=',F4.0,'LB/100SQ.FT,N=',F4.2,',K=',F5.0,'EQ.VIS.'/
     220X,67(1H-))
      GO TO 281
  280 WRITE(6,86)DENS,UA
   86 FORMAT(20X,'WATER DENSITY=',F4.2,'PPG,VISCOSITY=',F2.0,'CP'/1X,38(
     11H-))
  281 CONTINUE
      WRITE(6,313)
  313 FORMAT(1X,'Q=FLOW RATE , V=VELOCITY , NR=REYNOLDS NO., DP=PRESS.LO
     1SS , DE=EQUIVALENT DIAMETER,'
     2 /1X,'TPL=TOTAL PRESS.LOSS IN THE SYSTEM,HP=PUMP HORSEPOWER.')
      WRITE(6,14)
   14 FORMAT(/8X,'1.315X27/8IN.DRILL PIPE',9X,'27/8X75/8IN.CASING'
     1,11X,'23/8IN.CHOKE LINE')
      WRITE(6,103) DE1,DE2,DE3
  103 FORMAT(14X,'DE=',F5.3,'IN.',18X,'DE=',F5.3,'IN.',18X,'ID=',F5.3,
     1'IN.'/ 8X,25(1H-), 4X,24(1H-), 4X,24(1H-))
      WRITE(6,70)DEPB,DEPC,DEPC
   70 FORMAT( 2X,'Q',5X,'V',5X ,'NR' ,2X,'DP/',I4,'FT',1X,'8V/DE',4X,'V'
     1,5X ,'NR' ,1X,'DP/',I4,'FT',1X,'8V/DE',4X,'V',4X ,'NR', 2X,'DP/',I
     24,'FT',1X,'8V/DE',3X,'TPL',5X,'HP'
     1,3X,'NRE DP',2X,'NRE CSG',1X,'NRE CH')
      WRITE(6,80)
   80 FORMAT(1X,'GPM',3X,'FPS',11X,'PSI',4X,'1/SEC',3X,'FPS',10X
     1,'PSI',4X,'1/SEC',3X,'FPS', 10X, 'PSI',4X,'1/SEC',3X
     2,'PSI')
      DO 100 J=1,NO
C
C     CALCULATION OF PRESSURE LOSS IN EACH CONDUIT(P1,P2,P3) BY CALLING
C     SUBROUTINE" PL"
      CALL PL(IR,DENS,T600,T300,DEPB,OD1,ID2,MT,DE1,Q(J),V1(J),P1(J),
     1NR1(J),NRE1(J))
      CALL PL(IR,DENS,T600,T300,DEPD,OD2,IDC,MT,DE2,Q(J),V2(J),P2(J),
     1NR2(J),NRE2(J))
      CALL PL(IR,DENS,T600,T300,DEPC,0.0,ID3,MT,DE3,Q(J),V3(J),P3(J),
     1NR3(J),NRE3(J))
C
C     CALCULATION OF TOTAL PRESSURE LOSS IN THE SYSTEM
      TPL(J)=P1(J)+P2(J)+P3(J)
C
      PHP(J)=TPL(J)*FLOAT(Q(J))/1714.
C
C     CALCULATION OF 8V/D OR THE NEWTONIAN SHEAR RATE
      SR1(J)=(8.*V1(J)/(DE1/12.))
      SR2(J)=(8.*V2(J)/(DE2/12.))
      SR3(J)=(8.*V3(J)/(DE3/12.))
```

```
      WRITE(6,212)Q(J),V1(J),NR1(J),P1(J),SR1(J),V2(J),NR2(J),P2(J),SR2(
     1J),V3(J),NR3(J),P3(J),SR3(J),TPL(J),PHP(J)
     2,NRR1(J),NRR2(J),NRR3(J)
  212 FORMAT(/1X,I3,2X,F4.1,1X,I6,2X,F6.1,2X,F6.1,3X,F3.1,1X,I6,3X,F5.1,
     12X,F5.1,3X,F4.1,1X,I6,1X,F6.1,2X,F6.1,2X,F6.1,1X,F5.1
     2,1X,I6,1X,I6,1X,I6)
  100 CONTINUE
  329 CONTINUE
   10 CONTINUE
      WRITE(6,55)
   55 FORMAT(1H1)
      STOP
      END
C
C

      SUBROUTINE VIS(T600,T300,PV,YP,UA,N,K)
C     SUBROUTINE"VIS"CALCULATES PLASTIC VISCOSITY,YIELD POINT,
C     APPERANT VISCOITY,FLOW BEHAVIOR INDEX,AND CONSISTENCY INDEX
C     FOR A FANN VISCOMETER MODEL 35.
C
      REAL N,K
      PV=T600-T300
      YP=T300-PV
      N=3.322*ALOG10(T600/T300)
      K=510.*T300/511.**N
      UA=300.*T600/600.
      RETURN
      END
C
C

      SUBROUTINE FFAN(IR,DE,XN,RN,RNR,F)
C     SUBROUTINE"FFAN"CALCULATES FANNING FRICTION FACTOR,F
C
C     I=NO. OF TRIAL
      E=0.00065
C     CHECKING FOR LAMINAR FLOW
      IF(RNR.LT.1000.)GO TO 30
C
C     TURBULENT FLOW EQUATION
      FO=.01
      I=0
   10 IF(IR.EQ.1)GO TO 50
C
C     POWER LAW MODEL
      F=(1./(4./XN**.75*ALOG10(RN*FO**(1.-XN/2))-.395/XN**1.2))**2
      GO TO 60
C
C     BINGHAM PLASTIC FLUID ,COLEBROOK FUNCTION
   50 F=1./(-4.*ALOG10(E/(3.72*DE)+1.255/(RN*(FO**.5))))**2
   60 CONTINUE
      I=I+1
      IF(I.GT.50)GO TO 20
      IF(ABS((F-FO)/FO).LT.1.E-04)RETURN
      FO=F
```

```
      GO TO 10
   20 WRITE(6,26)
   26 FORMAT(1X,22HFFPOW DID NOT CONVERGE)
C
C     LAMINAR FLOW EQUATION
C
   30 F=16./RN
      RETURN
      END
C
C
      SUBROUTINE VEL(NT,D1,D2,Q,DE,V)
C     SUBROUTINE"VEL"ALCULATES AVERAGE FLUID VELOCITY,V,AND EQUIVALENT
C     DIAMETER ,DE.
C
C     CHECKING FOR ANNULUR FLOW
      IF(D1.GT.0.0) GO TO 10
C
C     PIPE FLOW,EQUIVALENT DIAMETER EQUATION
      DE=D2
      DV=D2**2
      GO TO 20
C
C     ANNULAR FLOW,EQUIVALENT DIAMETER EQUATION(CRITTENDON CRITERIA)
   10 X=(D2**4-D1**4)
      Y=((D2**2-D1**2)**2)/ALOG(D2/D1)
      Z=(D2**2-D1**2)**.5
      DE=.5*(((X-Y)**.25)+Z)
      DV=DE**2
C
C     ANNULAR FLOW,EQUIVALENT DIAMETER EQUATION(HYDRAULIC RADIUS CRITERIA)
      IF(NT.EQ.2)DE=D2-D1
C
C     ANNULAR FLOW,EQUIVALENT DIAMETER EQUATION(SLOT FLOW CRITERIA)
      IF(NT.EQ.3)DE=.816*(D2-D1)
C
C     ANNULAR FLOW,EQUIVALENT DIAMETER EQUATION(GEOMETRY TERM CRITERIA)
      IF(NT.EQ.4)DE=SQRT(D2**2+D1**2-((D2**2-D1**2)/ALOG(D2/D1)))
      IF(NT.NE.1)DV=(D2**2-D1**2)
   20 V=Q/2.448/DV
      RETURN
      END
C
C
      SUBROUTINE EQVIS(IR,D1,D2,V,XN,XK,PV,YP,EU,EUR)
C     SUBROUTINE"EQVIS"CALCULATES EQUIVALENT VISCOSITY ,EU
C
      IF(IR.EQ.2)GO TO 140
C
C     BINGHAM PLASTIC MODEL
      EU=PV
      IF(D1.GT.0.)GO TO 16
      EUR=PV+6.66*YP*D2/V
      GO TO 60
```

```
   16 EUR=PV+5.*YP*(D2-D1)/V
      GO TO 60
  140 IF(D1.GT.0.)GO TO 30
C     POWER LAW MODEL
      EU=XK/96.*(D2/V)**(1.-XN)*((3.+(1./XN))/.0416)**XN
      EUR=EU
      GO TO 60
   30 EU=XK/144.*((D2-D1)/V)**(1.-XN)*((2.+1./XN)/.0208)**XN
      EUR=EU
   60 CONTINUE
      RETURN
      END
C
C

      SUBROUTINE REYNOLD(W,EU,DE,V,RN,EUR,RNR)
C     SUBROUTINE"REYNOLD"CALCULATES REYNOLDS NUMBER,RN
      RN=928.*W*V*DE/EU
      RNR=928.*W*V*DE/EUR
      RETURN
      END
C
C

      SUBROUTINE PGRAD(IR,D1,D2,DE,F,W,V,YP,EU ,GP)
C     SUBROUTINE"PGRAD" CALCULATES FRICTIONAL PRESSURE GRADIENT
C     PRESSURE GRADIENT IS CALCULATE WITH FANNING EQUATION AND EIGHTER
C     HAGEN-POISEUILLE LAW (PIPE FLOW) OR SLOT FLOW EQUATION (ANNULUR
C     FLOW) IN BOTH LAMINER AND TURBULENT REGIMES
C
C     CHECKING FOR PRESSURE GRADIENT USING FANNING EQUATION
      GP=F*W*V**2/25.8/DE
C
C     CHECKING FOR ANNULUR FLOW
      IF(D1.GT.0.)GO TO 70
C
C     CHECKING FOR PRESSURE GRADIENT(PIPE FLOW) USING HAGEN-POISEUILLE LAW
      GP2=EU *V/1500./D2**2
C
C     BINGHAM PLASTIC MODEL
      IF(IR.EQ.1)GP2=GP2+YP/225./D2
      GO TO 80
C
C     CHECKING FOR  PRESSURE GRADIENT(ANNULAR FLOW) USING SLOT FLOW EQUATION
   70 GP2=EU *V/1000./(D2-D1)**2
C     BINGHAM PLASTIC MODEL
C
      IF(IR.EQ.1)GP2=GP2+YP/200./(D2-D1)
   80 IF(GP2.GT.GP)GP=GP2
      RETURN
      END
```

```
      SUBROUTINE PL(IR,DENS,T600,T300,DEPTH,D1,D2,NT,DE,Q,V,P,NR,NRR)
C     SUBROUTINE "PL" CALCULATES FRICTIONAL PRESSURE LOSS
C
      REAL N,K
      INTEGER Q,DEPTH
      QQ=FLOAT(Q)
C
C     CALCULATION OF VISCOUS PROPERTIES BY CALLING SUBROUTINE"VIS"
      CALL VIS(T600,T300,PV,YP,UA,N,K)
C     CALCULATION OF AVERAGE FLUID VELOCITY (V) AND EQUIVALENT
C     DIAMETER (DE) BY CALLING SUBROUTINE "VEL"
      CALL VEL(NT,D1,D2,QQ,DE,V)
C
C     CALCULATION OF EQUIVALENT VISCOSITY (EU) BY CALLING
C     SUBROUTINE "EQVIS"
      CALL EQVIS(IR,D1,D2,V, N, K,PV,YP,EU,EUR)
C
C     CALCULATION OF REYNOLDS NO. AND FLOW REGIME REYNOLDS NO.
C     BY CALLING SUBROUTINE"RYNOLD"
      CALL RYNOLD(DENS,EU,DE,V,RN,EUR,RNR)
C
C     CALCULATION OF FANNING FRICTION FACTOR "F" BY CALLING
C     SUBROUTINE "FFAN"
      CALL FFAN(IR,DE,N,RN,RNR,F)
C
C     CALCULATION OF FRICTIONAL PRESSURE GRADIENT "GF" BY
C     CALLING SUBROUTINE "PGRAD"
      CALL PGRAD(IR,D1,D2,DE,F,DENS,V,YP,EU ,GF)
      NR=IFIX(RN)
      NRR=IFIX(RNR)
      P=GF*FLOAT(DEPTH)
      RETURN
      END
```

APPENDIX B

The Fortran computer program "TWPHAS" calculates total pressure losses (frictional, elevation, and acceleration) of nitrogen gas-drilling fluid mixtures flowing in pipes. The two-phase flow subroutines were originally designed by Brill and Beggs.[6] These subroutines include the following correlations, 1) Poettmann and Carpenter, 2) Baxendell and Thomas, 3) Fancher and Brown, 4) Hagedorn and Brown, 5) Orkiszewski, and 6) Beggs and Brill. Nomenclature and units are provided in the main program or subroutines. The following is a list of subroutines used in the program. Variables in the argument lists with an asterisk are calculated in the subroutines.

B-1) SURF (P, T, SURL*)

B-2) VISN (PSIA, TFAH, VISN2*)

B-3) ZNZ (P, T, Z*)

B-4) EQVIS (IR, D, V, XK, XN, PV, YP, EU*)

B-5) VIS (T600, T300, PV*, YP*, UA*, N*, K*)

B-6) TEMP (Q, TD, DELH)

B-7) FFAN (IR, ED, XN, RN, F*)

B-8) FLAGR2 V, H, F, NV, NH, IV, IH, VARG*, HARG*)

B-9) FLAGR (X, Y, XARG*, IDEG, NPTS)

B-10) CATEGA (DIA, ED, RP, VM, HLNS, DENG, DENL, CVIS, VISL, DPDL*, KCODE, IR, XN)

B-11) HAGR (DIA, ED, P, VM, HLNS, DENG, DENL, GVIS,
XNLV, VISL, XNGV, XNL, XND, HL*, DPDL*, IR, XN)

B-12) ORKIS (DIA, ED, P, VM, HLNS, DENG, DENL, GVIS,
SURL, XNLV, VISL, XNGV, HL*, DPDL*, IR, XN, IREG*)

B-13) BEGBR (DIA, ED, P, VM, HLNS, DENG, DENL, GVIS,
XNLV, HL*, VISL, DPDL*, IR, XN, IREG*)

```
$JOB TWPHAS
C
C      SUBROUTINE"TWPHAS"CALCULATES NITROGEN GAS-MUD MIXTURES TOTAL
C      PRESSURE DROP IN PIPES. TOTAL PRESSURE DROPS ARE CALCULATES
C      BASED ON THE FOLLOWING TWO-PHASE FLOW CORRELATIONS:
C      1) POETTMANN & CARPENTER , K=1
C      2) BAXENDELL & THOMAS , K=2
C      3) FANCHER & BROWN , K=3
C      4) HAGEDORN & BROWN , K=4
C      5)ORKISZEWSKI ,K=5
C      6) BEGGS & BRILL ,K=6
C
C      THE MUD VISCOSITY IS DEFINED BY THE BINGHAM MODEL PLASTIC
C      VISCOSITY,PV,WHEN IR=1,OR BY THE POWER LAW EQUIVALENT VISCOSITY,
C      EU,WHEN IR=2.
C
C    THE FOLLOWING IS A LIST OF THE VARIABLES USED IN THE PROGRAM LISTED
C    IN ALPHABETICAL ORDER:
C      ACCGR=ACCELERATION PRESSURE GRADIENT,PSI/FT.
C      AP=CROSS-SECTIONAL AREA OF PIPE,FT.
C      BM=MUD VOLUME FACTOR ,BBL/STB
C      BW=WATER FORMATION VOLUME FACTOR,BBL/STB
C      CP=MUD HEAT CAPACITY,BTU/(LB-DEG.F)
C      DCSG=CASING INSIDE DIAMETER,IN.
C      DENG=GAS DENSITY,LBM/CU.FT.
C      DENL=LIQUID DENSITY,LBM/CU.FT.
C      DENS=MUD DENSITY,LB/GAL
C      DEPTH=DEPTH,FT.
C      DI=PIPE DIAMETER,IN.
C      DIA=PIPE DIAMETER,FT.
C      DLTA=LENGTH INCREMENT,FT.
C      DP=DRILL PIPE INSIDE DIAMETER,IN.
C      DP= PRESSURE DROP ,PSI/INCREMENT.
C      DPDL=TOTAL PRESSURE GRADIENT,PSI/FT.
C      E=ABSOLUTE PIPE ROUGHNESS ,IN.
C      ED=RELATIVE PIPE ROUGHNESS,DIMENSIONLESS
C      ELGR=ELEVATION PRESSURE GRADIENT,PSI/FT.
C      EU=EQUIVALENT VISCOSITY,CP
C      F=FANNING FRICTION FACTOR,DIMENSIONLESS
C      FF=MOODY FRICTION FACTOR,DIMENSIONLESS
C      FM=MASS FLOW RATE,LB/HR.
C      FRGR=FRICTION PRESSSURE GRADIENT,PSI/FT.
C      G=GEOTHERMAL GRADIENT DEG.F/FT.
C      GLR=GAS/LIQUID RATIO,SCF/STB
C      GSG=GAS GRAVITY(AIR=1.0)
C      GVIS=GAS VISCOSITY,CP
C      HL=LIQUID HOLD UP,FRACTION
C      HLNS=NO-SLIP LIQUID HOLD UP,FRACTION
C      HP=OVERALL HEAT TRANSFER COEFFICIENT,BTU/(SQ.FT-DEG.F-HR)
C      IR=1 , BINGHAM PLASTIC MODEL
C      IR=2 , POWER LAW MODEL
C      IREG=TWO-PHASE FLOW REGIME SEE SUBROUTINES "ORKIS" AND "BEGBR"
C      K=CONSISTENCY INDEX,EQ.CP
C      N=FLOW BEHAVIOR INDEX,DIMENSIONLESS
C      NINC=NO.OF INCREMENTS
C      NO=NUMBER OF DATA POINTS
C      P=PRESSURE,PSIA
C      PA=PRESSURE , PSIA
```

```
C     PATHM=ATMOSPHERIC PRESSUR=14.7 PSI
C     PBAR=PRESSURE,BAR
C     PD=DOWNSTREAM PRESSURE ,PSIG
C     PDP=DOWNSTREAM PRESSURE ,PSIA
C     PSIA=PRESSURE,PSIA
C     PV=PLASTIC VISCOMETER,CP
C     QG=GAS FLOW RATE,SCF/DAY
C     QGPT=GAS FLOW RATE AT T AND P ,CU.FT/DAY
C     QL=LIQUID FLOW RATE,STB/D
C     QLPT=LIQUID FLOW RATE AT T AND P,BBL/DAY
C     QM=MUD FLOW RATE,GPM
C     QN=NITROGEN FLOW RATE,SCF/MIN
C     QW=WATER FLOW RATE,STB/D
C     RN=REYNOLDS NO.
C     RP=PIPE RADIUS,FT
C     RSN=SOLUTION NITROGEN/WATER RATIO,SCF/CU.FT.
C     RW=WELL RADIUS,FT
C     SGL=LIQUID(MUD)SPECIFIC GRAVITY(WATER=1.0)
C     SLDS=SOLIDS CONTENT,FRACTION BY VOLUME
C     SURL=GAS-LIQUID SURFACE TENSION,DYNES/CM.
C     T300=VISCOMETER DIAL READING AT 300 RPM
C     T600=VISCOMETER DIAL READING AT 600 RPM
C     T=TEMPERATURE,DEG.F
C     TA=TEMPERATURE IN DEG.R
C     TABS=ABSOLUTE TEMPERATURE,DEG.R
C     TC=TEMPERATURE,DEG.C
C     TD=TOTAL DEPTH,FT.
C     TF=FLOWING TEMPERATURE,DEG.F
C     TFAR=TEMPERATURE,DEG.F
C     TIN= FLOWING INLET TEMPERATURE ,DEG.F
C     TKEL=TEMPERATURE,DEG.K
C     TO=ABSOLUTE TEMPERATURE =460 DEG.
C     TS=SURFACE TEMPERATURE,DEG.F
C     U=OVERALL HEAT TRANSFER COEFFICIENT CROSS WELLBORE,
C     BTU/(SQ.FT.-DEG.F-HR.)
C     UA=APPERANT VISCOSITY ,CP
C     V=AVERAGE FLUID VELOCITY,FT./SEC
C     VISL=LIQUID VISCOSITY,CP
C     VISN2=NITROGEN GAS VISCOSITY,CP
C     VM=SUPERFICIAL MIXTURE VELOCITY,FT/SEC.
C     VSG=SUPERFICIAL GAS VELOCITY,FT/SEC.
C     VSL=SUPERFICIAL LIQUID VELOCITY,FT/SEC.
C     XK=CONSISTENCY INDEX,EQ.CP
C     XN=FLOW BEHAVIOR INDEX,DIMENSIONLESS
C     XND=DIAMETER NUMBER,DIMENSIONLESS
C     XNGV=GAS VELOCITY NUMBER,DIMENSIONLESS
C     XNL=LIQUID VISCOSITY NUMBER,DIMENSIONLESS
C     XNLV=LIQUID VELOCITY NUMBER,DIMENSIONLESS
C     YP=YIELD POINT ,LB/100 SQ.FT.
C     Z=COMPRESSIBILITY FACTOR
C
      DIMENSION DEPTH(250),PDP(250),PD(250),P1(250),P2(250),P3(250),
     1P4(250),P5(250),P6(250),DP1(250),DP2(250),DP3(250),DP4(250)
     2 ,DP5(250),DP6(250),HL4(250),HL5(250),HL6(250),QM(250)
     3,IREGO(250),IREGB(250)
      COMMON /BL1/DCSG,DP,U,HP,CP,TIN,TS,G,DENS
```

```
      COMMON /BL2/TF(500)
      READ(5,*) SLDS,DENS,T600,T300,NO,TIN,QN
      READ(5,*) (QM(I),I=1,NO)
      READ(5,*) (PD(I),I=1,NO)
      DATA TD,DEP,DI,DCSG,DP/6000.,3000.,1.995,6.969,2.875/
      DATA U,HP,CP,G,TS/1.3,30.,.8,.011,75./
      E=.00065
      GSG=.94876
      SGL=DENS/8.33
      ED=E/DI
      DIA=DI/12.
      AP=3.14159*DIA**2/4.
      DO 122 IR=1,2
C
C     CALCULATION OF MUD VISCOUS PROPERTIES
      CALL VIS(T600,T300,PV,YP,UA,XN,XK)
C
      WRITE(6,75)
      WRITE(6,65) DI,DENS,PV
   65 FORMAT(10X,'CALCULATED TOTAL CHOKE LINE PRESSURE'/10X,36(1H-)/
     110X,'PIPE ID=',F5.3,'IN. ,MW=',F4.1,'PGG ,PV=',F4.0/10X,36(1H-))
      IF(IR.EQ.1) WRITE(6,16)
      IF(IR.EQ.2) WRITE(6,17)
   16 FORMAT(20X,'BINGHAM PLASTIC MUD BEHAVIOR')
   17 FORMAT(20X,'POWER LAW MUD BEHAVIOR')
      DO 400 I=1,NO
      PDP(I)=PD(I)+14.7
      QL=60.*24.*QM(I)/42.
      QG=60.*24.*QN
      GLR=QG/QL
       WRITE(6,15) QM(I),QN,GLR
   15 FORMAT( /01X,'MUD RATE =',F5.0,'GPM , GAS RATE =',F5.0,'SCF/MIN ,
     1 GLR =',F5.0,'SCF/STB'/1X,65(1H-))
      WRITE(6,45)
   45 FORMAT( /7X,'DEPTH',2X,'PTCR',3X,'BXTH',3X,'FNBN',3X,'HGBN',
     13X,'ORKS',3X,'BGBR',3X,'HGBN',3X,'ORKS',3X,'BGBR',3X,'ORKS',3X,
     2'BGBR')
      WRITE(6,55)
   55 FORMAT( 9X,'FT',3X,'PSI',4X,'PSI',4X,'PSI',4X,'PSI',4X ,'PSI',4X,
     1'PSI',5X,'HL',5X,'HL',5X,'HL',4X,'IREG',3X,'IREG')
      DO 500 K=1,6
      P=PDP(I)
      DLTA=20.
C
C     CALCULATION OF FLOWING TEMPERATURE
      CALL TEMP(QM(I),TD,DLTA)
C
      NINC=IFIX(DEP/DLTA)
      N=NINC+1
      IRUN=0
      DO 100 II=1,N
      T=TF(II)
      TABS=T+460.
      TC=(T-32.)*5./9.
      PBAR=P/14.504
      PA=P-14.7
```

```
C     CALCULATION OF NITROGEN "Z"FACTOR
      CALL ZN2(PA,T,Z)
C
C     CALAULATION OF NITROGEN/WATER RATIO
      RSN=5.3E-05*TC**2-.0105*TC+1.45+1.803*ALOG(PBAR)-8.23
      IF(PBAR.LT.100.)RSN=-.002*TC+.2+.175*ALOG(PBAR)+.14
C
C     CALAULATION OF NITROGEN/MUD  RATIO
      GLRC=GLR-RSN*(1.-SLDS)*5.165
C
      BW=1.+1.2E-4*(T-60.)+1.E-6*(T-60.)**2-3.33E-6*P
      BM=BW
      QLPT=QL*BM*5.615
      QGPT=QL*GLRC*Z*TABS*14.7/520./P
      VSL=QLPT/AP/24./3600.
      VSG=QGPT/AP/24./3600.
      VM=VSL+VSG
C
C     CALCULATION OF MUD EQUIVALENT VISCOSITY
      CALL EQVIS(IR,DI,VM,XN,XK,PV,YP,EU)
      VISL=EU
C
      HLNS=VSL/VM
      DENG=2.7*P*GSG/Z/TABS
      DENL=SGL*62.4/BM
C
C     CALCULATION OF NITROGEN VISCOSITY
      CALL VISN(P,T,GVIS)
C
C     CALCULATION OF GAS-WATER SURFACETENSION
      CALL SURF(P,T,SURL)
C
      XNLV=1.938*VSL*(DENL/SURL)**.25
      XNGV=1.938*VSG*(DENL/SURL)**.25
      XND=120.872*DIA*SQRT(DENL/SURL)
      XNL=.15726*VISL/(DENL*(SURL**3))**.25
      IF(K.EQ.1)GO TO 10
C     K=1,POETTMANN & CARPENTER CORRELATION.
      IF(K.EQ.2)GO TO 20
C     K=2,BAXENDELL & THOMAS CORRELATION
      IF(K.EQ.3)GO TO 30
C     K=3,FANCHER & BROWN CORRELATION.
      IF(K.EQ.4)GO TO 40
C     K=4,HAGEDORN & BROWN CORRELATION.
      IF(K.EQ.5)GO TO 50
C     K=5,ORKISZEWSKI CORRELATION.
      IF(K.EQ.6)GO TO 60
C     K=6,BEGGS & BRILL CORRELATION.
   10 CALL CATEGA(DIA,ED,GLR,VM,HLNS,DENG,DENL,GVIS,VISL,DPDL1,1,IR,XN)
      DP1(II)=-DPDL1*DLTA
      P1(II)=P
      P=P+DP1(II)
      GO TO 110
   20 CALL CATEGA(DIA,ED,GLR,VM,HLNS,DENG,DENL,GVIS,VISL,DPDL2,2,IR,XK)
      DP2(II)=-DPDL2*DLTA
      P2(II)=P
```

```
      P=P+DP2(II)
      GO TO 110
   30 CALL CATEGA(DIA,ED,GLR,VM,HLNS,DENG,DENL,GVIS,VISL,DPDL3,3,IR,XN)
      DP3(II)=-DPDL3*DLTA
      P3(II)=P
      P=P+DP3(II)
      GO TO 110
   40 CALL HAGBR(DIA,ED,P,VM,HLNS,DENG,DENL,GVIS,XNLV,VISL,
     1XNGV,XNL,XND,HL4(II),DPDL4,IR,XN)
      DP4(II)=-DPDL4*DLTA
      P4(II)=P
      P=P+DP4(II)
      GO TO 110
   50 CALL ORKIS(DIA,ED,P,VM,HLNS,DENG,DENL,GVIS,SUEL,XNLV,VISL,
     1XNGV,HL5(II),DPDL5,IR,XN,IREG)
      IREGO(II)=IREG
      DP5(II)=-DPDL5*DLTA
      P5(II)=P
      P=P+DP5(II)
      GO TO 110
   60 CALL BEGBR(DIA,ED,P,VM,HLNS,DENG,DENL,GVIS,XNLV,HL6(II),VISL,
     1DPDL6,IR,XN,IREG)
      IREGB(II)=IREG
      DP6(II)=-DPDL6*DLTA
      P6(II)=P
      P=P+DP6(II)
  110 CONTINUE
      DEPTH(II)=DLTA*IRUN
      IRUN=IRUN+1
  100 CONTINUE
  500 CONTINUE
      DO 600 J=1,N,25
      P1(J)=P1(J)-14.7
      P2(J)=P2(J)-14.7
      P3(J)=P3(J)-14.7
      P4(J)=P4(J)-14.7
      P5(J)=P5(J)-14.7
      P6(J)=P6(J)-14.7
      WRITE(6,25)DEPTH(J),P1(J),P2(J),P3(J),P4(J),P5(J),P6(J),HL4(J)
     1,HL5(J),HL6(J),IREGO(J),IREGB(J)
   25 FORMAT(/6X,F5.0,2X,F5.0,2X,F5.0,2X,F5.0,2X,F5.0,2X,F5.0,2X,F5.0
     1,3X,F5.3,2X,F5.3,2X,F5.3,3X,I2,5X,I2)
  600 CONTINUE
  400 CONTINUE
      WRITE(6,75)
   75 FORMAT('1')
  122 CONTINUE
      STOP
      END
```

```
      SUBROUTINE SURF(P,T,SURL)
C     SUBROUTINE"SURF"CALCULATES GAS-WATER SURFACE TENSION
C
      DIMENSION STVA(10),STV74(10),STV280(10)
      DATA STVA/
     10.,1000.,2000.,3000.,4000.,5000.,6000.,7000.,8000.,9000./
      DATA STV74/
     175.,63.,59.,57.,54.,52.,52.,51.,50.,49./
      DATA STV280/
     153.,46.,40.,33.,26.,21.,21.,22.,23.,24./
      STN74=FLAGR(STVA,STV74,P,2,10)
      STN280=FLAGR(STVA,STV280,P,2,10)
      SURL=(STN74-STN280)/(280.-74.)*(T-74.)*(-1)+STN74
      IF(T.LT.74.) SURL=STN74
      IF(T.GT.280.) SURL=STN280
      RETURN
      END
C
C
      SUBROUTINE EQVIS(IR,D,V,XN,XK,PV,YP,EU)
C     SUBROUTINE"EQVIS"CALCULATES EQUIVALENT VISCOSITY ,EU
      IF(IR.EQ.2)GO TO 140
C
C     BINGHAM PLASTIC MODEL
      EU=PV
      GO TO 60
C     POWER LAW MODEL
  140 EU=XK/96.*(D/V)**(1.-XN)*((3.+(1./XN))/.0416)**XN
   60 CONTINUE
      RETURN
      END
C
C
      SUBROUTINE VISN(PSIA,TFAH,VISN2)
C     SUBROUTINE"VISN"CALCULATES NITROGEN GAS VISCOSITY
C
      TKEL=(TFAH-32.)*5./9.+273.16
      VIS=((TKEL/273.16)**1.5)*(6.493256/(TKEL+118.))
      VISN2=VIS+1.51E-06*PSIA
      RETURN
      END
C
C
      SUBROUTINE ZN2(P,T,Z)
C     SUBROUTINE 'ZN2" CALCULATES THE AVERAGE COMPRESSIBILITY FACTOR(Z)
C     OF NITROGEN AT AVERAGE PRESSURE AND TEMPERATURE
C
      DIMENSION A0(3),A1(3),A2(3),A3(3),B0(3),B1(3),B2(3),C0(3),C1(3),C2
     1(3)
C     PA=PRESSURE,PSIG
      DATA A0(2),A0(3),A1(2),A1(3),A2(2),A2(3),A3(2),A3(3),C1(1),C2(1)/1
     10*0.0/
```

```
      A0(1)=1.679393E-7
      A1(1)=-6.2243E-10
      A2(1)=8.0385E-13
      A3(1)=-3.5472E-16
      B0(1)=-3.122E-4
      B1(1)=8.488E-7
      B2(1)=-5.37E-10
      C0(1)=1.0
      B0(2)=2.2817E-4
      B1(2)=-4.066E-7
      B2(2)=2.3E-10
      C0(2)=-0.0956
      C1(2)=2.5E-3
      C2(2)=-1.5E-6
      B0(3)=2.2042E-4
      B1(3)=-3.515E-7
      B2(3)=1.815E-10
      C0(3)=-0.1573
      C1(3)=2.438E-3
      C2(3)=-1.4E-6
      PATM=14.7
      TO=460.
      PA=PATM+P
      TA=TO+T
      I=3
      IF(PA.LT.8000.) I=2
      IF(PA.LT.4000.) I=1
      A=A0(I)+A1(I)*TA+A2(I)*TA**2+A3(I)*TA**3
      B=B0(I)+B1(I)*TA+B2(I)*TA**2
      C=C0(I)+C1(I)*TA+C2(I)*TA**2
      Z=A*PA**2+B*PA+C
      RETURN
      END
C
C

      SUBROUTINE VIS(T600,T300,PV,YP,UA,N,K)
C     SUBROUTINE"VIS"CALCULATES PLASTIC VISCOSITY,YIELD POINT,
C     APPEARANT VISCOITY,FLOW BEHAVIOR INDEX,AND CONSISTENCY INDEX
C     FOR A FANN VISCOMETER MODEL 35.
      REAL N,K
      PV=T600-T300
      YP=T300-PV
      N=3.322*ALOG10(T600/T300)
      K=510.*T300/511.**N
      UA=300.*T600/600.
      RETURN
      END
C
C

      SUBROUTINE TEMP(Q,TD,DELH)
C     SUBROUTINE"TEMP"CALCULATES FLOWING TEMPERATURE
C     N=NUMBER OF DEPTH INTERVALS
C     DELH=DISTANCE BETWEEN DEPTH STATIONS,FT
      DIMENSION DEPTH(500),TG(500),TP(500)
```

```
      COMMON /BL1/DW,DP,U,HP,CP,TPI,TS,G,RHO
      COMMON /BL2/TA(500)
      RW=DW/2./12.
      RP=DP/2./12.
      FM=Q*60.*RHO
      A =(FM*CP)/(2.*3.14159*RP*HP)
      B =(RW*U)/(RP*HP)
      C1=(B/(2.*A))*(1.+(1.+4./B)**0.5)
      C2=(B/(2.*A))*(1.-(1.+4./B)**0.5)
      C3= 1.+(B/2.)*(1.+(1.+4./B)**0.5)
      C4= 1.+(B/2.)*(1.-(1.+4./B)**0.5)
      AL1=G*A
      AL2=2.7183**(C1*TD)
      AL3=2.7183**(C2*TD)
      ALPHA=AL1-(TPI-TS+AL1)*AL2*(1.-C3)
      BETA=AL3*(1.-C4)-AL2*(1.-C3)
      CK2=ALPHA/BETA
      CK1=(TPI-CK2-TS+G*A)
      N=IFIX(TD)/IFIX(DELH)
      N=N+1
      NN=1
      DEPTH(NN)=0.0
      DO 50 NN=1,N
      TG(NN)=TS+G*DEPTH(NN)
      EX1=2.7183**(C1*DEPTH(NN))
      EX2=2.7183**(C2*DEPTH(NN))
      EX3=G*DEPTH(NN)
      TA(NN)=CK1*C3*EX1+CK2*C4*EX2+EX3+TS
      TP(NN)=CK1*EX1+CK2*EX2+EX3+TS-G*A
      DEPTH(NN+1)=DEPTH(NN)+DELH
   50 CONTINUE
      RETURN
      END
C
C

      SUBROUTINE FFAN(IR,ED,XN,RN,F)
C     SUBROUTINE"FFAN"CALCULATES FANNING FRICTION FACTOR,F
C
C     CHECKING FOR LAMINAR FLOW
      IF(RN.LT.1000.)GO TO 30
      FO=.01
C     I=NO. OF TRIAL
      I=0
   10 IF(IR.EQ.1)GO TO 50
C
C     POWER LAW MODEL
      F=(1./(4./XN**.75*ALOG10(RN*FO**(1.-XN/2))-.395/XN**1.2))**2
      GO TO 60
C
C     BINGHAM PLASTIC FLUID ,COLEBROOK FUNCTION
   50 F=1./(-4.*ALOG10(ED/3.72+1.255/(RN*(FO**.5))))**2
   60 CONTINUE
      I=I+1
      IF(I.GT.50)GO TO 20
      IF(ABS((F-FO)/FO).LT.1.E-04)RETURN
```

```
      FO=F
         GO TO 10
   20 WRITE(6,26)
   26 FORMAT(1X,22HFFPOW DID NOT CONVERGE)
C
C     LAMINAR FLOW EQUATION
   30 F=16./RE
      RETURN
      END
C
C
      FUNCTION FLAGR2 (V,H,F,NV,NH,IV,IH,VARG,HARG)
C
C     FLAGR2 IS A FUNCTION SUBPROGRAM FOR PERFORMING DOUBLE INTER-
C     POLATION.IT CALLS FLAGR (LISTED ON A FOLLOWING PAGE) FOR EACH
C     INTERPOLATION.
C     F IS THE FUNCTION VALUE MATRIX
C     H IS THE COLUMN (HORIZONTAL) ARRAY.
C     IV AND IH ARE DEGREES OF INTERPOLATION IN THE  V AND H ARRAYS.
C     NV AND NH ARE DIMENSIONS OF THE VERTICAL AND HORIZONTAL ARRAYS.
C     V IS THE ROW (VERTICAL) ARRAY.
C     VARG AND HARG ARE ARGUMENTS FOR WHICH INTERPOLATED FUNCTION
C     VALUES ARE DESIRED
C
      DIMENSION V(NV),H(NH),F(NV,NH),X(50),Y(50)
      DO 20 J=1,NH
      DO 10 I=1,NV
   10 X(I)=F(I,J)
   20 Y(J)=FLAGR(V,X,VARG,IV,NV)
      FLAGR2=FLAGR(H,Y,HARG,IH,NH)
      RETURN
      END
C
C
      FUNCTION FLAGR (X,Y,XARG,IDEG,NPTS)
C
C     INTERPOLATION ROUTINE SIMILAR TO FLAGR IN APPLIED NUMERICAL
C     METHODS BY CARNAHAN, LUTHER AND WILKES, JOHN WILEY AND SONS,
C     PG. 31.
C     FLAGR USES THE LAGRANGE FORMULA TO EVALUATE THE INTERPOLATING
C     POLYNOMIAL OF DEGREE IDEG FOR ARGUMENT XARG USING THE DATA
C     VALUES X(MIN).....X(MAX) AND Y(MIN).....Y(MAX) WHERE MIN =
C     MAX-IDEG. THE X(I) VALUES ARE NOT NECESSARILY EVENLY SPACED
C     AND CAN BE IN EITHER INCREASING OR DECREASING ORDER.
C     X IS THE ARRAY OF INDEPENDENT VARIABLE DATA POINTS.
C     Y IS THE ARRAY OF DEPENDENT VARIABLE DATA POINTS.
C     XARG IS THE ARGUMENT FOR WHICH AN INTERPOLATED VALUE IS DESIRED.
C     IDEG IS THE DEGREE OF INTERPOLATING POLYNOMIAL (1 IS LINEAR,
C     2 IS QUADRATIC, ETC).
C     NPTS IS THE NUMBER OF DATA POINTS IN X AND Y.
C
      DIMENSION X(NPTS),Y(NPTS)
      N=IABS(NPTS)
      N1=IDEG+1
```

```
      L=1
      IF (X(2).GT.X(1)) GO TO 1
      L=2
C
C     CHECK TO BE SURE THAT XARG IS WITHIN RANGE OF X(I) VALUES
C     FOR INTERPOLATION PURPOSES. IF IT IS NOT, SET FLAGR EQUAL
C     TO THE APPROPRIATE TERMINAL VALUE (Y(1) OR Y(N)) AND RETURN.
C     NOTE THAT THIS PRECLUDES EXTRAPOLATION OF DATA.
    1 GO TO (2,3),L
    2 IF (XARG.LE.X(1)) GO TO 4
      IF (XARG.GE.X(N)) GO TO 5
      GO TO 6
    3 IF (XARG.GE.X(1)) GO TO 4
      IF (XARG.LE.X(N)) GO TO 5
      GO TO 6
    4 FLAGR=Y(1)
      RETURN
    5 FLAGR=Y(N)
      RETURN
C
C     DETERMINE VALUE OF MAX.
    6 GO TO (10,20),L
C
C     DATA ARE IN ORDER OF INCREASING VALUES OF X.
   10 DO 11 MAX=N1,N
      IF (XARG.LT.X(MAX)) GO TO 12
   11 CONTINUE
C
C     DATA ARE IN ORDER OF DECREASING VALUES OF X.
   20 DO 21 MAX=N1,N
      IF (XARG.GT.X(MAX)) GO TO 12
   21 CONTINUE
C     COMPUTE VALUE OF FACTOR.
   12 MIN=MAX-IDEG
      FACTOR=1.
      DO 7 I=MIN,MAX
      IF (XARG.NE.X(I)) GO TO 7
      FLAGR=Y(I)
      RETURN
    7 FACTOR=FACTOR*(XARG-X(I))
C     EVALUATE INTERPOLATING POLYNOMIAL.
      YEST=0.
      DO 9 I=MIN,MAX
      TERM=Y(I)*FACTOR/(XARG-X(I))
      DO 8 J=MIN,MAX
      IF (I.NE.J) TERM=TERM/(X(I)-X(J))
    8 CONTINUE
    9 YEST=YEST+TERM
      FLAGR=YEST
      RETURN
      END
```

```
      SUBROUTINE CATEGA (DIA,ED,RP,VM,HLNS,DENG,DENL,GVIS,VISL,DPDL,
     1KCODE,IR,XN)
C
C     SUBROUTINE TO CALCULATE PRESSURE GRADIENT IN -PSI/FT USING
C     ANY OF THE CATEGORY A CORRELATIONS.  THE CORRELATION
C     SELECTED IS DETERMINED BY THE VALUE OF KCODE.
C     IF KCODE.EQ.1  POETTMANN AND CARPENTER CORRELATION
C     IF KCODE.EQ.2  BAXENDELL AND THOMAS CORRELATION
C     IF KCODE.EQ.3  FANCHER AND BROWN CORRELATION
C
      DIMENSION XF(10) ,FPC(10),FBT(10),FFB(3,10)
      DIMENSION XFL(10),FPCL(10),FBTL(10),FFBL(3,10),FFBBL(10)
C
C     DATA FOR ABSCISSA OF FRICTION FACTOR CORRELATIONS
      DATA XF/
     1 3.,5.,10.,20.,30.,40.,50.,60.,80.,120./
C     FRICTION FACTOR DATA FOR POETTMANN AND CARPENTER
      DATA FPC/
     1 8.,1.2,.26,0.072,.038,.024,.0176,.0136,.0088,.0048/
C     FRICTION FACTOR DATA FOR BAXENDELL AND THOMAS
      DATA FBT/
     1 8.,1.2,.26,.072,.038,.0268,.0236,.0220,.0204,.0188/
C     FRICTION FACTOR DATA FOR FANCHER AND BROWN
      DATA FFB/
     1 1.6,.38,.18,.4,.21,.095,.145,.09,.04,.063,.04,.016,
     2 .042,.026,.0092,.0292,.018,.0064,.0240,.014,.0047,
     3 .02,.011,.004,.0148,.008,.003,.01,.005,.0022/
C
C     PREPARE FRICTION FACTOR ARRAYS FOR INTERPOLATION.
      DO 1 I=1,10
      XFL(I)=ALOG(XF(I))
      FPCL(I)=ALOG(FPC(I))
      FBTL(I)=ALOG(FBT(I))
      DO 1 J=1,3
    1 FFBL(J,I)=ALOG(FFB(J,I))
C
C     CHECK FOR SINGLE PHASE GAS OR LIQUID FLOW.
      IF (HLNS.LT.1.) GO TO 2
      HL=1.
      DENNS=DENL
      IREG=1
      GO TO 9
    2 IF (HLNS.GT.0.) GO TO 3
      HL=0.
      DENNS=DENG
      VIS=GVIS
      IREG=2
      XN=1.
      IR=1
      GO TO 9
C     CALCULATE ABSCISSA OF FRICTION FACTOR CORRELATIONS.
    3 DENNS=DENL*HLNS+DENG*(1.-HLNS)
      X=DENNS*VM*DIA
      XL=ALOG(X)
      IREG=3
```

```
C     CALCULATE FRICTION FACTOR.
      GO TO (4,5,6),KCODE
C     CALCULATE POETTMANN AND CARPENTER FRICTION FACTOR.
    4 FF=EXP(FLAGR(XFL,FFCL,XL,2,10))
      GO TO 10
C
C     CALCULATE BAXENDELL AND THOMAS FRICTION FACTOR.
    5 FF=EXP(FLAGR(XFL,FBTL,XL,2,10))
      GO TO 10
C     CALCULATE FANCHER AND BROWN FRICTION FACTOR.
    6 J=3
      IF (REP.LT.3000.) J=1
      DO 7 I=1,10
    7 FFBBL(I)=FFBL(J,I)
      FF=EXP(FLAGR(XFL,FFBBL,XL,2,10))
      GO TO 10
C
C     CALCULATE SINGLE PHASE FLOW FRICTION FACTOR.
    9 REYN=1488.*DENNS*VM*DIA/VIS
C
C      CALLING FANNING FRICTION FACTOR.
      CALL FFAN(IR,ED, XN,REYN,F)
C
C     CALCULATING MOODY FRICTION FACTOR
      FF=4.*F
C
C     CALCULATE FRICTION, ELEVATION AND TOTAL PRESSURE GRADIENTS.
   10 FRGR=FF*DENNS*VM**2/(2.0*32.2*DIA*144.)
      ELGR=DENNS/144.
      DPDL=-(FRGR+ELGR)
      RETURN
      END
C
C


      SUBROUTINE HAGBR (DIA,ED,P,VM,HLNS,DENG,DENL,GVIS,
     1 XNLV,VISL,XNGV,XNL,XND,HL,DPDL,IR,XN)
C
C     SUBROUTINE TO CALCULATE LIQUID HOLDUP AND PRESSURE GRADIENT
C     USING THE HAGEDORN AND BROWN CORRELATION.  THE ACCELERATION
C     PRESSURE GRADIENT IS CALCULATED WITH THE DUNS AND ROS EQUATION.
C     THE FLOW REGIMES CORRESPONDING TO IREG ARE-
C     IREG=1  LIQUID
C     IREG=2  GAS
C     IREG=3  BUBBLE
C     IREG=4  SLUG
C
      DIMENSION XHL(12),YHL(12),XCNL(10),YCNL(10),XPSI(12),YPSI(12)
      DIMENSION XHLL(12),XCNLL(10),YCNLL(10)
C     KHL>0,NO SLIP HOLD UP IF GREATER THAN H&B HOLD UP
C     KREG>0,GRIFFITH AND WALLIS CORRELATION FOR BUBBLE FLOW
C
      KREG=1
      KHL=1
C     ENTER DATA ARRAYS FOR LIQUID HOLDUP CORRELATION.
      DATA XHL/
```

```
     1.2,.5,1.,2.,5.,10.,20.,50.,100.,200.,300.,1000./
      DATA YHL/
     1.04,.09,.15,.18,.25,.34,.44,.65,.82,.92,.96,1./
      DATA XCNL/
     1.002,.005,.01,.02,.03,.06,.1,.15,.2,.4/
      DATA YCNL/
     1.0019,.0022,.0024,.0028,.0033,.0047,.0064,.008,.009,.0115/
      DATA XPSI/
     1.01,.02,.025,.03,.035,.04,.045,.05,.06,.07,.08,.09/
      DATA YPSI/
     11.,1.1,1.23,1.4,1.53,1.6,1.65,1.68,1.74,1.78,1.8,1.83/
      VSL=VM*HLNS
      VSG=VM-VSL
C
C     CHECK FOR SINGLE PHASE GAS OR LIQUID FLOW.
      IF (HLNS.LT.1.) GO TO 1
      HL=1.
      DENNS=DENL
      IREG=1
      GO TO 6
    1 IF (HLNS.GT.0.) GO TO 2
      HL=0.
      DENNS=DENG
      XN=1.
      IR=1
      IREG=2
      GO TO 6
C
C     CHECK FOR BUBBLE FLOW.
    2 XLB=1.071-.2281*VM**2/DIA
      IF (XLB.LT..13) XLB=.13
      HGNS=1.-HLNS
      IF (HGNS.GT.XLB) GO TO 3
      IREG=3
      IF (KREG.EQ.0) GO TO 3
      VS=.8
      HL=1.-.5*(1.+VM/VS-SQRT((1.+VM/VS)**2.-4.*VSG/VS))
      IF (HL.LT.HLNS) HL=HLNS
      DENS=DENL*HL+DENG*(1.-HL)
      REYNB=1488.*DENL*(VSL/HL)*DIA/VISL
C     CALLING FANNING FRICTION FACTOR
      CALL FFAN(IR,ED, XN,REYNB,F)
C     CALCULATING MOODY FRICTION FACTOR
      FF=4.*F
C
C     CALCULATE ELEVATION AND FRICTION GRADIENTS AND ACCELERATION TERM
C     FOR BUBBLE FLOW.
      ELGR=DENS/144.
      FRGR=FF*DENL*(VSL/HL)**2/(2.*32.2*DIA*144.)
      EKK=0.
      GO TO 7
C     PREPARE HOLDUP CORRELATION ARRAYS FOR INTERPOLATION,
C
    3 DO 4 K=1,10
      XCNLL(K)=ALOG(XCNL(K))
    4 YCNLL(K)=ALOG(YCNL(K))
```

```
      DO 5 K=1,12
    5 XHLL(K)=ALOG(1.E-05*XHL(K))
C
C     CALCULATE LIQUID HOLDUP.
      XX=ALOG(XNL)
      CNL =EXP(FLAGR(XCNLL,YCNLL,XX,2,10))
      XX=ALOG(XNLV*CNL/(XNGV**.575*XND)*(P/14.7)**.1)
      HL=FLAGR(XHLL,YHL,XX,2,12)
      XX=XNGV*XNL**0.38/XND**2.14
      PSI=FLAGR(XPSI,YPSI,XX,2,12)
      IF (PSI.LT.1.) PSI=1.
      HL=HL*PSI
      IF (HL.LT.0) HL=0.
      IF (HL.GT.1.) HL=1.
      IF (HL.GT.HLNS) GO TO 6
      IF ( KHL.GT.0) HL=HLNS
C
C     CALCULATE NO-SLIP AND SLIP MIXTURE DENSITIES.
    6 DENNS=DENL*HLNS+DENG*(1.-HLNS)
      DENS=DENL*HL+DENG*(1.-HL)
C
C     CALCULATE FRICTION FACTOR
      VISS=VISL**HL*GVIS**(1.-HL)
      REYN=1488.*DENNS*VM*DIA/VISS
C     CALLING FANNING FRICTION FACTOR
      CALL FFAN(IR,ED, XN,REYN,F)
C     CALCULATING MOODY FRICTION FACTOR
      FF=4.*F
C
C     CALCULATE ELEVATION, FRICTION, ACCELERATION, AND TOTAL PRESSURE
C     GRADIENTS.
      ELGR=DENS/144.
      FRGR=FF*DENNS**2*VM**2/(2.*32.2*DIA*DENS*144.)
      VSG=VM*(1.-HLNS)
      EKK=DENS*VM*VSG/(32.2*P*144.)
      IF (EKK.GT..95) GO TO 8
    7  DPDL=-(ELGR+FRGR)/(1.-EKK)
      ACCGR=-DPDL*EKK
      RETURN
    8 WRITE (6,9)
    9 FORMAT (1X,'APPROACHING CRITICAL FLOW. STOP CALCULATIONS')
      STOP
      END
C
C


      SUBROUTINE ORKIS (DIA,ED,P,VM,HLNS,DENG,DENL,GVIS,
     1 SURL,XNLV,VISL,XNGV,HL,DPDL,IR,XN,IREG)
C
C     SUBROUTINE TO CALCULATE PRESSURE GRADIENT IN PSI/FT USING
C     THE ORKISZEWSKI CORRELATION.
C     THE FLOW REGIMES CORRESPONDING TO IREG ARE:
C     IREG=1  LIQUID
C     IREG=2  GAS
C     IREG=3  BUBBLE
C     IREG=4  SLUG
```

```
C      IREG=5  MIST
C      IREG=6  TRANSITION
C
       DIMENSION REBS(5),RELS(3),C2S(5,3)
C
C      ENTER DATA ARRAYS NEEDED FOR INTERPOLATION OF C2 FOR OBTAINING
C      BUBBLE VELOCITY IN SLUG FLOW.
       DATA REBS/ 3000.,4000.,5000.,6000.,8000./
       DATA RELS/ 0.,2900.,6000./
       DATA C2S/
      1 1.,1.,1.,1.,1.,1.5,1.24,1.15,1.115,1.08,1.71,1.5,1.3,1.23,1.165/
C
C      CALCULATE SUPERFICIAL VELOCITIES.
       VSL=VM*HLNS
       VSG=VM-VSL
C
C       CALCULATE LIQUID AND GAS REYNOLDS NUMBERS.
       REYNL=1488.*DENL*VM*DIA/VISL
       REYNG=1488.*DENG*VSG*DIA/GVIS
       ITRAN=1
C
C      CHECK FOR SINGLE PHASE FLOW
       IF (HLNS.GT..99999) GO TO 20
       IF (HLNS.LT..00001) GO TO 21
C
C      DETERMINE FLOW REGIME.
       XLS=50.+36.*XNLV
       XLM=75.+84*(XNLV**.75)
       HGNS=VSG/VM
       XLB=1.071-.2281*VM**2/DIA
       IF (XLB.LT..13) XLB=.13
       IF (HGNS.LT.XLB) GO TO 1
       IF (XNGV.LT.XLS) GO TO 2
       IF (XNGV.GT.XLM) GO TO 13
       ITRAN=2
       GO TO 2
C
C      BUBBLE FLOW REGIME
     1 IREG=3
       VS=.8
       HL=1.-.5*(1.+VM/VS-SQRT((1.+VM/VS)**2.-4.*VSG/VS))
       IF (HL.LT.HLNS) HL=HLNS
       DENS=DENL*HL+DENG*(1.-HL)
       REYNB=1488.*DENL*(VSL/HL)*DIA/VISL
C      CALLING FANNING FRICTION FACTOR
       CALL FFAN(IR,ED,XN,REYNB,F)
C      CALCULATING MOODY FRICTION FACTOR
       FF=4.*F
C
C      CALCULATE ELEVATION AND FRICTION GRADIENTS AND ACCELERATION TERM
C      FOR BUBBLE FLOW.
       ELGR=DENS/144.
       FRGR=FF*DENL*(VSL/HL)**2/(2.*32.2*DIA*144.)
       EKK=0.
       GO TO 22
```

```
C       SLUG FLOW REGIME
    2 IREG=4
      KSIG=0
      IC=2
      IB=1
      IF (VM.GT.10.) IB=2
      II=IB+IC
C
C       CALCULATE LIQUID DISTRIBUTION COEFFICIENT.
      XX1=.01*ALOG10(VISL+1.)/DIA**1.571
      XX=-ALOG10(VM)*(XX1+.397+.63*ALOG10(DIA))
      GO TO (3,4,5,6),II
    3 XX2=.0127*ALOG10(VISL+1.)/DIA**1.415
      SIG=XX2-.284+.167*ALOG10(VM)+.133*ALOG10(DIA)
      GO TO 7
    4 XX3=.0274*ALOG10(VISL+1.)/DIA**1.371
      SIG=XX3+.161+.569*ALOG10(DIA)+XX
      GO TO 7
    5 XX4=.013*ALOG10(VISL)/DIA**1.38
      SIG=XX4-.681+.232*ALOG10(VM)-.428*ALOG10(DIA)
      GO TO 7
    6 XX5=.045*ALOG10(VISL)/DIA**.799
      SIG=XX5-.709-.162*ALOG10(VM)-.888*ALOG10(DIA)
    7 CONTINUE
      IF (VM.LT.10..AND.SIG.LT.-.065*VM) SIG=-.065*VM
C
C       TRIAL AND ERROR CALCULATION OF BUBBLE VELOCITY, VB.
      VBG=.5*SQRT(32.2*DIA)
      I=0
    8 REYNB=1488.*DENL*VBG*DIA/VISL
      I=I+1
      IF (I.GT.10) GO TO 11
      XX=SQRT(32.2*DIA)
      IF (REYNL.GT.6000.) GO TO 9
C       CALCULATE VB BY INTERPOLATION OF CURVES.
      C2=FLAGR2(REBS,RELS,C2S,5,3,2,2,REYNB,REYNL)
      VB=.35*C2*XX
      GO TO 10
C       CALCULATE VB USING EQUATIONS.
    9 TX=(.251+8.74E-06*REYNL)*XX
      VB=(TX+SQRT(TX**2+(13.59*VISL)/(DENL*SQRT(DIA))))/2.
      IF (REYNB.LE.3000.) VB=(.546+8.74E-06*REYNL)*XX
      IF (REYNB.GE.8000.) VB=(.35+8.74E-06*REYNL)*XX
   10 IF (ABS(VB-VBG).LT..001) GO TO 11
      VBG=VB
      GO TO 8
   11 CONTINUE
C
C       CALCULATE MIXTURE DENSITY FOR SLUG FLOW.
      DENS=(DENL*(VSL+VB)+DENG*VSG)/(VM+VB)+DENL*SIG
      IF (VM.LE.10.) GO TO 12
      XX=-VB*(1.-DENS/DENL)/(VM+VB)
      IF (SIG.GE.XX) GO TO 12
      IF (KSIG.EQ.1) GO TO 12
      SIG=XX
      KSIG=1
```

```
      GO TO 11
   12 CONTINUE
C
C     CALCULATE EQUIVALENT LIQUID HOLDUP.
      HL=(DENS-DENG)/(DENL-DENG)
C
C     CALCULATE ELEVATION AND FRICTION GRADIENTS AND ACCELERATION
C     TERM FOR SLUG FLOW.
      ELGR=DENS/144.
C     CALLING FANNING FRICTION FACTOR
      CALL FFAN(IR,ED,XN,REYNL,F)
C     CALCULATING MOODY FRICTION FACTOR
      FF=4.*F
      FRGR=(FF*DENL*VM**2/(2.*32.2*DIA*144.))*((VSL+VB)/(VM+VB)+SIG)
      EKK=0.
      IF (ITRAN.GT.1) GO TO 18
      GO TO 22
C
C      MIST FLOW REGIME
   13 IREG=5
C
C     TRIAL AND ERROR CALCULATION FOR ED AND CORRECTED VSG.
      VSGP=VSG
      EDG=ED
   14 REYG=1488.*DENG*VSGP*DIA/GVIS
      XWEB=454.*DENG*VSGP**2*(EDG*DIA)/SURL
      XVIS=.0002048*VISL**2/(DENL*SURL*(EDG*DIA))
      PR=XWEB*XVIS
      EDC=.0749*SURL/(DENG*VSGP**2*DIA)
      IF (PR.GT..005) EDC=.3713*SURL*PR**.302/(DEN3*VSGP**2*DIA)
      VSGP=VSG/(1.-EDC)**2
      IF (ABS(EDC-EDG).LT.1.E-7) GO TO 15
      EDG=EDC
      GO TO 14
C
C     CALCULATE FRICTION GRADIENT FOR MIST FLOW
   15 IF (EDC.LT..05) GO TO 16
      FF=(1./(4.*ALOG10(.27*EDC))**2.+.067*EDC**1.73)*4.
      GO TO 17
C     CALLING FANNING FRICTION FACTOR
   16 CALL FFAN(1,EDC,1.,REYG,F)
C     CALCULATING MOODY FRICTION FACTOR
      FF=4.*F
   17 FRGR=FF*DENG*VSGP**2/(2.*32.2*DIA*144.)
C
C     CALCULATE ELEVATION GRADIENT AND ACCELERATION TERM FOR MIST FLOW.
      DENS=DENL*HLNS+DENG*(1.-HLNS)
      ELGR=DENS/144.
      EKK=DENS*VM*VSGP/(32.2*P*144.)
      IF (EKK.GT..95) GO TO 23
C
C     CHECK FOR TRANSITION REGION.
      IF (ITRAN.GT.1) GO TO 19
      GO TO 22
C
C     TRANSITION FLOW REGIME
```

```
   18 FRGRS=FRGR
      ELGRS=ELGR
      GO TO 13
   19 FRGRM=FRGR
      ELGRM=ELGR*XNGV/XLM
      DPDLM=-(FRGRM+ELGRM)/(1.-EKK)
      ACCGRM=-EKK*DPDLM
C
C     DETERMINE TRANSITION REGION WEIGHTING FACTORS.
      XS=(XLM-XNGV)/(XLM-XLS)
      XM=1.-XS
C
C     CALCULATE TRANSITION REGION FRICTION,ELEVATION,ACCELERATION AND
C     TOTAL PRESSURE GRADIENTS.
      FRGR=XS*FRGRS+XM*FRGRM
      ELGR=XS*ELGRS+XM*ELGRM
      ACCGR=XM*ACCGRM
      DPDL=-(FRGR+ELGR+ACCGR)
      IREG=6
      RETURN
C
C     SINGLE PHASE LIQUID FLOW
   20 IREG=1
      REYNL=1488.*DENL*VSL*DIA/VISL
C     CALLING FANNING FRICTION FACTOR
      CALL FFAN(IR,ED,XN,REYNL,F)
C     CALCULATING MOODY FRICTION FACTOR
      FF=4.*F
      FRGR=FF*DENL*VSL**2/(2.*32.2*DIA*144.)
      ELGR=DENL/144.
      HL=HLNS
      EKK=0.
      GO TO 22
C
C     SINGLE PHASE GAS FLOW
   21 IREG=2
      REYNG=1488.*DENG*VSG*DIA/GVIS
C     CALLING FANNING FRICTION FACTOR
      CALL FFAN( 1,ED,1.,REYNG,F)
C     CALCULATING MOODY FRICTION FACTOR
      FF=4.*F
      FRGR=FF*DENG*VSG**2/(2.*32.2*DIA*144.)
      ELGR=DENG/144.
      HL=HLNS
      EKK=DENG*VSG**2/(32.2*P*144.)
C
C     CALCULATE TOTAL AND ACCELERATION PRESSURE GRADIENTS FOR BUBBLE,
C     SLUG AND SINGLE PHASE FLOW.
   22 DPDL=-(FRGR+ELGR)/(1.-EKK)
      ACCGR=-EKK*DPDL
C
      RETURN
   23 WRITE (6,24)
   24 FORMAT (1X,'APPROACHING CRITICAL FLOW.STOP CALCULATIONS')
      STOP
      END
```

```
      SUBROUTINE BEGBR (DIA,ED,P,VM,HLNS,DENG,DENL,GVIS,
     1 XNLV,HL,VISL,DPDL,IR,XN,IREG)
C
C     SUBROUTINE TO CALCULATE PRESSURE GRADIENT IN PSI/FT USING A
C     MODIFIED BEGS AND BRILL CORRELATION.
C
C     THE HORIZONTAL FLOW REGIMES CORRESPONDING TO IREG ARE:
C     IREG=1 LIQUID
C     IREG=2 GAS
C     IREG=3 DISTRIBUTED
C     IREG=4 INTERMITTENT
C     IREG=5 SEGREGATED
C     IREG=6 TRANSITION
C     ANG=ANGLE OF FLOW FROM HORIZONTAL,DEG.
C     IHL=0,NO INCLIND FLOW HOLD UP CORRECTION
      IHL=0
      ANG=90.
C
C     CONVERT INCLINATION ANGLE TO RADIANS.
      A=ANG*3.1416/180.
C
C     CALCULATE SUPERFICIAL VELOCITIES AND MIXTURE FROUDE NUMBER.
      VSL=VM*HLNS
      VSG=VM-VSL
      XNFR=VM**2/(32.2*DIA)
C
C     CHECK FOR SINGLE PHASE FLOW.
      IREG=5
      IF (HLNS.GT..99999) IREG=1
      IF (HLNS.LT..00001) IREG=2
      IF (IREG.GT.2) GO TO 1
      HL=HLNS
      GO TO 12
C
C     DETERMINE FLOW REGIME USING REVISED FLOW PATTERN MAP.
    1 ITRAN=0
      XL1=316*HLNS**.302
      XL2=.0009252/HLNS**2.46842
      XL3=.1/HLNS**1.45155
      XL4=.5/HLNS**6.738
      XDD=XL1
      IF (HLNS.LT..01) GO TO 2
      IF (HLNS.GT..4) XDD=XL4
      IF (XNFR.GE.XL2.AND.XNFR.LT.XL3) ITRAN=1
      IF (XNFR.GE.XL3.AND.XNFR.LT.XDD) IREG=4
      IF (XNFR.GE.XDD) IREG=3
      GO TO 3
    2 IF (XNFR.GE.XL1) IREG=3
C
C     DETERMINE HORIZONTAL FLOW LIQUID HOLDUP AND C-FACTOR COEFFICIENTS
C     FOR UPHILL FLOW
    3 I=IREG-2
      GO TO (4,5,6),I
C
C     DISTRIBUTED FLOW.
```

```
    4 HLO=1.065*HLNS**.5824/XNFR**.0609
      D=1.
      E=0.
      F=0.
      G=0.
      GO TO 7
C
C     INTERMITTENT FLOW.
    5 HLO=.845*HLNS**.5351/XNFR**.0173
      D=2.96
      E=.305
      F=-.4473
      G=.0978
      GO TO 7
C
C     SEGREGATED FLOW.
    6 HLO=.98*HLNS**.4846/XNFR**.0868
      D=.011
      E=-3.768
      F=3.539
      G=-1.614
C
C     RESTRICT MINIMUM VALUE OF HLO.
    7 IF (HLO.LT.HLNS) HLO=HLNS
C
C     CHECK FOR HORIZONTAL FLOW.
      IF (A.NE.0.) GO TO 8
      HL =HLO
      GO TO 10
C
C     FLOW IS INCLINED,CALCULATE C-FACTOR.
    8 IF (A.GT.0.) GO TO 9
C     DOWNHILL C-FACTOR COEFFICIENTS.
      D=4.7
      E=-.3692
      F=.1244
      G=-.5056
C
C     CALCULATE THE C-FACTOR
    9 C=(1.-HLNS)*ALOG(D*HLNS**E*XNLV**F*XNFR**G)
      IF (C.LT.0.) C=0.
C
C     CALCULATE THE ANGLE CORRECTION FACTOR AND THE CORRECTED LIQUID
C     HOLDUP FRACTION.
      XX=SIN(1.8*A)
      FAC=1.+C*(XX-.333*XX**3)
C     CHECK TO BE SURE FAC IS NOT NEGATIVE.
      IF (FAC.LT.0.) FAC=0.
      HL=HLO*FAC
      IF (HL.GT.1) HL=1.
C
C     APPLY PALMER HOLDUP CORRECTION FACTORS IF DESIRED.
      IF (IHL.EQ.0) GO TO 10
      IF (ANG.LT.0.) HL=HL*.541
      IF (ANG.GT.0.) HL=HL*.918
```

```
C     CHECK FOR TRANSITION FLOW.
   10 IF (ITRAN.LT.1) GO TO 12
      IF (IREG.LT.5) GO TO 11
      HLS=HL
      IREG=4
      GO TO 3
   11 HLI=HL
      AA=(XL3-XNPR)/(XL3-XL2)
      B=1.-AA
      HL=HLS*AA+HLI*B
C
C     CALCULATE MIXTURE FLUID PROPERTIES.
   12 DENNS=DENL*HLNS+DENG*(1.-HLNS)
      DENS=DENL*HL+DENG*(1.-HL)
      VISNS=VISL*HLNS+GVIS*(1.-HLNS)
C
C     CALCULATE THE FRICTION FACTOR
      REYN=1488.*DENNS*VM*DIA/VISNS
C     CALLING FANNING FRICTION FACTOR
      CALL FFAN(IR,ED,XN,REYN,F)
C     CALCULATING MOODY FRICTION FACTOR
      FF=4.*F
      IF (IREG.LE.2) GO TO 13
C
C     CALCULATE TWO PHASE FRICTION FACTOR.
      Y=HLNS/(HL**2)
      X=ALOG(Y)
      S=X/(-.0523+3.182*X-.8725*X**2+.01853*X**4)
      IF (Y.GT.1.AND.Y.LT.1.2) S=ALOG(2.2*Y-1.2)
      FF=FF*EXP(S)
C
C     CALCULATE FRICTION,ELEVATION,ACCELERATION AND TOTAL PRESSURE
C     GRADIENTS.
   13 FRGR=FF*DENNS*VM**2/(2.*32.2*DIA*144.)
      ELGR=DENS*SIN(A)/144
      EKK=DENS*VM*VSG/(32.2*P*144.)
      IF (EKK.GT..95) GO TO 14
      DPDL=-(FRGR+ELGR)/(1.-EKK)
      ACCGR=-EKK*DPDL
C
      RETURN
   14 WRITE(6,15)
   15 FORMAT (1X,'APPROACHING CRITICAL FLOW.STOP CALCULATIONS')
      STOP
      END
```